

REFERENCES

- Anquetil, P.A., Yu, H., Madden, J.D., Madden, P.G., Swager, T.M., and Hunter, I.W. (2002) Thiophene-based conducting polymer molecular actuators. Proceedings of SPIE, 4695, 424-434.
- Boochathum, P., and Prajudtake, W. (2001) Vulcanization of *cis*- and *trans*-polyisoprene and their blends: cure characteristics and crosslink distribution. European Polymer Journal, 37, 417-427.
- Chandrasekhar, P. (1999) Fundamentals and Applications of Conducting Polymers Handbook, USA: Kluwer Academic Publishers.
- Choi, S-S. (1999) Correlation of crosslink density with pyrolysis pattern of natural Rubber vulcanizates with efficient vulcanizing cure system. Journal of Analytical and Applied Pyrolysis, 52, 105-112.
- Chotpattananont, D., Sirivat, A., and Jamieson, A.M. (2004) Electrorheological properties of perchloric acid-doped polythiophene suspensions. Colloid Polym Sci, 282, 357-365.
- Davidson, K., and Ponsonby, A.M. (1999) Synthesis of cross-linked electrically conductive polymers. Synthetic Metals, 102, 1512-1513.
- Deependra, K., Shahid, A., and Seungyong, Y. (2004) Semiconducting and Metallic Polymers. Condensed matter physics II, 1-19.
- Demanze, F., Yassar, A., and Garnier, F. (1996) Alternating Donor-Acceptor Substitutions in Conjugated Polythiophenes. Macromolecules, 29, 4267-4273.
- Faez, R., and De Paoli, M-A. (2001) A conductive rubber based on EPDM and Polyaniline I. Dopping method effect. European Polymer Journal, 37, 1139-1143.
- Faez, R., Schuster, R-H., and De Paoli, M-A. (2002) A conductive elastomer based on EPDM and polyaniline II. Effect of the crosslinking method. European Polymer Journal, 38, 2459-2463.
- Grulke, E.A. Solubility Parameter Values. Polymer Handbook Volume 2, Brandrup & Immernut Publisher, 519-552.

- Holmes, A.B., Peter, L., Sano, T., Morrison, J.J., Feeder, N., and Kraft, A. (2001) Supramolecular assemblies with dithieno[3, 2-b;2', 3'-d] thiophenes and other conjugated thiophene-containing π -systems. Synthetic Metals, 119, 175-176
- Horkay, F., McKenna, G.B., Deschamps, P., and Geissler, E. (2000) Neutron Scattering Properties of Randomly Crosslinked Polyisoprene Gels. Macromolecules, 33, 5215-5220.
- Jacqueline, I.K. (1990) Concise Encyclopedia of Polymer Science and Engineering. 2nd edition. New York: A Wiley-Interscience Publication.
- Kawai, T., Tanaka, F., Kojima, S., and Yoshino, K. (1999) Electrical and optical properties of poly(3-alkoxythiophen) and their application for gas sensor. Synthetic Metals, 102, 1358-1359.
- Khan, I.M., Waugaman, M., Sannigrahi, B., and McGeady, P. (2003) Synthesis, characterization and biocompatibility studies of oligosiloxane modified polythiophenes. European Polymer Journal, 39, 1405-1412.
- Kim, B., Chen, L., Gong, J.P., and Osada, Y. (1999) Titration Behavior and Spectral Transitions of Water-Soluble Polythiophene Carboxylic Acids Macromolecules, 32, 3964-3969.
- Kim, B., Chen, L., Gong, J.P., Nishino, M., and Osada, Y. (2000) Environmental Responses of Polythiophene Hydrogels. Macromolecules, 33, 1232-1236.
- Kim, B., Fukuoka, H., Gong, J.P., and Osada, Y. (2001) Titration Behavior and Spectral Transitions of hydrophobically modified water-soluble polythiophenes. European Polymer Journal, 37, 2499-2503.
- Kim, S.R., Choi, S.A., Kim, J.D., Lee, C., Rhee, S.B., and Kim, K.J. (1995) Preparation of polythiophene LB films and their gas sensitivities by the quartz crystal microbalance. Synthetic Metals, 71, 2027-2028.
- Knite, M., Teteris, V., Kiploka, A., and Kaupuzs, J. (2004) Polyisoprene-carbon Black nanocomposites as tensile strain and pressure sensor materials. Sensors and Actuators A, 110, 142-149.
- Kornbluh, R., Perlrine, R., Joseph, J., Heydt, R., Pei, Q., and Chiba, S. (1999) High-Field Electrostriction of Elastomeric Polymer Dielectrics for Actuation. Proceeding of SPIE, 3669, 149-161.

- Krause, S., and Bohon, K. (2001) Electromechanical response of electrorheological fluids and Poly(dimethylsiloxane) networks. Macromolecules, 34, 7179-7189.
- Küçükyavuz, S., Sankir, M., and Küçükyavuz, Z. (2002) Electrochemical preparation and characterization of carbon fiber reinforced PDMS/Pth composites. Synthetic Metals, 128, 247-251.
- Küçükyavuz, Z., and Kiralp, S. (2003) Preparation and Characterization of Conducting Polybutadiene/Polythiophene Composites. Turk J. Chem, 27, 417-422.
- Kumar, D., and Sharma, R.C. (1998) Advances in conductive polymers. European Polymer Journal, 34, 1053-1060.
- Lee, C., Kim, K.J., and Rhee, S.B. (1995) The effect of ester substitution and alkyl chain length on the properties of polythiophenes. Synthetic Metals, 69, 295-296.
- Liu, B., and Shaw, T.M. (2001) Electrorheology of filled silicone elastomers. Journal of Rheology, 45(3), 641-657.
- McCullough, R.D., and Ewbank, P.C. (1997) Self-Assembly and Chemical Response of Conducting Polymer Superstructure. Synthetic Metals, 84, 311-312.
- Mu, S., and Park, S.M. (1995) Preparation and characterization of polythiophene in aqueous solutions. Synthetic Metals, 69, 311-312.
- Painter, P.C., and Coleman, M.M. (1997) Fundamentals of Polymer Science: An Introductory text, U.S.A: Technomic Publishing Company.
- Raphael, M.O., Samuel, J.H., and Kinam, P. (1996) Hydrogels and Biodegradable Polymer for bioapplications. Washington, D.C: American Chemical Society.
- Reedijk, J.A., Martens, H.C.F., van Bohemen, S.M.C., Hilt, O., Brom, H.B., and Michels, M.A.J. (1999) Charge transport in doped polythiophene. Synthetic Metals, 101, 475-476.
- Salaneck, W.R., Luncstrom, I., and Ranby, B. (1993) Conjugated polymer and related materials: The interconnection of chemical and electronic structure. New York: Oxford Science Publications.

- Shen, Z., Xue, H., and Li, Y. (2001) Polyaniline-polyisoprene composite film Based glucose biosensor with high permselectivity. Synthetic Metals, 124, 345-349.
- Stenger-Smith, J.D. (1998) Intrinsically electrically conducting polymers: Synthesis, Characterization, and their applications. Prog. Polym. Sci., 23, 57-79.
- Tolbert, L., Edmond, C., and Kowalik, J. (1999) Charge-transfer doping of poly (3-alkyl-2, 2'-bithiophene). Synthetic Metals, 101, 500-501.
- Torsi, L., Tafuri, A., Cioffi, N., Gallazzi, M.C., Sassella, A., Sabbatini, L., and Zambonin, P.G. (2003) Regioregular polythiophene field-effect transistors employed as chemical sensors. Sensors and Actuators B, 93, 257-262.
- Van Vught, F.A. (2000) Transparent and conductive polymer layers by gas plasma techniques. The Netherlands: L.M.H. Groenewoud.
- Wallance, G. G., Small, C. J., and Too, C. O. (1997) Responsive conducting polymer-hydrogel composites. Polymer Gels and Networks, 5, 251-265.
- Wang, D.W. (1992) Encyclopedia of Polymer Science and Engineering. 2nd Edition, vol. 1. New York: A Wiley-Interscience Publication.
- Wang, F., Lai, Y-H., and Han, M-Y. (2004) Stimuli-Responsive Conjugated Copolymers Having Electro-Active Azulene and Bithiophene Units in the Polymer Skeleton: Effect of Protonation and p-Doping on conducting Properties. Macromolecules, 37, 3222-3230.
- Zrínyi, M., Fehér, J., and Filipcsei, G. (2000) Novel gel actuator containing TiO₂ particles operated under static electric field. Macromolecules, 33, 5751-5753

APPENDICES

Appendix A Identification of Characteristic FT-IR Spectrum of Undoped and Doped Poly(3-thiophene acetic acid)

The undoped and doped poly(3-thiophene acetic acid) (PTAA) was first characterized by FT-IR spectroscopy in order to identify functional groups. An FT-IR spectrometer (Thermo Nicolet, Nexus 670) operated in the absorption mode with 32 scans and a resolution of $\pm 4 \text{ cm}^{-1}$, covering a wavenumber range of $4000\text{-}400 \text{ cm}^{-1}$ using a deuterated triglycine sulfate detector. Optical grade KBr (Carlo Erba Reagent) was used as the background material. The synthesized P3TAA was intimately mixed with dried KBr at a ratio of P3TAA:KBr = 1:20.

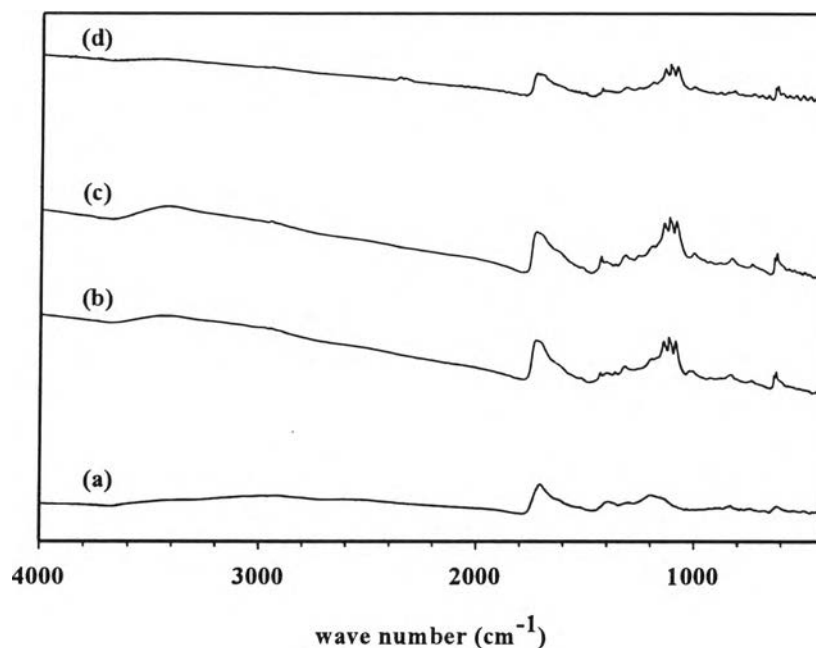


Figure A1 The FT-IR spectrum of : a) undoped poly(3-thiophene acetic acid); and poly(3-thiophene acetic acid) doped with HClO_4 at various mole ratios of acid to monomer unit; b) 1:1; c) 10:1; and d) 200:1.

The assignments of peaks in the spectrum are shown in Table A1. The characteristic peaks of P3TAA were found at $3200\text{-}3000 \text{ cm}^{-1}$ and can be assigned to

the stretching vibration of the C-H bond on the thiophene ring; peaks at 3000-2800 cm^{-1} represent the aliphatic C-H bonds; peak at 1700 cm^{-1} represents the C=O stretching vibration; peak at 1400 cm^{-1} represents the thiophene ring stretching vibration; and peaks at 1300-1200 cm^{-1} represent the C-O stretching vibration. The most distinct feature in this spectrum is the extremely broad O-H absorption occurring in the region from 3400 to 2400 cm^{-1} , which is attributed to the strong hydrogen bonding of the dimer. This absorption often obscures the C-H stretching vibrations occurring in the same region. It is obvious from the absorption peak at around 1700 cm^{-1} that the ester groups were not deteriorated during the oxidative polymerization (Kim *et al.*, 1999). After the neutral polythiophene was doped with perchloric acid, some characteristic peaks of acid appeared on FT-IR spectra: a broad peak around 3400-3000 cm^{-1} , and a sharp peak at 1400 cm^{-1} .

Table A1 The FT-IR absorption spectrum of undoped and doped PTAA with HClO_4

Wavenumber (cm^{-1})	Assignments	References
3400	O-H stretching vibration	Kim <i>et al.</i> (1999)
3200 – 3000	C-H stretching of thiophene ring	Kim <i>et al.</i> (1999)
3000 – 2800	C-H stretching of aliphatic	Kim <i>et al.</i> (1999)
1700	C=O stretching vibration	Kim <i>et al.</i> (1999)
1400	Thiophene ring stretching vibration	Kim <i>et al.</i> (1999)
1300 – 1200	C-O stretching vibration	Kim <i>et al.</i> (1999)
835	C-H stretching, out of plane of thiophene ring	Kim <i>et al.</i> (1999)

Appendix B Identification of Characteristic Peaks of Undoped and Doped Poly(3-thiophene acetic acid) from UV-Visible Spectroscopy

The UV-Visible spectra of undoped and doped polythiophene recorded with a UV-Vis absorption spectrometer (Perkin-Elmer, Lambda 10). Measurements were taken in the absorbance mode in the wavelength range of 200-800 nm. Synthesized P3TAA was grinded into a fine powder, dissolved in DMSO at the concentration of 6.0×10^{-5} M and pipetted into the sample holder. Scan speed was 240 mm/min, and a slit width of 2.0 nm using a deuterium lamp as the light source.

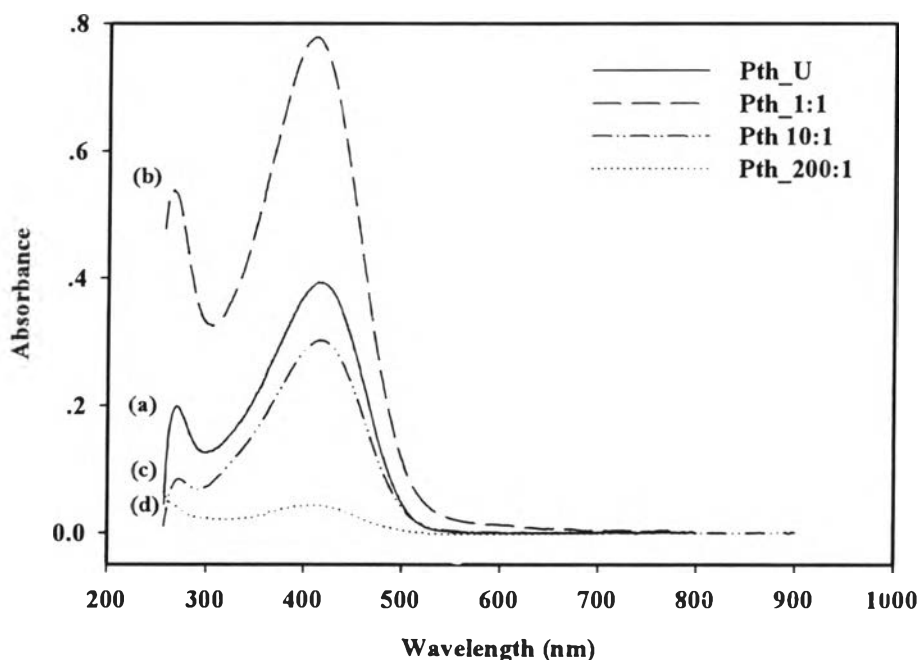


Figure B1 The UV-Visible spectra of : a) undoped poly(3-thiophene acetic acid); and poly(3-thiophene acetic acid) doped with HClO_4 at various mole ratios of acid to monomer unit; b) 1:1; c) 10:1; and d) 200:1.

The UV-Visible spectra of undoped and doped poly(3-thiophene acetic acid) from the references are shown in Table B1. The wavelength in [] refers to the results of the assignments cited from references.

Table B1 Assignment peaks of UV-Visible peaks of undoped and doped polythiophene

Wavelength (nm)	Assignments	References
264±5 [264]	π - π^* transitions of the bithiophene unit	Wang <i>et al.</i> (2004)
435±10 [435]	π - π^* transitions of the conjugated polymer chains	Demanze <i>et al.</i> (1996)
735±5 [735]	localized of polaron state	Demanze <i>et al.</i> (1996)

The data from UV-Visible spectra are summarized in Table B2, whereas N/A means not detectable.

Table B2 The UV-Visible spectrum of undoped (Pth_U) and doped polythiophene as various doping ratios

Doping ratio	Absorbance		
	Wavelength (cm ⁻¹)		
	265-275	400-420	730-750
Pth U	0.199	0.393	N/A
Pth 1:1	0.539	0.779	N/A
Pth 10:1	0.085	0.302	N/A
Pth 200:1	N/A	0.045	0.002

Appendix C The Thermogravimetric Thermogram of Undoped and Doped PTAA, Crosslinked Polyisoprene (PI_03) and Polythiophene/Polyisoprene (Pth_U/PI_03)

A thermal gravimetric analyzer (DuPont, model TGA 2950) was used to determine amount of moisture content and dopant, and the decomposition temperature of undoped, doped poly(3-thiophene acetic acid) (P3TAA) at various mole ratios of dopant, of crosslinked polyisoprene (PI_03) and polythiophene/polyisoprene blends (Pth_U/PI_03) with the temperature scan from 30 to 800°C and a heating rate of 10°C/min. The samples were weighted in the range of 5-10 mg and loaded into a platinum pan, and then were heated under an oxygen gas flow. Three transitions were observed in undoped poly(3-thiophene acetic acid), 30-120°C, 120-280°C and 280-600°C; they can be referred to as the losses of water and residue solvent, the side chain degradation and the backbone degradation, respectively (Chotpattananont *et al.*, 2004; Hu *et al.*, 2000). After doping, the thermograms show the degradation temperature of perchloric acid dopant at around 148 °C and a decrease in the thermal stability of main chain as compared to that of the undoped P3TAA. For the polythiophene/polyisoprene blends, the blends have a better thermal stability with increasing polythiophene particles concentration.

Table C1 Summary of undoped and doped P3TAA degradation steps

Sample	Transition temperature (°C)			% Weight loss			% Residue
	1 st	2 nd	3 rd	1 st	2 nd	3 rd	
Pth U	30-120	120-280	280-600	4.69	20.82	68.79	6.27
Pth 1:1	30-110	110-250	250-600	7.57	17.76	72.74	2.98
Pth 10:1	30-110	110-255	255-600	8.56	17.89	72.04	2.50
Pth 200:1	30-115	115-265	265-600	5.88	17.15	75.80	2.13

Table C2 Summary of PI_03, Pth_U5/PI_03, Pth_U10/PI_03, Pth_U20/PI_03, and Pth_U30/PI_03 degradation steps

Sample	Transition temperature (°C)			% Weight loss			% Residue
	1 st	2 nd	3 rd	1 st	2 nd	3 rd	
PI 03	30-450	450-600	-	91.77	7.668	-	0.424
PI 03/Pth U5	30-360	360-440	440-600	63.52	15.86	20.51	0.954
PI 03/Pth U10	30-390	390-440	440-600	66.78	10.12	22.36	1.61
PI 03/Pth U20	30-385	385-450	450-600	53.98	17.50	32.94	1.48
PI 03/Pth U30	30-395	395-600	-	54.75	44.99	-	2.33

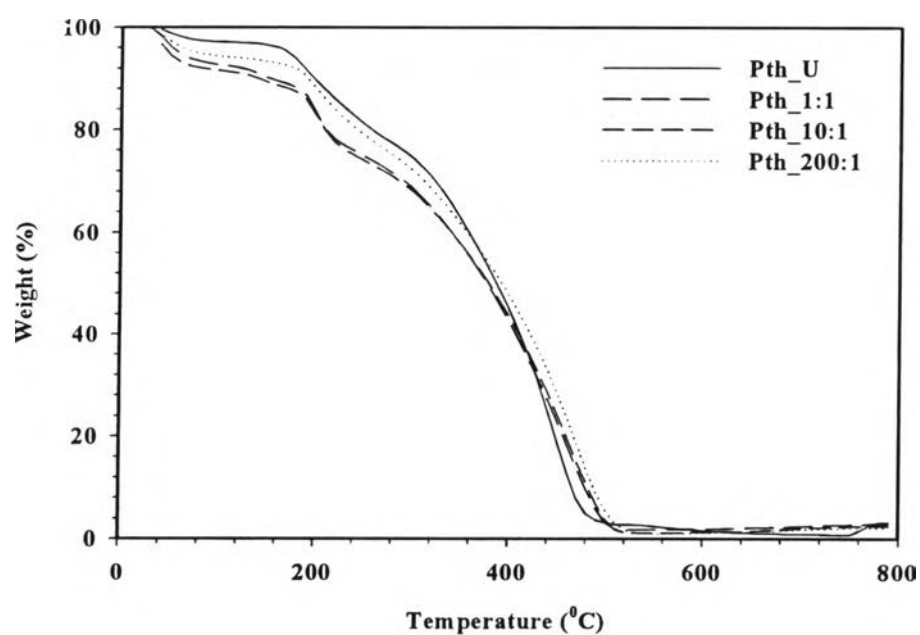


Figure C1 The TGA thermograms of undoped and doped P3TAA with HClO₄.

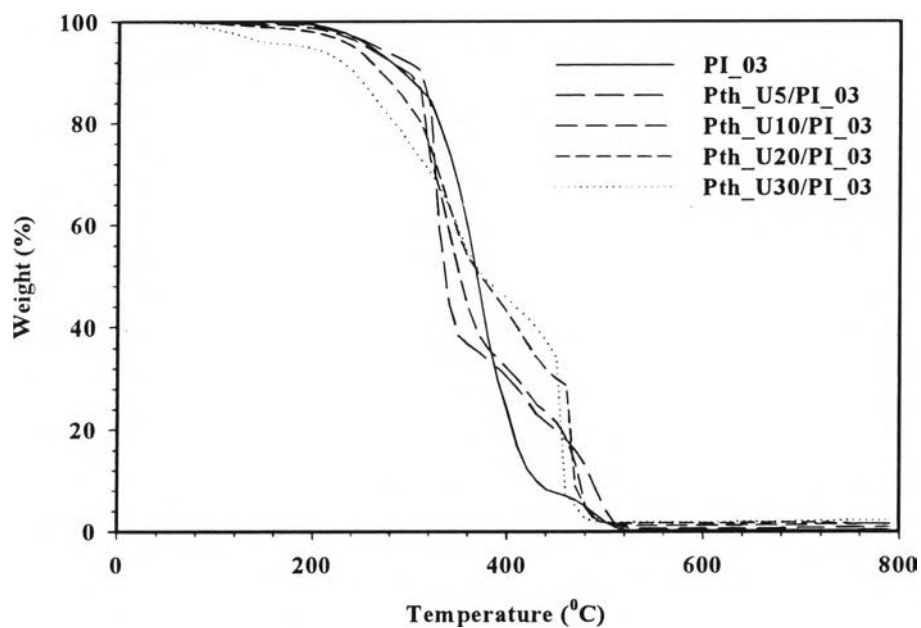


Figure C2 The TGA thermograms of crosslinked polyisoprene (PI_03) and polythiophene/polyisoprene blends (Pth_U/PI_03).

Appendix D Determination of Particle Sizes of Undoped and Doped P3TAA

Table D1 Summary of the particles diameter of undoped P3TAA (Pth_U), P3TAA doping ratio 1:1 (Pth_1:1), P3TAA doping ratio 10:1 (Pth_10:1), and P3TAA doping ratio 200:1 (Pth_200:1)

Samples	Particle diameter (μm)				
	1	2	3	Avg.	STD
Pth U	20.19	21.6	15.6	19.13	3.14
Pth 1:1	18.25	17.41	17.33	17.66	0.51
Pth 10:1	17.61	16.8	16.6	17.00	0.53
Pth 200:1	23.42	23.46	23.81	22.56	0.21

Table D2 The raw data from particle size analysis of undoped P3TAA

Size		Undoped polythiophene					
Low (μm)	High (μm)	In%	Under%	In%	Under%	In%	Under%
0.05	0.12	0.00	0.00	0.00	0.00	0.00	0.00
0.12	0.15	0.11	0.12	0.00	0.00	0.02	0.02
0.15	0.19	0.22	0.34	0.00	0.00	0.06	0.08
0.19	0.23	0.33	0.67	0.00	0.00	0.11	0.19
0.23	0.28	0.43	1.10	0.00	0.00	0.19	0.38
0.28	0.35	0.52	1.61	0.00	0.00	0.29	0.67
0.35	0.43	0.59	2.20	0.00	0.00	0.41	1.08
0.43	0.53	0.64	2.84	0.00	0.00	0.55	1.63
0.53	0.65	0.65	3.49	0.00	0.00	0.67	2.30
0.65	0.81	0.61	4.10	0.00	0.00	0.75	3.04
0.81	1.00	0.53	4.63	0.00	0.00	0.74	3.78
1.00	1.23	0.42	5.05	0.00	0.00	0.62	4.40
1.23	1.51	0.33	5.38	0.00	0.00	0.46	4.86
1.51	1.86	0.33	5.71	0.00	0.00	0.34	5.20
1.86	2.30	0.39	6.10	0.00	0.00	0.31	5.52
2.30	2.83	0.53	6.63	0.41	0.41	0.42	5.94
2.83	3.49	0.76	7.39	1.08	1.49	0.73	6.67
3.49	4.30	1.10	8.49	1.86	3.35	1.25	7.91
4.30	5.29	1.59	10.07	2.80	6.15	1.97	9.89
5.29	6.52	2.21	12.29	4.03	10.18	2.82	12.71
6.52	8.04	2.96	15.25	5.54	15.72	3.73	16.43
8.04	9.91	3.81	19.06	7.51	23.23	4.74	21.17
9.91	12.21	4.78	23.84	10.10	33.33	5.94	27.11
12.21	15.04	6.03	29.87	14.05	47.39	7.51	34.63
15.04	18.54	7.66	37.52	18.46	65.83	9.54	44.16
18.54	22.84	9.54	47.07	19.14	84.94	11.81	55.98
22.84	28.15	11.35	58.41	11.87	96.80	13.57	69.54
28.15	34.69	12.36	70.77	2.99	99.81	13.50	83.03
34.69	42.75	11.85	82.61	0.17	100.00	10.70	93.72
42.75	52.68	9.39	92.01	0.00	100.00	5.62	99.35
52.68	64.92	5.87	97.86	0.00	100.00	0.64	99.99
64.92	80.00	2.12	100.00	0.00	100.00	0.00	100.00

Table D3 The raw data from particle size analysis of doped P3TAA, as doping ratio 1:1

Size		Doped polythiophene 1:1					
Low (μm)	High (μm)	In%	Under%	In%	Under%	In%	Under%
0.05	0.12	0.02	0.02	0.02	0.02	0.01	0.02
0.12	0.15	0.32	0.34	0.34	0.36	0.33	0.35
0.15	0.19	0.61	0.95	0.66	1.02	0.63	0.98
0.19	0.23	0.87	1.82	0.94	1.96	0.90	1.88
0.23	0.28	1.08	2.90	1.19	3.15	1.13	3.01
0.28	0.35	1.23	4.13	1.37	4.52	1.31	4.32
0.35	0.43	1.30	5.42	1.48	5.99	1.41	5.73
0.43	0.53	1.28	6.71	1.50	7.49	1.43	7.15
0.53	0.65	1.19	7.90	1.43	8.93	1.36	8.51
0.65	0.81	1.02	8.91	1.28	10.20	1.21	9.72
0.81	1.00	0.81	9.72	1.07	11.27	1.02	10.74
1.00	1.23	0.64	10.36	0.89	12.17	0.85	11.59
1.23	1.51	0.61	10.97	0.86	13.03	0.82	12.41
1.51	1.86	0.77	11.74	1.05	14.08	1.02	13.43
1.86	2.30	1.11	12.85	1.40	15.48	1.39	14.83
2.30	2.83	1.55	14.41	1.81	17.29	1.85	16.68
2.83	3.49	2.08	16.49	2.26	19.55	2.35	19.03
3.49	4.30	2.68	19.17	2.75	22.29	2.87	21.90
4.30	5.29	3.33	22.50	3.30	25.59	3.42	25.33
5.29	6.52	4.02	26.52	3.91	29.50	4.01	29.34
6.52	8.04	4.70	31.22	4.56	34.05	4.61	33.95
8.04	9.91	5.36	36.58	5.21	39.26	5.25	39.20
9.91	12.21	6.05	42.62	5.92	45.18	5.97	45.17
12.21	15.04	6.91	49.53	6.79	51.97	6.88	52.05
15.04	18.54	7.93	57.46	7.79	59.75	7.91	59.95
18.54	22.84	8.88	66.34	8.60	68.36	8.74	68.70
22.84	28.15	9.44	75.78	8.99	77.35	9.08	77.78
28.15	34.69	9.11	84.89	8.53	85.88	8.52	86.29
34.69	42.75	7.66	92.55	7.16	93.03	6.98	93.26
42.75	52.68	5.15	97.70	4.83	97.86	4.64	97.90
52.68	64.92	2.29	99.98	2.13	99.98	2.09	99.98
64.92	80.00	0.00	100.00	0.00	100.00	0.00	100.00

Table D4 The raw data from particle size analysis of doped PTAA, as doping ratio 10:1

Size		Doped polythiophene 10:1					
Low (μm)	High (μm)	In%	Under%	In%	Under%	In%	Under%
0.05	0.12	0.02	0.02	0.02	0.02	0.01	0.02
0.12	0.15	0.28	0.30	0.30	0.31	0.29	0.30
0.15	0.19	0.53	0.83	0.56	0.87	0.56	0.86
0.19	0.23	0.75	1.58	0.79	1.66	0.80	1.66
0.23	0.28	0.92	2.50	0.97	2.63	1.00	2.65
0.28	0.35	1.03	3.53	1.09	3.72	1.15	3.80
0.35	0.43	1.07	4.60	1.14	4.85	1.23	5.03
0.43	0.53	1.04	5.63	1.11	5.96	1.24	6.27
0.53	0.65	0.93	6.56	1.00	6.96	1.17	7.45
0.65	0.81	0.76	7.32	0.83	7.79	1.02	8.46
0.81	1.00	0.57	7.89	0.63	8.42	0.81	9.27
1.00	1.23	0.40	8.29	0.45	8.87	0.60	9.87
1.23	1.51	0.30	8.59	0.34	9.21	0.49	10.36
1.51	1.86	0.30	8.89	0.35	9.56	0.55	10.91
1.86	2.30	0.42	9.31	0.51	10.06	0.80	11.71
2.30	2.83	0.73	10.04	0.87	10.93	1.27	12.98
2.83	3.49	1.32	11.36	1.52	12.45	2.04	15.02
3.49	4.30	2.28	13.65	2.55	15.00	3.10	18.11
4.30	5.29	3.63	17.28	3.93	18.93	4.40	22.51
5.29	6.52	5.24	22.52	5.52	24.45	5.75	28.26
6.52	8.04	6.81	29.32	7.00	31.45	6.82	35.08
8.04	9.91	7.91	37.23	7.99	39.43	7.31	42.39
9.91	12.21	8.35	45.58	8.34	47.77	7.29	49.68
12.21	15.04	8.40	53.98	8.36	56.13	7.18	56.86
15.04	18.54	8.37	62.35	8.32	64.45	7.29	64.15
18.54	22.84	8.30	70.65	8.22	72.67	7.56	71.71
22.84	28.15	8.19	78.84	7.99	80.66	7.85	79.56
28.15	34.69	7.66	86.50	7.28	87.94	7.63	87.19
34.69	42.75	6.51	93.00	6.00	93.94	6.56	93.75
42.75	52.68	4.59	97.60	4.08	98.03	4.42	98.18
52.68	64.92	2.36	99.95	1.97	99.98	1.82	99.99
64.92	80.00	0.04	100.00	0.00	100.00	0.00	100.00

Table D5 The raw data from particle size analysis of doped P3TAA, as doping ratio 200:1

Size		Doped polythiophene 200:1					
Low (μm)	High (μm)	In%	Under%	In%	Under%	In%	Under%
0.05	0.12	0.00	0.00	0.00	0.00	0.00	0.00
0.12	0.15	0.00	0.00	0.00	0.00	0.00	0.00
0.15	0.19	0.00	0.00	0.00	0.00	0.00	0.00
0.19	0.23	0.00	0.00	0.00	0.00	0.00	0.00
0.23	0.28	0.00	0.00	0.00	0.00	0.00	0.00
0.28	0.35	0.00	0.00	0.00	0.00	0.00	0.00
0.35	0.43	0.00	0.00	0.00	0.00	0.00	0.00
0.43	0.53	0.59	0.59	0.36	0.37	0.35	0.35
0.53	0.65	0.92	1.51	1.01	1.37	1.03	1.38
0.65	0.81	0.82	2.33	0.94	2.30	0.97	2.35
0.81	1.00	0.54	2.87	0.60	2.90	0.64	2.98
1.00	1.23	0.33	3.20	0.36	3.27	0.40	3.38
1.23	1.51	0.20	3.40	0.22	3.49	0.25	3.63
1.51	1.86	0.13	3.53	0.14	3.63	0.18	3.81
1.86	2.30	0.18	3.71	0.19	3.82	0.24	4.05
2.30	2.83	0.32	4.02	0.34	4.16	0.38	4.43
2.83	3.49	0.55	4.57	0.57	4.73	0.61	5.04
3.49	4.30	0.90	5.47	0.89	5.61	0.91	5.96
4.30	5.29	1.41	6.88	1.32	6.94	1.33	7.29
5.29	6.52	2.22	9.10	1.93	8.87	1.90	9.19
6.52	8.04	3.43	12.53	2.78	11.65	2.69	11.88
8.04	9.91	5.08	17.62	3.95	15.60	3.80	15.69
9.91	12.21	7.20	24.81	5.55	21.16	5.33	21.01
12.21	15.04	9.81	34.63	7.73	28.90	7.44	28.46
15.04	18.54	12.59	47.21	10.41	39.30	10.09	38.54
18.54	22.84	14.53	61.74	12.91	52.21	12.62	51.16
22.84	28.15	14.63	76.36	14.36	66.56	14.21	65.37
28.15	34.69	12.26	88.62	13.63	80.19	13.73	79.09
34.69	42.75	8.09	96.68	10.85	91.04	11.12	90.21
42.75	52.68	3.28	99.99	6.61	97.66	6.99	97.20
52.68	64.92	0.00	100.00	2.34	99.97	2.79	99.97
64.92	80.00	0.00	100.00	0.00	100.00	0.00	100.00

Appendix E Calculation of Doping Level from EDX

The % doping levels of the doped polythiophene powder at various ratios of $N_{\text{acid}}/N_{\text{Pth}}$ were calculated from the amounts of carbon (C), oxygen (O), sulfur (S) and chlorine (Cl) mol percents obtained from EDX. For HClO_4 doped polythiophene, the % doping level was calculated from amounts of Cl as shown in the equation (E.1)

$$\% \text{ doping level of Pth-HClO}_4 = \frac{\% \text{Cl}_{\text{HClO}_4}}{\% \text{S}} \times \frac{M_{\text{S}}}{M_{\text{ClO}_4^-}} \times 100 \quad (\text{E.1})$$

Table E1 Doping level of HClO_4 doped polythiophene from EDX

Doping ratio ($N_{\text{acid}}/N_{\text{Pth}}$)	EDX data				EDX data				%Doping level
	% mole of Cl				% mole of S				
	1	2	3	Average	1	2	3	Average	
Pth 1:1	0.61	0.71	0.66	0.66	3.95	5.82	5.40	5.06	4.27 ± 0.60
Pth 10:1	1.01	0.66	0.74	0.80	1.33	1.77	2.09	1.73	15.93 ± 7.36
Pth 200:1	0.68	0.72	1.10	0.83	1.13	0.91	1.98	1.34	20.89 ± 4.02

Appendix F Determination of the Correction Factor (K)

The electrical conductivity of undoped and doped P3TAA was measured by a two-point probe meter. The meter consists of two probes, making contact on the surface of film sample. These probes were connected to a source meter (Keithley, Model 6517A) for a constant voltage source and reading the resultant current.

The geometrical correction factor was taken into account of geometric effects, depending on the configuration and probe tip spacing.

$$K = \frac{w}{l} \quad (\text{F.1})$$

K is geometrical correction factor, w is width of probe tip spacing (cm), l is the length between probes (cm).

In this measurement, the constant K value was determined by using standard materials where specific resistivity values were known; we used silicon wafer chips (SiO₂). In our case, the sheet resistivity was measured by using our custom made two-point probe and then the geometric correction factor was calculated by equation (F.2) as follows:

$$K = \frac{\rho}{R \times t} = \frac{I \times \rho}{V \times t} \quad (\text{F.2})$$

K is geometric correction factor, ρ is resistivity of standard silicon wafer, which calibrated by using a four point probe at King Mongkut's Institute Technology of Lad Krabang (Ω.cm), t is film thickness (cm), R is film resistance (Ω), I is measure current (A), and V is voltage drop (V).

Standard Si wafer were cleaned to remove organic impurities prior to be used according to the standard RCA method (Kem, 1993).

Materials

Acetones (Scharlau, 99.5%), Methanol (CARLO ERBA, 99.9%), Ammonium hydroxide (Merk, 99.9%), Hydrogen peroxide (CARLO ERBA, 30% in water), and dilute (2%) Hydrofuric acid

Experiment

The cleaning procedures contain 3 steps: the solvent clean, the RCA01 and the HF dip. The first step is the solvent clean step, employed to remove oils and organic residues that appeared on Si wafer surface. The Si wafer was placed into the acetone at 55°C for 10 min, removed and placed in methanol for 2-5 min, subsequently rinsed with deionized water and blown dried with nitrogen gas. Second step is the RCA clean, to remove organic residues from silicon wafers. This process oxidized the silicon wafer and left a thin oxide on the surface of the wafer. RCA solution was prepared with 5 parts of water (H₂O), 1 part of 27% ammonium hydroxide (NH₄OH), and 1 part of 30% hydrogen peroxide (H₂O₂). 65 ml of NH₄OH (27%) was added into 325 ml of deionized water in a beaker and then heated to 70 ± 5°C. The mixture would bubble vigorously after 1-2 min, indicated that it was ready to use. Silicon wafer was soaked in the solution for 15 min, consequently overflowed with deionized water in order to rinse and remove the solution. The third step is the HF dip, which was carried out to remove native silicon dioxide from wafer. 480 ml of deionised water was added to the polypropylene bottle and then added to 20 ml HF. Wafer was soaked in this solution for 2 min, removed and checked for hydrophobicity by performing the wetting test. Deionized water was poured onto the surface wafer; the clean silicon surface would shows that the beads of water would roll off. Clean Si wafer was further blown dried with nitrogen and stored in a clean and dry environment.

Table F1 Determination the correction factor of probe A

Probe	K (correction factor)				
	1	2	3	Average	STD
A	2.07E-04	2.07E-04	3.11E-04	2.42E-04	6.00E-05

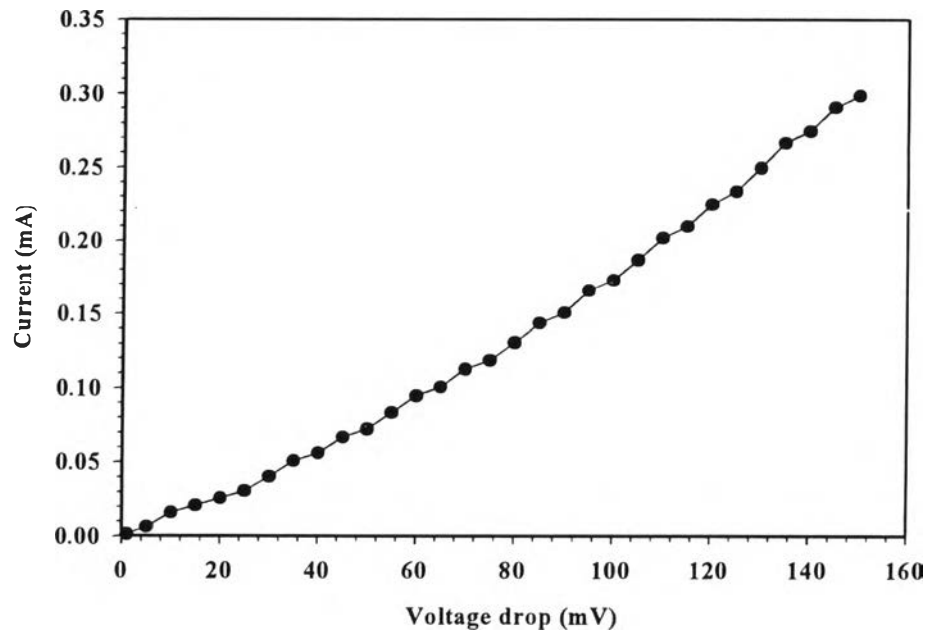


Figure F1 The calibration data of Si-wafer: K tay which specific resistivity (ρ) 0.014265 $\Omega \cdot \text{cm}$, thickness 0.0724 cm, 27-28°C, 36-38%R.H.

Table F2 Determination the correction factor of probe A with standard Si wafer
(specific resistivity 0.014265 Ω .cm, thickness 0.0724 cm, 27-28°C, 36-38%R.H)

Volt Applied (mV)			Current (mA)		
1	2	3	1	2	3
1	1	1	0.0016	0.0033	0.0030
5	5	5	0.0065	0.0067	0.0062
10	10	10	0.0162	0.0129	0.0127
15	15	15	0.0211	0.0162	0.0160
20	20	20	0.0259	0.0197	0.0194
25	25	25	0.0308	0.0230	0.0228
30	30	30	0.0407	0.0299	0.0295
35	35	35	0.0510	0.0369	0.0363
40	40	40	0.0564	0.0405	0.0398
45	45	45	0.0670	0.0477	0.0470
50	50	50	0.0725	0.0513	0.0506
55	55	55	0.0836	0.0587	0.0579
60	60	60	0.0950	0.0663	0.0655
65	65	65	0.1010	0.0702	0.0694
70	70	70	0.1130	0.0780	0.0774
75	75	75	0.1190	0.0823	0.0813
80	80	80	0.1310	0.0906	0.0896
85	85	85	0.1440	0.0989	0.0982
90	90	90	0.1510	0.1030	0.1030
95	95	95	0.1660	0.1120	0.1120
100	100	100	0.1730	0.1170	0.1160
105	105	105	0.1870	0.1260	0.1260
110	110	110	0.2020	0.1360	0.1350
115	115	115	0.2100	0.1410	0.1400
120	120	120	0.2250	0.1510	0.1510
125	125	125	0.2340	0.1570	0.1570
130	130	130	0.2500	0.1670	0.1680
135	135	135	0.2670	0.1770	0.1780
140	140	140	0.2750	0.1830	0.1840
145	145	145	0.2910	0.1940	0.1950
150	150	150	0.2990	0.1990	0.2000

Appendix G Conductivity Measurement

The specific conductivity, which is the inversion of specific resistivity (ρ) of undoped and doped P3TAA pellets were measured by using the two-point probe connected to a source meter (Keithley, Model 6517A) for a constant voltage source and reading resultant current under the atmospheric pressure, 54-60% relative humidity and 25-28°C. The correction factor (K) of probe A is 2.42×10^{-4} . The thickness of pellets was measured by a thickness gauge. The applied voltage was plotted versus the current change to determine the linear ohmic regime of each sample. The applied voltage and the current change in the linear ohmic regime were converted to the electrical conductivity of the polymer by using equation (G.1) as follows:

$$\sigma = \frac{1}{\rho} = \frac{1}{R_s \times t} = \frac{I}{K \times V \times t} \quad (\text{G.1})$$

where σ is specific conductivity (S/cm), ρ is specific resistivity ($\Omega \cdot \text{cm}$), R_s is sheet resistivity (Ω), I is measure current (A), K is geometric correction factor, V is applied voltage (voltage drop) (V), t is pellet thickness (cm).

Table G1 Determination the specific conductivity (S/cm) of polyisoprene fluid (PI₀₀), undoped and doped polythiophene at various mole ratios of acid to monomer unit

Code	Specific conductivity (S/cm)	STD
PI 00	8.18×10^{-7}	1.13×10^{-7}
Pth U	3.01×10^{-6}	1.01×10^{-7}
Pth 1:1	1.54×10^{-3}	3.72×10^{-4}
Pth 10:1	3.66×10^{-3}	2.00×10^{-4}
Pth 200:1	1.12×10^{-1}	1.53×10^{-2}

Table G2 The raw data of the determination of linear regime of polyisoprene fluid

Sample	Thickness (cm)	Applied voltage (V)			Mesuered Current (A)			Conductivity (S/cm)		
		1	2	3	1	2	3	1	2	3
PI_00	1) 0.0637	1	1	1	5.59E-11	7.14E-11	7.12E-11	3.63E-06	4.71E-06	4.58E-06
	2) 0.0627	10	10	10	6.27E-11	7.50E-11	7.55E-11	4.07E-07	4.95E-07	4.86E-07
	3) 0.0643	20	20	20	5.09E-11	7.82E-11	8.19E-11	1.65E-07	2.58E-07	2.63E-07
		30	30	30	7.39E-11	8.12E-11	8.57E-11	1.60E-07	1.79E-07	1.84E-07
		40	40	40	7.83E-11	7.58E-11	8.61E-11	1.27E-07	1.25E-07	1.38E-07
		50	50	50	8.46E-11	7.87E-11	8.55E-11	1.10E-07	1.04E-07	1.10E-07
		60	60	60	8.83E-11	9.06E-11	8.97E-11	9.56E-08	9.90E-08	9.61E-08
		70	70	70	9.04E-11	8.42E-11	9.56E-11	8.38E-08	7.93E-08	8.79E-08
		80	80	80	8.22E-11	9.46E-11	9.90E-11	6.67E-08	7.80E-08	7.96E-08
		90	90	90	9.34E-11	9.64E-11	1.01E-10	6.74E-08	7.06E-08	7.22E-08
		100	100	100	9.60E-11	9.41E-11	1.04E-10	6.23E-08	6.21E-08	6.70E-08
		110	110	110	9.99E-11	1.00E-10	1.06E-10	5.90E-08	6.00E-08	6.17E-08
		120	120	120	1.04E-10	1.00E-10	1.01E-10	5.62E-08	5.52E-08	5.39E-08
		130	130	130	1.06E-10	9.91E-11	1.07E-10	5.31E-08	5.03E-08	5.29E-08
		140	140	140	1.11E-10	1.10E-10	1.10E-10	5.13E-08	5.18E-08	5.04E-08
		150	150	150	1.10E-10	1.07E-10	1.10E-10	4.77E-08	4.70E-08	4.71E-08
		160	160	160	1.10E-10	1.08E-10	1.05E-10	4.45E-08	4.46E-08	4.24E-08
		170	170	170	1.13E-10	1.15E-10	1.07E-10	4.32E-08	4.44E-08	4.05E-08
		180	180	180	1.15E-10	1.18E-10	1.09E-10	4.14E-08	4.34E-08	3.88E-08
		190	190	190	1.14E-10	1.18E-10	1.11E-10	3.89E-08	4.10E-08	3.77E-08
		200	200	200	1.17E-10	1.20E-10	1.21E-10	3.80E-08	3.95E-08	3.88E-08
		210	210	210	1.18E-10	1.16E-10	1.17E-10	3.66E-08	3.66E-08	3.59E-08
		220	220	220	2.40E-09	2.51E-09	2.76E-09	7.08E-07	7.52E-07	8.07E-07
		225	225	225	2.50E-09	2.61E-09	2.82E-09	7.20E-07	7.66E-07	8.05E-07
		230	230	230	2.54E-09	2.90E-09	2.87E-09	7.17E-07	8.31E-07	8.02E-07
	235	235	235	2.54E-09	3.21E-09	2.91E-09	7.02E-07	9.00E-07	7.97E-07	
240	240	240	2.65E-09	3.33E-09	3.06E-09	7.17E-07	9.15E-07	8.19E-07		
245	245	245	2.65E-09	3.45E-09	3.13E-09	7.03E-07	9.29E-07	8.22E-07		
250	250	250	2.75E-09	3.49E-09	3.25E-09	7.14E-07	9.21E-07	8.36E-07		
255	255	255	2.91E-09	3.59E-09	3.38E-09	7.40E-07	9.27E-07	8.53E-07		
260	260	260	3.05E-09	3.71E-09	3.64E-09	7.61E-07	9.41E-07	9.00E-07		

Table G3 The raw data of the determination of linear regime of P3TAA

Sample	Thickness (cm)	Applied voltage (V)			Mesuered Current (A)			Conductivity (S/cm)		
		1	2	3	1	2	3	1	2	3
Pth_U	1) 0.03937	5.0	5.0	10.0	1.44E-10	1.36E-10	1.37E-10	3.03E-06	2.56E-06	2.30E-06
	2) 0.04388	10.0	10.0	20.0	1.47E-10	1.39E-10	1.39E-10	1.54E-06	1.31E-06	1.17E-06
	3) 0.02466	15.0	15.0	30.0	1.50E-10	1.43E-10	1.42E-10	1.05E-06	8.99E-07	7.94E-07
		20.0	20.0	40.0	1.52E-10	1.45E-10	1.46E-10	7.98E-07	6.83E-07	6.12E-07
		25.0	25.0	50.0	1.54E-10	1.48E-10	1.48E-10	6.47E-07	5.58E-07	4.96E-07
		30.0	30.0	60.0	1.55E-10	1.51E-10	1.50E-10	5.43E-07	4.74E-07	4.19E-07
		35.0	35.0	70.0	1.57E-10	1.53E-10	1.52E-10	4.71E-07	4.12E-07	3.64E-07
		40.0	40.0	80.0	1.59E-10	1.54E-10	1.54E-10	4.18E-07	3.63E-07	3.23E-07
		45.0	45.0	90.0	1.61E-10	1.58E-10	1.54E-10	3.76E-07	3.31E-07	2.87E-07
		50.0	50.0	100.0	1.64E-10	1.60E-10	1.58E-10	3.45E-07	3.02E-07	2.65E-07
		55.0	55.0	110.0	1.66E-10	1.61E-10	1.61E-10	3.17E-07	2.76E-07	2.45E-07
		60.0	60.0	120.0	1.67E-10	1.62E-10	1.61E-10	2.92E-07	2.54E-07	2.25E-07
		65.0	65.0	130.0	1.70E-10	1.64E-10	2.09E-09	2.75E-07	2.38E-07	2.70E-06
		70.0	70.0	135.0	1.71E-10	2.21E-09	2.27E-09	2.57E-07	2.98E-06	2.82E-06
		75.0	75.0	140.0	2.13E-09	2.43E-09	2.35E-09	2.98E-06	3.05E-06	2.82E-06
		80.0	80.0	145.0	2.28E-09	2.61E-09	2.48E-09	2.99E-06	3.07E-06	2.87E-06
		85.0	85.0	150.0	2.45E-09	2.79E-09	2.59E-09	3.03E-06	3.09E-06	2.90E-06
90.0	90.0	155.0	2.59E-09	2.98E-09	2.62E-09	3.02E-06	3.12E-06	2.83E-06		
100.0	100.0	160.0	2.90E-09	3.38E-09	2.70E-09	3.05E-06	3.19E-06	2.83E-06		
Pth_1:1	1) 0.02995	0.045	0.045	0.045	6.63E-10	4.06E-10	2.80E-10	2.03E-03	1.25E-03	8.71E-04
	2) 0.02981	0.050	0.050	0.050	6.98E-10	4.65E-10	3.53E-10	1.93E-03	1.29E-03	9.89E-04
	3) 0.02954	0.055	0.055	0.055	8.05E-10	5.76E-10	4.46E-10	2.02E-03	1.45E-03	1.13E-03
		0.060	0.060	0.060	8.14E-10	6.82E-10	5.19E-10	1.87E-03	1.58E-03	1.21E-03
		0.065	0.065	0.065	8.60E-10	6.93E-10	6.09E-10	1.83E-03	1.48E-03	1.31E-03
		0.070	0.070	0.070	9.52E-10	7.48E-10	7.02E-10	1.88E-03	1.48E-03	1.40E-03
		0.075	0.075	0.075	1.04E-09	7.39E-10	6.79E-10	1.92E-03	1.37E-03	1.27E-03
		0.080	0.080	0.080	1.13E-09	8.18E-10	7.09E-10	1.96E-03	1.42E-03	1.24E-03
		0.085	0.085	0.085	1.23E-09	9.40E-10	7.72E-10	1.99E-03	1.53E-03	1.27E-03
		0.090	0.090	0.090	1.29E-09	9.95E-10	8.09E-10	1.98E-03	1.53E-03	1.26E-03
		0.095	0.095	0.095	1.34E-09	1.07E-09	8.83E-10	1.94E-03	1.56E-03	1.30E-03
		0.100	0.100	0.100	1.34E-09	1.10E-09	9.51E-10	1.85E-03	1.53E-03	1.33E-03
		0.105	0.105	0.105	1.41E-09	1.16E-09	9.72E-10	1.86E-03	1.53E-03	1.30E-03

Table G3 (cont.)

Sample	Thickness (cm)	Applied voltage (V)			Mesuered Current (A)			Conductivity (S/cm)		
		1	2	3	1	2	3	1	2	3
Pth_10:1	1) 0.02455	0.001	0.001	0.001	4.42E-10	3.87E-10	4.46E-10	7.44E-02	6.72E-02	8.14E-02
	2) 0.02383	0.005	0.005	0.005	4.56E-10	4.25E-10	4.71E-10	1.54E-02	1.48E-02	1.72E-02
	3) 0.02264	0.010	0.010	0.010	5.14E-10	4.80E-10	4.69E-10	8.66E-03	8.33E-03	8.57E-03
		0.015	0.015	0.015	5.42E-10	4.79E-10	4.76E-10	6.08E-03	5.54E-03	5.79E-03
		0.020	0.020	0.020	5.61E-10	5.29E-10	4.95E-10	4.72E-03	4.59E-03	4.52E-03
		0.025	0.025	0.025	2.13E-09	5.34E-10	5.34E-10	1.43E-02	3.70E-03	3.91E-03
		0.030	0.030	0.030	2.28E-09	2.06E-09	6.79E-10	1.28E-02	1.19E-02	4.13E-03
		0.035	0.035	0.035	2.41E-09	2.20E-09	2.15E-09	1.16E-02	1.09E-02	1.12E-02
		0.040	0.040	0.040	2.46E-09	2.28E-09	2.20E-09	1.04E-02	9.87E-03	1.01E-02
		0.045	0.045	0.045	2.58E-09	2.39E-09	2.31E-09	9.67E-03	9.21E-03	9.37E-03
		0.050	0.050	0.050	2.62E-09	2.44E-09	2.34E-09	8.83E-03	8.47E-03	8.57E-03
		0.055	0.055	0.055	2.76E-09	2.56E-09	2.46E-09	8.46E-03	8.08E-03	8.19E-03
		0.060	0.060	0.060	2.89E-09	2.70E-09	2.58E-09	8.10E-03	7.80E-03	7.85E-03
		0.065	0.065	0.065	2.95E-09	2.74E-09	2.63E-09	7.65E-03	7.33E-03	7.38E-03
		0.070	0.070	0.070	3.08E-09	2.87E-09	2.73E-09	7.40E-03	7.11E-03	7.12E-03
		0.075	0.075	0.075	3.15E-09	2.93E-09	2.79E-09	7.07E-03	6.78E-03	6.79E-03
		0.080	0.080	0.080	3.27E-09	3.05E-09	2.88E-09	6.89E-03	6.62E-03	6.58E-03
		0.085	0.085	0.085	3.41E-09	3.16E-09	2.99E-09	6.76E-03	6.46E-03	6.44E-03
		0.090	0.090	0.090	3.47E-09	3.21E-09	3.07E-09	6.49E-03	6.19E-03	6.22E-03
		0.095	0.095	0.095	3.58E-09	3.35E-09	3.16E-09	6.35E-03	6.11E-03	6.08E-03
		0.100	0.100	0.100	3.67E-09	3.37E-09	3.19E-09	6.19E-03	5.84E-03	5.83E-03
		0.110	0.110	0.110	3.93E-09	3.63E-09	3.43E-09	6.03E-03	5.73E-03	5.70E-03
		0.120	0.120	0.120	4.10E-09	3.85E-09	3.60E-09	5.76E-03	5.57E-03	5.48E-03
		0.130	0.130	0.130	4.27E-09	4.04E-09	3.74E-09	5.53E-03	5.39E-03	5.26E-03
		0.140	0.140	0.140	4.45E-09	4.20E-09	3.89E-09	5.36E-03	5.21E-03	5.07E-03
		0.150	0.150	0.150	4.62E-09	4.37E-09	4.06E-09	5.18E-03	5.06E-03	4.94E-03
		0.200	0.200	0.200	5.67E-09	5.38E-09	4.96E-09	4.78E-03	4.67E-03	4.53E-03
		0.250	0.250	0.250	6.72E-09	6.38E-09	5.82E-09	4.53E-03	4.43E-03	4.25E-03
		0.300	0.300	0.300	7.85E-09	7.36E-09	6.68E-09	4.41E-03	4.26E-03	4.07E-03
		0.350	0.350	0.350	8.97E-09	8.35E-09	7.56E-09	4.32E-03	4.14E-03	3.95E-03
	0.400	0.400	0.400	1.00E-08	9.31E-09	8.47E-09	4.22E-03	4.04E-03	3.87E-03	
	0.450	0.450	0.450	1.11E-08	1.03E-08	9.32E-09	4.15E-03	3.97E-03	3.78E-03	
	0.500	0.500	0.500	1.22E-08	1.13E-08	1.02E-08	4.09E-03	3.92E-03	3.73E-03	
	0.550	0.550	0.550	1.32E-08	1.22E-08	1.11E-08	4.05E-03	3.86E-03	3.68E-03	
	0.600	0.600	0.600	1.43E-08	1.32E-08	1.20E-08	4.01E-03	3.82E-03	3.64E-03	
	0.650	0.650	0.650	1.54E-08	1.42E-08	1.28E-08	3.98E-03	3.79E-03	3.61E-03	
	0.700	0.700	0.700	1.65E-08	1.52E-08	1.37E-08	3.96E-03	3.76E-03	3.57E-03	
	0.750	0.750	0.750	1.75E-08	1.61E-08	1.46E-08	3.93E-03	3.73E-03	3.55E-03	
	0.800	0.800	0.800	1.86E-08	1.71E-08	1.55E-08	3.92E-03	3.72E-03	3.54E-03	
	0.850	0.850	0.850	1.97E-08	1.81E-08	1.64E-08	3.91E-03	3.69E-03	3.51E-03	
	0.900	0.900	0.900	2.09E-08	1.90E-08	1.72E-08	3.91E-03	3.67E-03	3.50E-03	
	0.950	0.950	0.950	2.19E-08	2.00E-08	1.81E-08	3.89E-03	3.65E-03	3.49E-03	
	1.000	1.000	1.000	2.30E-08	2.09E-08	1.91E-08	3.88E-03	3.63E-03	3.48E-03	
	1.050	1.050	1.050	2.41E-08	2.20E-08	2.00E-08	3.86E-03	3.64E-03	3.47E-03	

Pth_10:1		1.100	1.100	1.100	2.54E-08	2.30E-08	2.08E-08	3.89E-03	3.63E-03	3.45E-03
		1.150	1.150	1.150	2.63E-08	2.40E-08	2.16E-08	3.85E-03	3.62E-03	3.44E-03
		1.200	1.200	1.200	2.75E-08	2.53E-08	2.25E-08	3.87E-03	3.65E-03	3.43E-03
		1.250	1.250	1.250	2.86E-08	2.61E-08	2.35E-08	3.85E-03	3.63E-03	3.43E-03
		1.300	1.300	1.300	2.98E-08	2.70E-08	2.44E-08	3.86E-03	3.61E-03	3.42E-03
		1.350	1.350	1.350	3.08E-08	2.79E-08	2.56E-08	3.85E-03	3.59E-03	3.46E-03
		1.400	1.400	1.400	3.18E-08	2.88E-08	2.63E-08	3.82E-03	3.57E-03	3.44E-03
		1.450	1.450	1.450	3.29E-08	2.98E-08	2.71E-08	3.83E-03	3.57E-03	3.41E-03
		1.500	1.500	1.500	3.41E-08	3.09E-08	2.81E-08	3.83E-03	3.57E-03	3.42E-03
Pth_200:1	1) 0.04876	0.001	0.001	0.001	4.64E-08	2.29E-08	1.97E-08	3.9353	2.6391	1.8926
	2) 0.03581	0.005	0.005	0.005	4.63E-08	2.40E-08	2.13E-08	0.7862	0.5543	0.4094
	3) 0.04304	0.010	0.010	0.010	5.12E-08	2.89E-08	2.75E-08	0.4342	0.3343	0.2638
		0.015	0.015	0.015	5.24E-08	3.12E-08	3.05E-08	0.2964	0.2403	0.1956
		0.020	0.020	0.020	5.50E-08	3.41E-08	3.21E-08	0.2333	0.1967	0.1543
		0.025	0.025	0.025	5.91E-08	3.72E-08	3.30E-08	0.2003	0.1719	0.1270
		0.030	0.030	0.030	6.51E-08	4.28E-08	3.79E-08	0.1841	0.1646	0.1215
		0.035	0.035	0.035	6.95E-08	4.77E-08	4.40E-08	0.1683	0.1575	0.1208
		0.040	0.040	0.040	7.21E-08	5.01E-08	4.74E-08	0.1529	0.1446	0.1140
		0.045	0.045	0.045	7.82E-08	5.52E-08	5.25E-08	0.1473	0.1416	0.1120
		0.050	0.050	0.050	8.23E-08	5.80E-08	5.50E-08	0.1396	0.1340	0.1058
		0.055	0.055	0.055	9.00E-08	6.34E-08	6.02E-08	0.1388	0.1331	0.1051
		0.060	0.060	0.060	9.77E-08	6.83E-08	6.62E-08	0.1380	0.1314	0.1060
		0.065	0.065	0.065	1.01E-07	7.10E-08	6.89E-08	0.1319	0.1261	0.1019
		0.070	0.070	0.070	1.09E-07	7.65E-08	7.51E-08	0.1322	0.1262	0.1031
		0.075	0.075	0.075	1.12E-07	7.89E-08	7.85E-08	0.1262	0.1215	0.1005
		0.080	0.080	0.080	1.20E-07	8.52E-08	8.47E-08	0.1275	0.1230	0.1018
		0.085	0.085	0.085	1.29E-07	9.07E-08	9.03E-08	0.1289	0.1232	0.1021
		0.090	0.090	0.090	1.34E-07	9.36E-08	9.31E-08	0.1260	0.1202	0.0994
		0.095	0.095	0.095	1.41E-07	9.96E-08	9.80E-08	0.1262	0.1210	0.0991
		0.100	0.100	0.100	1.47E-07	1.03E-07	1.01E-07	0.1245	0.1188	0.0967
		0.105	0.105	0.105	1.55E-07	1.09E-07	1.06E-07	0.1248	0.1198	0.0966
		0.110	0.110	0.110	1.62E-07	1.15E-07	1.11E-07	0.1247	0.1208	0.0974
		0.115	0.115	0.115	1.66E-07	1.18E-07	1.13E-07	0.1226	0.1187	0.0947
		0.120	0.120	0.120	1.74E-07	1.24E-07	1.18E-07	0.1227	0.1193	0.0947
	0.125	0.125	0.125	1.79E-07	1.27E-07	1.21E-07	0.1217	0.1174	0.0932	
	0.130	0.130	0.130	1.87E-07	1.33E-07	1.27E-07	0.1223	0.1181	0.0942	
0.135	0.135	0.135	1.96E-07	1.39E-07	1.34E-07	0.1231	0.1187	0.0950		
0.140	0.140	0.140	2.00E-07	1.42E-07	1.38E-07	0.1214	0.1169	0.0945		
0.145	0.145	0.145	2.08E-07	1.48E-07	1.46E-07	0.1218	0.1177	0.0965		
0.150	0.150	0.150	2.14E-07	1.53E-07	1.57E-07	0.1208	0.1178	0.1008		

Appendix H The Differential Scanning Calorimeter Thermogram of Undoped and P3TAA, Crosslinked Polyisoprene (PI_03) and Polythiophene/Polyisoprene Blends (Pth_U/PI_03)

A Mettler-Toledo DSC822 differential scanning calorimeter (DSC) was used to record the nonisothermal exotherms as well as the subsequent melting endotherms for crosslinked polyisoprene (PI_03), undoped polythiophene (Pth_U), and polythiophene/polyisoprene blends (Pth_U/PI_03). Calibration for the temperature scale was carried out with a pure indium standard ($T_m^\circ = 156.6^\circ\text{C}$ and $\Delta H_f^\circ = 28.5 \text{ J.g}^{-1}$) on every other run to ensure accuracy and reliability of the data obtained. To minimize thermal lag between the polymer sample and the DSC furnace, each sample holder was loaded with a disc-shaped sample weighing around $8.0 \pm 0.5 \text{ mg}$. Each sample was used only once, and all the runs were carried out under nitrogen atmosphere to prevent extensive thermal degradation.

The experiments started with heating PI_03 from -60°C to 200°C , Pth_U from 25°C to 300°C , and 20Pth_U/PI_03 from -60°C to 300°C at a rate of $10^\circ\text{C}/\text{min}$. These experiments allow one to obtain values for the glass transition temperature (T_g) and side chain degradation temperature (T_d) of polythiophene at 70°C and 160°C (Hu *et al.*, 2000). It is also observed the exotherm at $150\text{-}170^\circ\text{C}$ corresponding to crosslink reaction of polyisoprene (Faez *et al.*, 1999). For 20Pth_U/PI_03 blends sample, it shows the temperature located between those of the pure component. The results clearly suggest that these components (PI_03 and Pth_U) are immiscible blends and do not have interaction together.

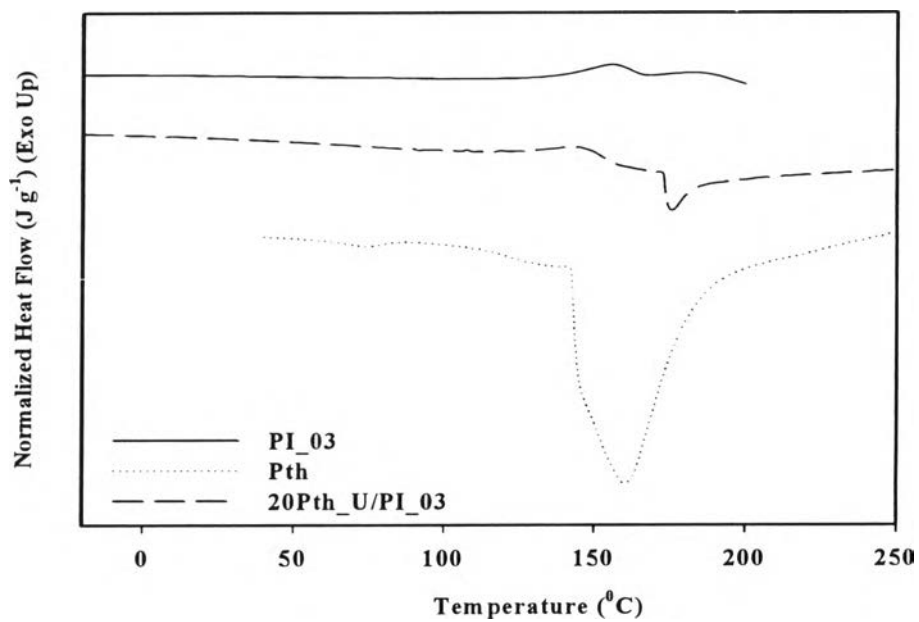


Figure H1 The DSC thermograms of crosslinked polyisoprene (PI_03) undoped P3TAA with HClO₄.

Appendix I Scanning Electron Micrograph of Undoped P3TAA, Doped P3TAA and Polythiophene/polyisoprene Blends (Pth_U/PI_03)



Figure I1 The morphology of undoped poly(3-thiophene acetic acid) (P3TAA) powder at magnification of 1,500.



(a)



(b)



(c)

Figure I2 The morphology of doped PTAA powder with HClO_4 as various doping ratio at magnification of 1,500: a) 1:1; b) 10:1; and c) 200:1.

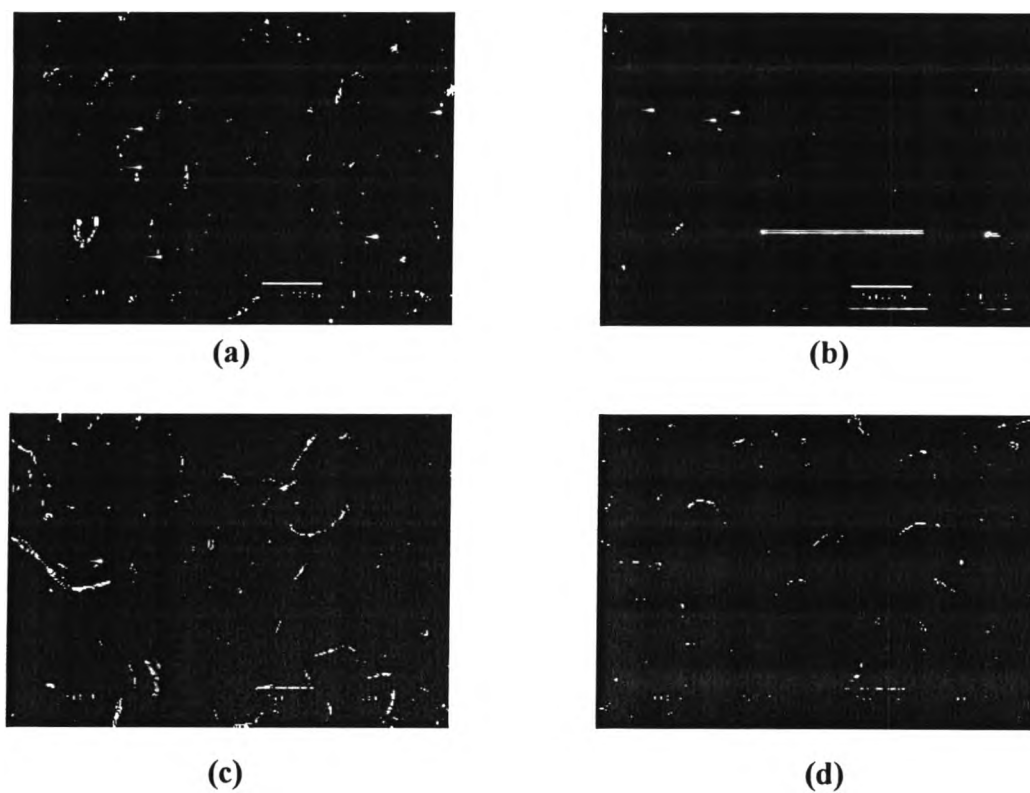


Figure 13 The morphology of polythiophene/polyisoprene blends as various polythiophene particle concentrations (%vol./vol.) at magnification of 350: a) 5%; b) 10%; c) 20%; and d) 30%.

Appendix J Determination of the Crosslink Density

The crosslink density can be determined by the measurement of M_c . We can determine M_c from knowing the swelling ability of certain solvents in a crosslinked network. A crosslinked polymer network cannot dissolve because the polymer chains are bound together and therefore cannot disentangle. It can, however, absorb a large quantity of a suitable liquid with which it is placed in contact. The driving force for swelling is the increase in entropy (the entropy of dilution) which occurs as polymer network chains spread apart and mix with solvent molecules. The mixing may be augmented ($\chi_1 < 0$) or diminished ($\chi_1 > 0$) by the heat of dilution. The thermodynamic treatment of a crosslinked polymer is based on the hypothesis that the mixing and elastic components of the free energy are additive and separable. The change in the Gibbs free energy which occurs during swelling can be divided between the ordinary free energy of mixing (ΔG_m) and the elastic free energy change (ΔG_{el}) which results from the expansion of the network as follows; $\Delta G = \Delta G_m + \Delta G_{el}$ (Horkey *et al.*, 2000).

From Flory-Huggins Theory; $\Delta G = kT(n_1 \ln v_1 + n_2 \ln v_2 + \chi n_1 v_2)$, where k is Boltzmann's constant, n_1 and n_2 are number of solvent and polymer molecules, respectively, v_1 and v_2 are volume fractions of solvent and polymer, respectively, and χ is polymer-solvent interaction parameter.

It should be noted that n_2 above is equal to zero ($n_2 = 0$) in this experiment due to the absence of individual polymer molecules. In other words, since all the chains are tied together in a network, there are no polymers floating around freely in the solution.

The expression for G_{el} can be derived from the statistical theory of rubber elasticity assuming $\Delta G_{el} = -T\Delta S$, i.e., no change in internal energy of the network structure occurs upon stretching.

$$G_{el} = \frac{kmT}{2}(3\alpha_s^2 - 3) = \frac{RnT}{2}(3\alpha_s^2 - 3) \quad (J.1)$$

m is number of effective chains in network, and α_δ is extension ratio for isotropic swelling.

The chemical potential of the solvent in the swollen gel is given by;

$$\mu_1 - \mu_1^\circ = N_A \left(\frac{\partial \Delta G_m}{\partial n_1} \right)_{T,P} = N_A \left(\frac{\partial \Delta G_{el}}{\partial \alpha_\delta} \right)_{T,P} \left(\frac{\partial \alpha_\delta}{\partial n_1} \right)_{T,P} \quad (J.2)$$

N_A is Avagadro's number, μ_1 is chemical potential of slovent in swollen gel, and μ_1° is chemical potential of neat soivent.

$$\alpha_\delta^3 = \frac{V}{V_0} = \frac{1}{V_2} = \frac{V_{solvent} + V_{polmer}}{V_{polymer}} + \frac{V_1 + V_2}{V_2} \quad (J.3)$$

$w_0/\rho_2 = V_0$ is volume of the non-swollen network = $V_1 + V_2$, and $V = V_{equil}$ is volume of swollen gel = V_2 .

The three partial derivatives in Equation (J.2) can be solved to yield the following (with m expressed as number of moles of network chains, or moles of chain segments between crosslinks).

$$\mu_1 - \mu_1^\circ = RT \left[\ln(1 - v_2) + v_2 + \chi_1 v_2^2 + v_1 \left(\frac{m}{v_0} \right) \left(v_2^{1/3} - \frac{v_2}{2} \right) \right] \quad (J.4)$$

v_1 is molar volume of solvent.

Equilibrium swelling is reached when

$$\mu_1 - \mu_1^\circ = 0 \quad (J.5)$$

and thus, from Equation (J.4) with $\mu_1 - \mu_1^\circ = 0$,

$$-\left[\ln(1 - v_{2m} + v_{2m} + \chi_1 v_{2m}^2) \right] = v_1 \left(\frac{m}{v_0} \right) \left(v_{2m}^{1/3} - \frac{v_{2m}}{2} \right) \quad (J.6)$$

and since $m/V_0 = \rho/M_c$, then:

$$-\left[\ln(1 - v_{2m} + v_{2m} + \chi_1 v_{2m}^2) \right] = v_1 \left(\frac{\rho}{M_c} \right) \left(v_{2m}^{1/3} - \frac{v_{2m}}{2} \right) \quad (J.7)$$

or

$$M_c = \frac{v_1 \rho_2 \left(v_{2m}^{1/3} - \frac{v_{2m}}{2} \right)}{- \left[\ln(1 - v_{2m}) + v_{2m} + \chi_1 v_{2m}^2 \right]} \quad (\text{J.8})$$

$$v_{2m} = \frac{w_0}{v_{equil} \times \rho_2} \quad (\text{J.9})$$

$$v_{equil} = \frac{w_0}{\rho_2} + \frac{w_s - w_0}{\rho_1} \quad (\text{J.10})$$

$$\chi = 0.34 + \frac{v_1}{RT} (\delta_1 - \delta_2)^2 \quad (\text{J.11})$$

and

$$\text{crosslink density} = [2M_c]^{-1} \quad (\text{J.12})$$

v_1 = the molar volume of solvent, $M_w/\text{density}$, ρ_2 = polymer density, polyisoprene $\approx 0.92 \text{ g/cm}^3$, ρ_1 = solvent density, toluene $\approx 0.867 \text{ g/cm}^3$, w_0 = original polymer weight, w_s = swollen polymer weight, χ = polymer-solvent interaction parameter, R = Gas constant, 8.29 N.m/mol.K , T = temperature, 298 K , δ_1 = solubility parameter of polymer, polyisoprene $\approx 17.02 \text{ (MPa)}^{1/2}$, δ_2 = solubility parameter of solvent, toluene $\approx 18.20 \text{ (MPa)}^{1/2}$.

Experiment

The procedure of the crosslink density measurement was as follows; initially the samples were cut to a dimension of $\approx 10 \times 10 \text{ mm}$, then weights of each specimen were then measured. Then we placed each specimen in a vial containing toluene for 3 days and the weight of the swollen sample was remeasured again. The crosslink density was calculated from the equations (J.8-J.12) (Painter *et al.*, 1997; Choi, 1999; Hokey *et al.*, 2000; Boochathum *et al.*, 2001). Experiments for each crosslinking ratio were carried out using three samples and data obtained were averaged. The crosslink densities of each specimen are listed in Table J1.

Table J1 Summary the crosslink density of pure polyisoprene

Systems	No.	M_c	Crosslink density (10⁻⁵ mol/cm³)
PI_02	1	13463	3.417
	2	11567	3.977
	3	12009	3.805
Average		12346	3.733
PI_03	1	6763	6.802
	2	7616	6.040
	3	8396	5.479
Average		7592	6.107
PI_05	1	4002	11.494
	2	4430	10.384
	3	4307	10.680
Average		4246	10.853
PI_07	1	3150	14.603
	2	2707	16.993
	3	3302	13.929
Average		3053	15.175

Appendix K Electrorheological Properties Measurement of Pure Polyisoprene at Various Degree of Crosslinking

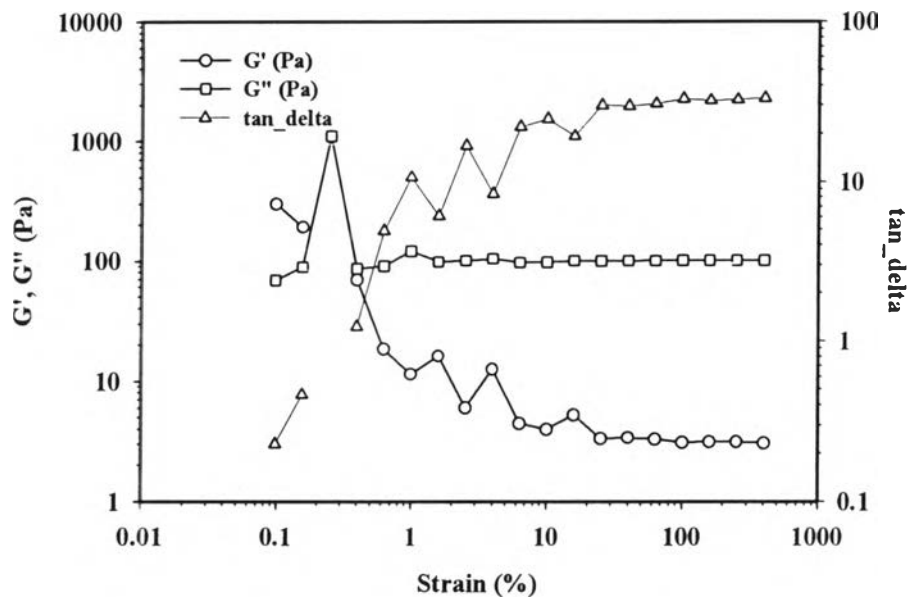
The electrorheological properties of pure polyisoprene at various degrees of crosslinking were measured by the melt rheometer (Rheometric Scientific, ARES) under oscillatory shear mode and applied electric field strength varying from 0 to 2 kV/mm. In these experiments, the dynamic moduli (G' and G'') were measured as functions of frequency and electric field strength. Strain sweep tests were first carried out to determine the suitable strain to measure G' and G'' in the linear viscoelastic regime as showed in Table K1.

Table K1 Summary of the linear viscoelastic regime of pure polyisoprene at various crosslinking ratios

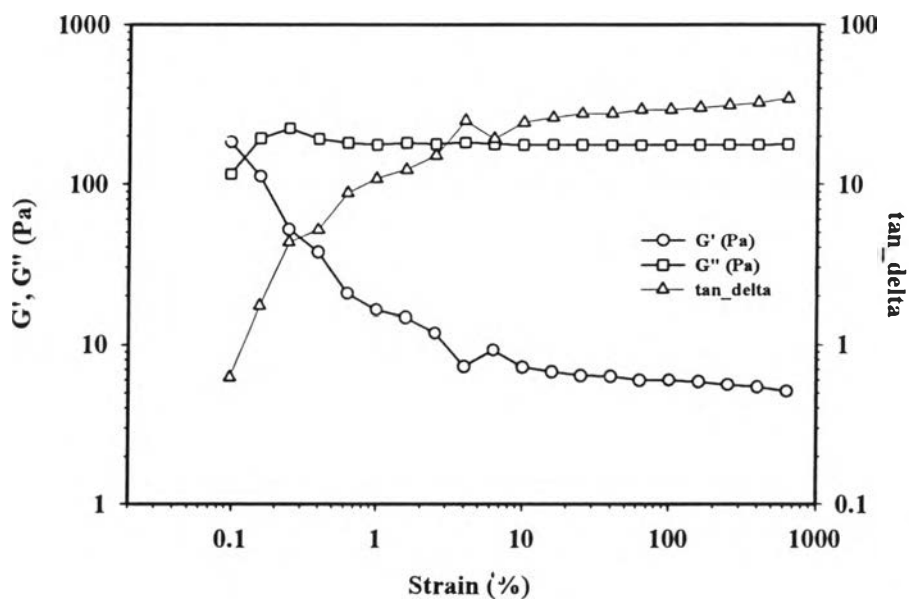
Systems	Crosslinking ratio (N_{DCP}/N_{PI})	Linear Viscoelastic Range (% Strain)
PI 00	0	220
PI 02	2	1
PI 03	3	1
PI 05	5	1
PI 07	7	1

Table K2 Induction time and recovery time of pure polyisoprene systems and polythiophene/polyisoprene blends

Samples	Electric field (kV/mm)	Induction time (τ_{ind})(s)	Recovery time (τ_{rec}) (s)	$\Delta G'_{ind}$	$\Delta G'_{rec}$
PI_03	1	107	76	195	188
	2	75	83	110	106
PI_05	2	73	74	202	175
PI_07	2	78	64	851	821
Pth_U20/PI_03	1	157	59	2257	35
	2	121	66	4794	80

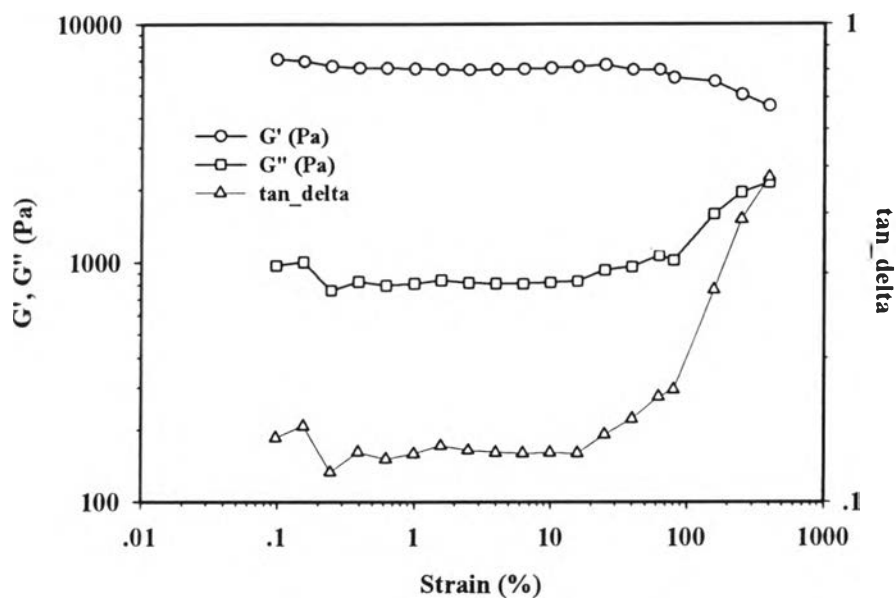


(a)

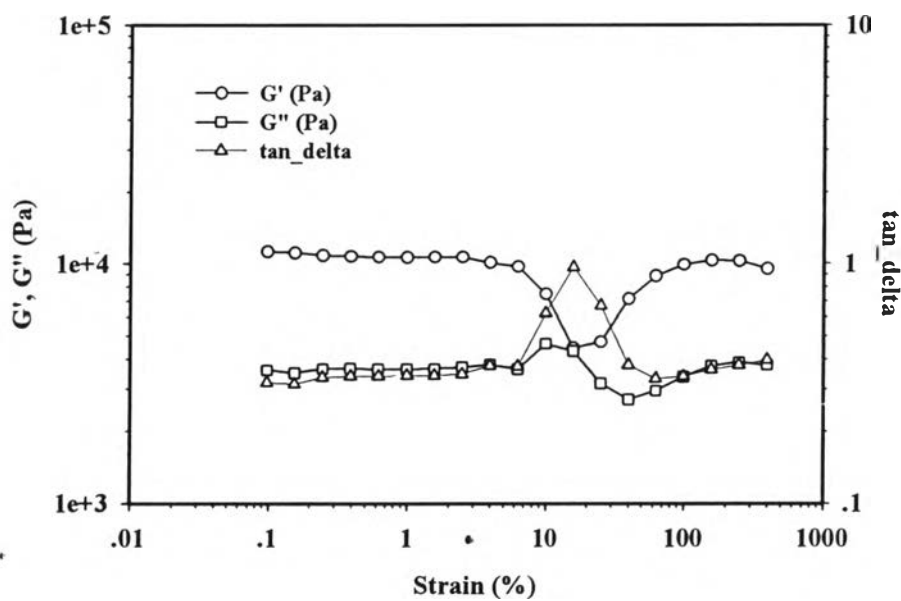


(b)

Figure K1 Strain sweep tests of pure polyisoprene fluid (PI_00), frequency 1.0 rad/s, 27°C, gap 0.500 mm: a) E 0 V/mm ; b) E 2 kV/mm.

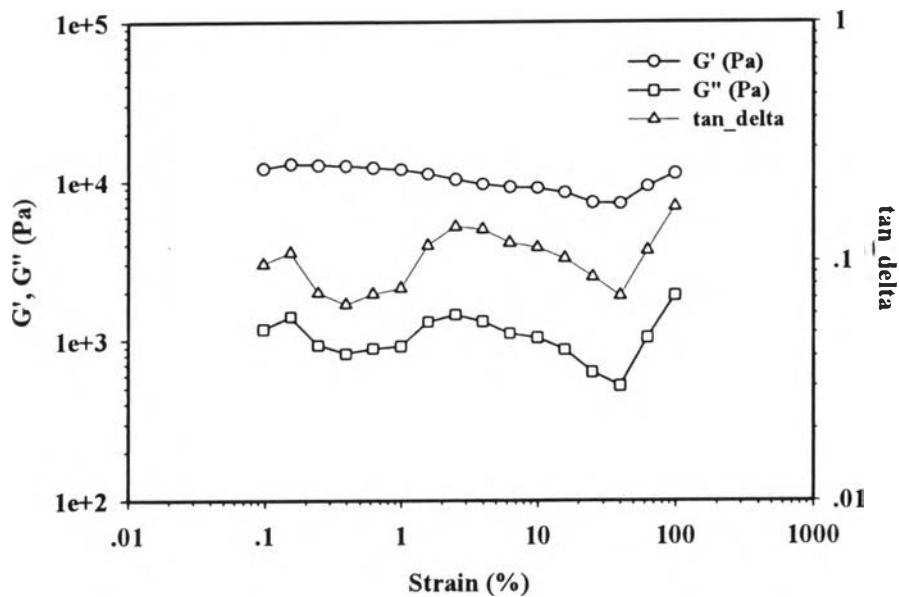


(a)

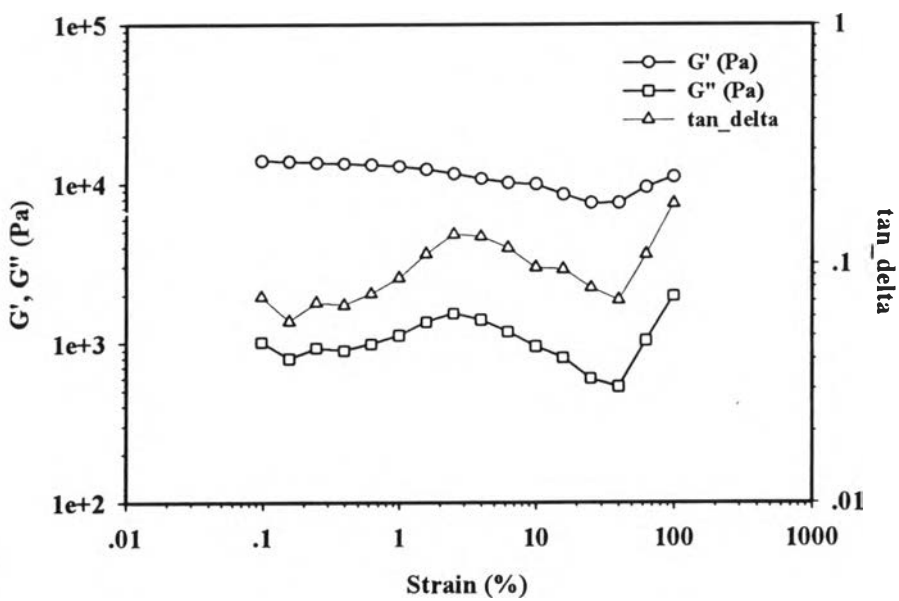


(b)

Figure K2 Strain sweep tests of pure polyisoprene with crosslinking ratio of 2 (PI₀₂), frequency 1.0 rad/s, 27°C, gap 0.870 mm: a) E 0 V/mm; b) E 2 kV/mm.

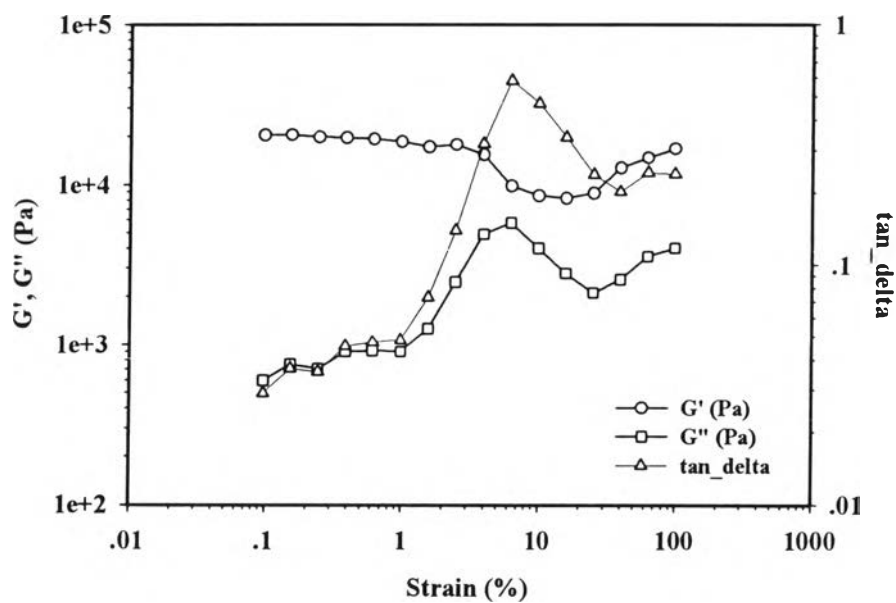


(a)

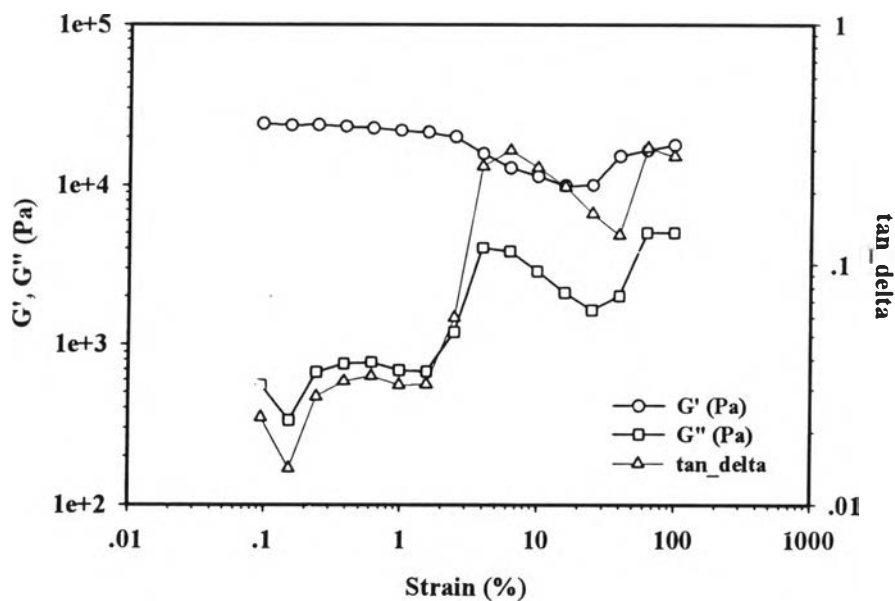


(b)

Figure K3 Strain sweep tests of pure polyisoprene with crosslinking ratio of 3 (PI_03), frequency 1.0 rad/s, 27°C, gap 0.930 mm: a) E 0 V/mm; b) E 2 kV/mm.

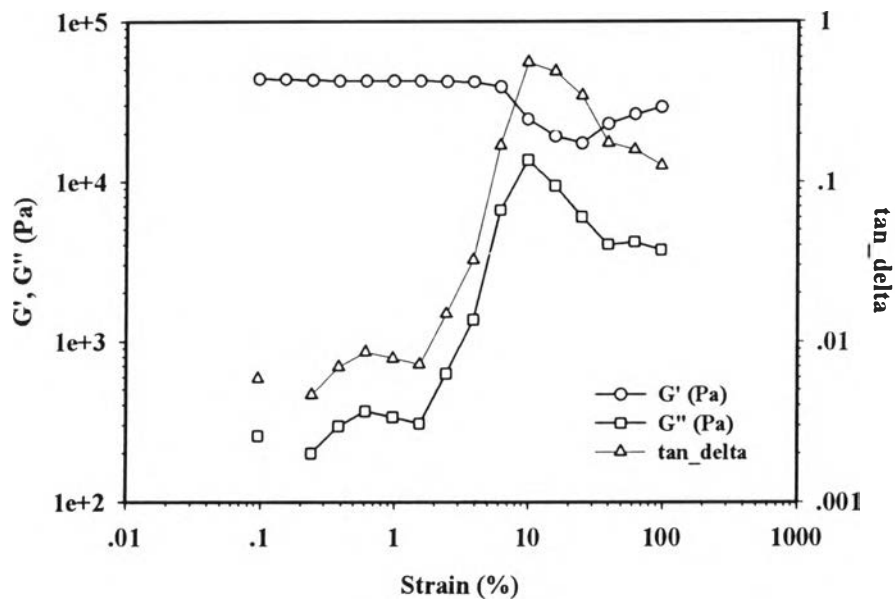


(a)

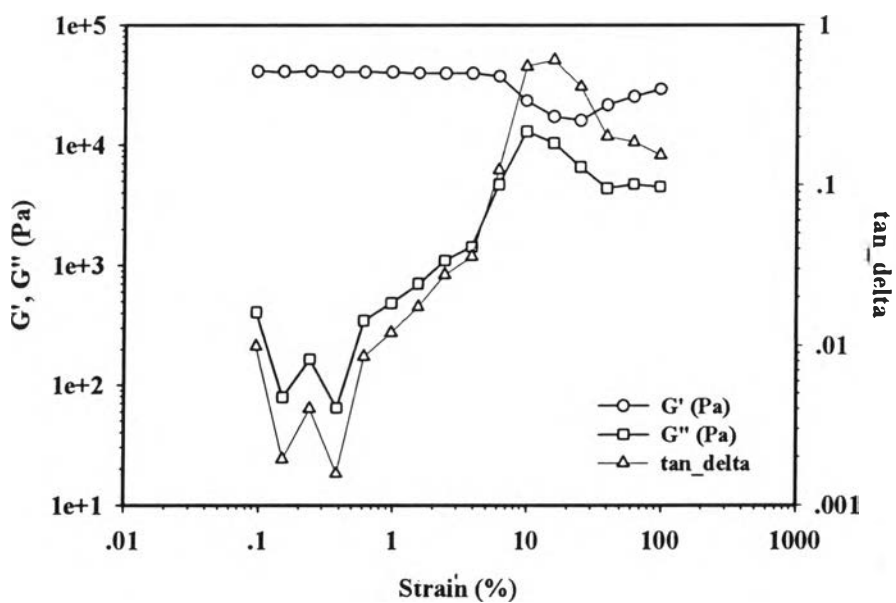


(b)

Figure K4 Strain sweep tests of pure polyisoprene with crosslinking ratio of 5 (PI_05), frequency 1.0 rad/s, 27°C, gap 0.930 mm: a) E 0 V/mm; b) E 2 kV/mm.

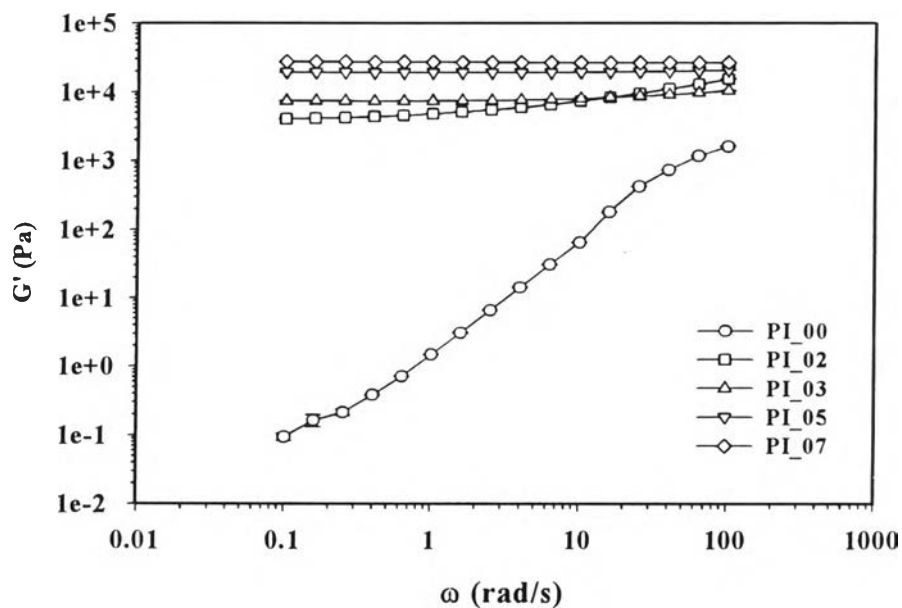


(a)

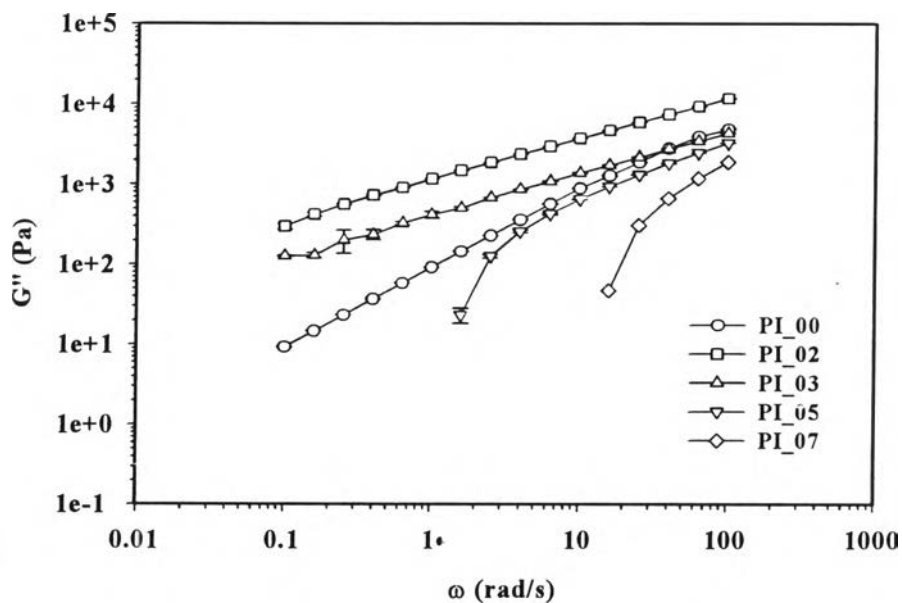


(b)

Figure K5 Strain sweep tests of pure polyisoprene with crosslinking ratio of 7 (PI_07), frequency 1.0 rad/s, 27°C, gap 0.940 mm: a) E 0 V/mm; b) E 2 kV/mm.

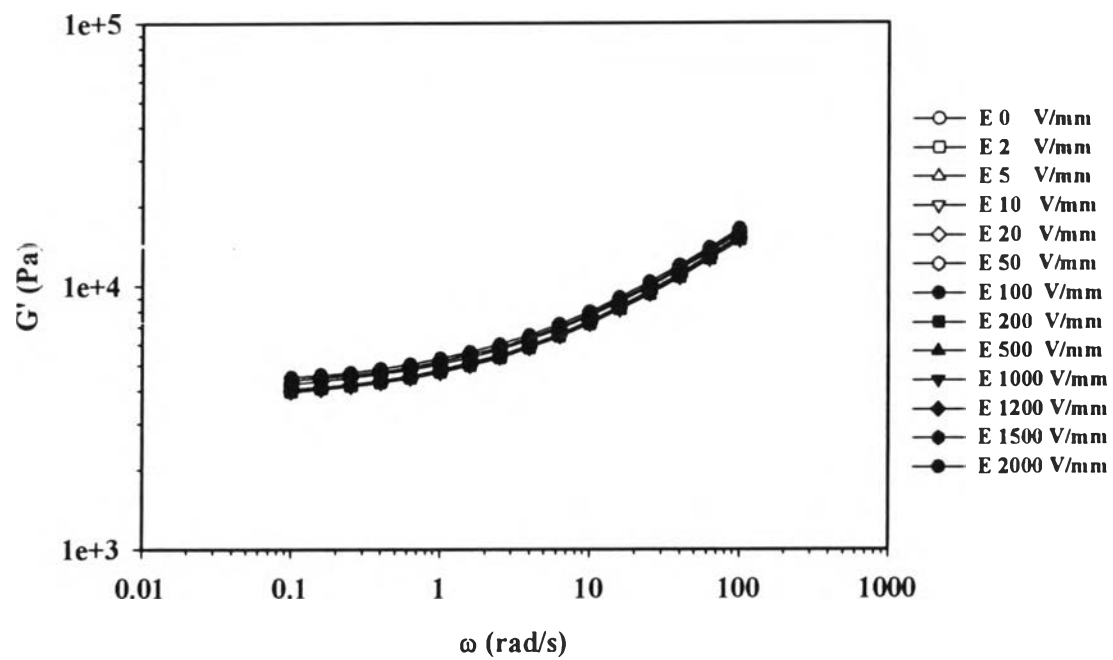


(a)

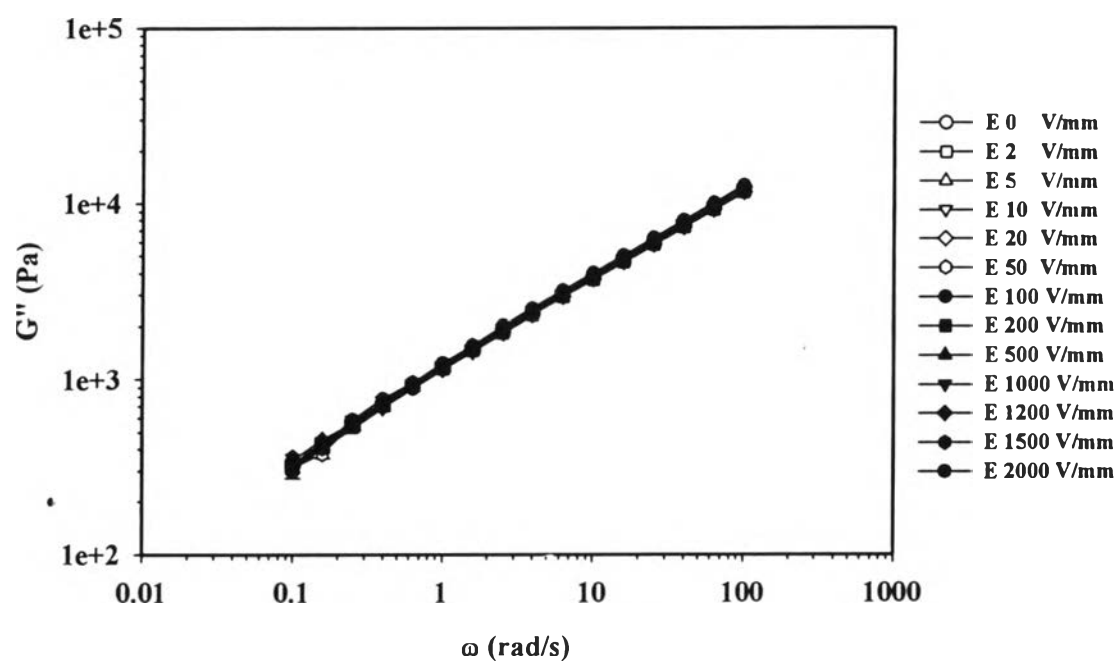


(b)

Figure K6 Storage and loss moduli of Polyisoprene at various crosslinking ratios, strain 1%, (PI_00 system, strain 220%), 27°C, electric field strength 0 V/mm: (a) the storage modulus, G' ; (b) the loss modulus, G'' .

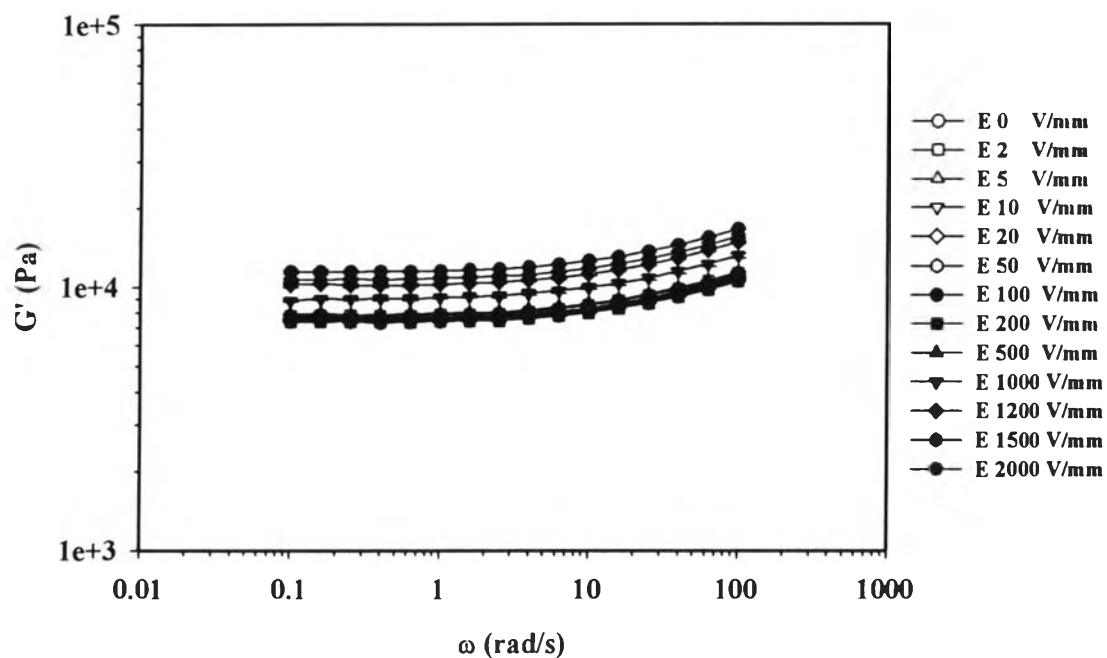


(a)

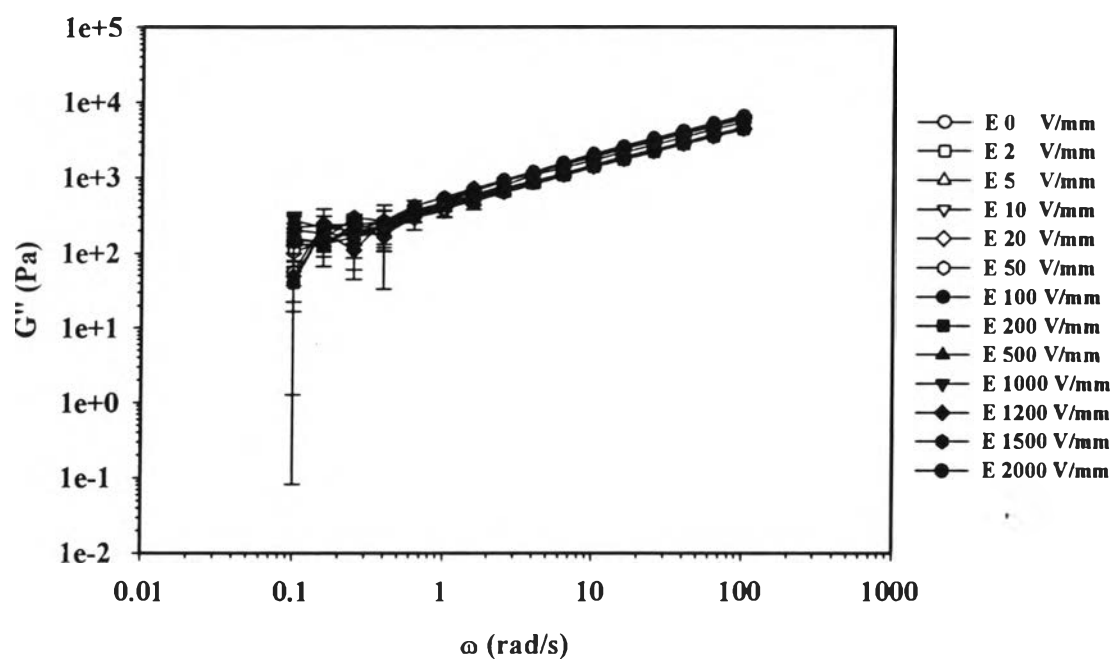


(b)

Figure K7 Frequency sweep tests of pure polyisoprene with crosslinking ratio of 2 (PI_02), strain 1.0%, 27°C, gap 0.895 mm, various electric field strengths: a) G' ; b) G'' .

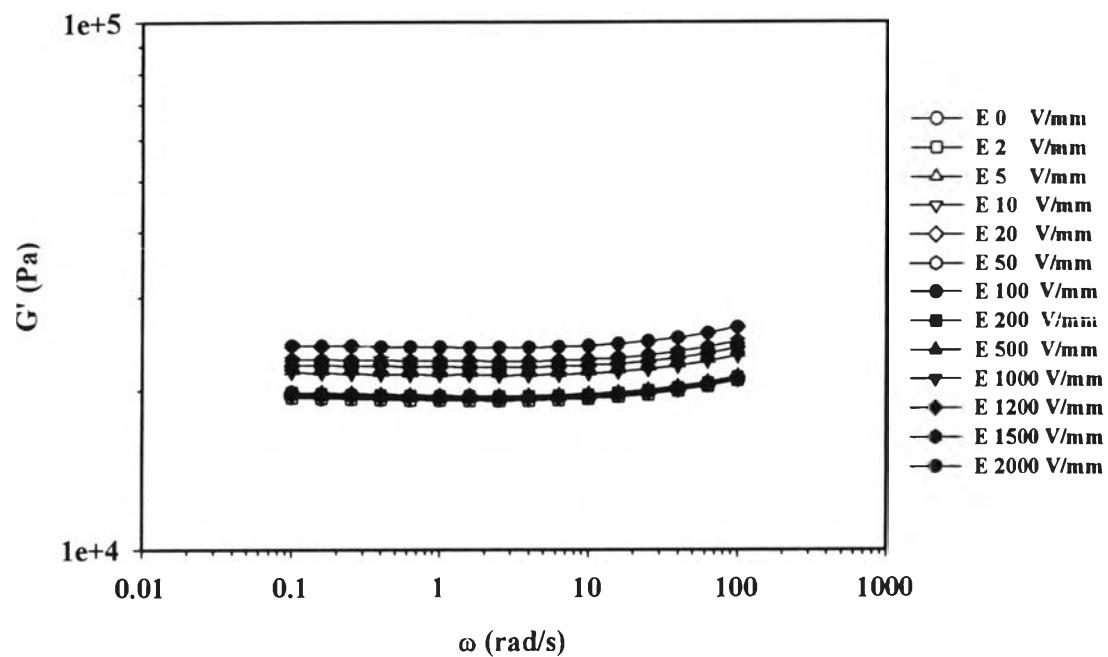


(a)

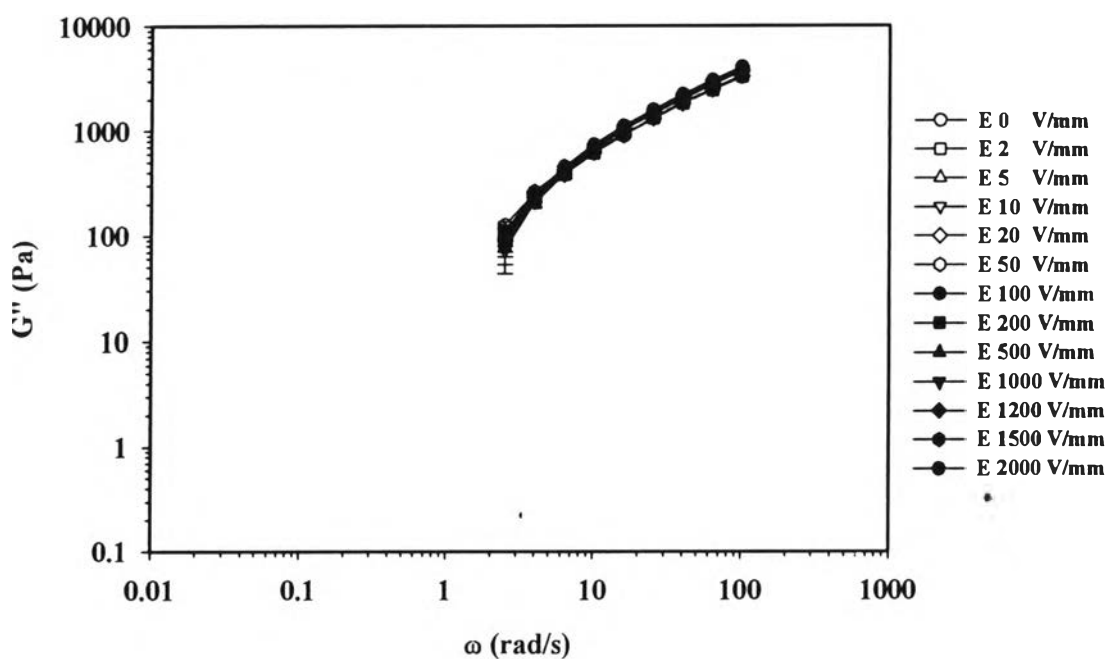


(b)

Figure K8 Frequency sweep tests of pure polyisoprene with crosslinking ratio of 3 (PI_03), strain 1.0%, 27°C, gap 0.894 mm, various electric field strength: a) G' ; b) G'' .

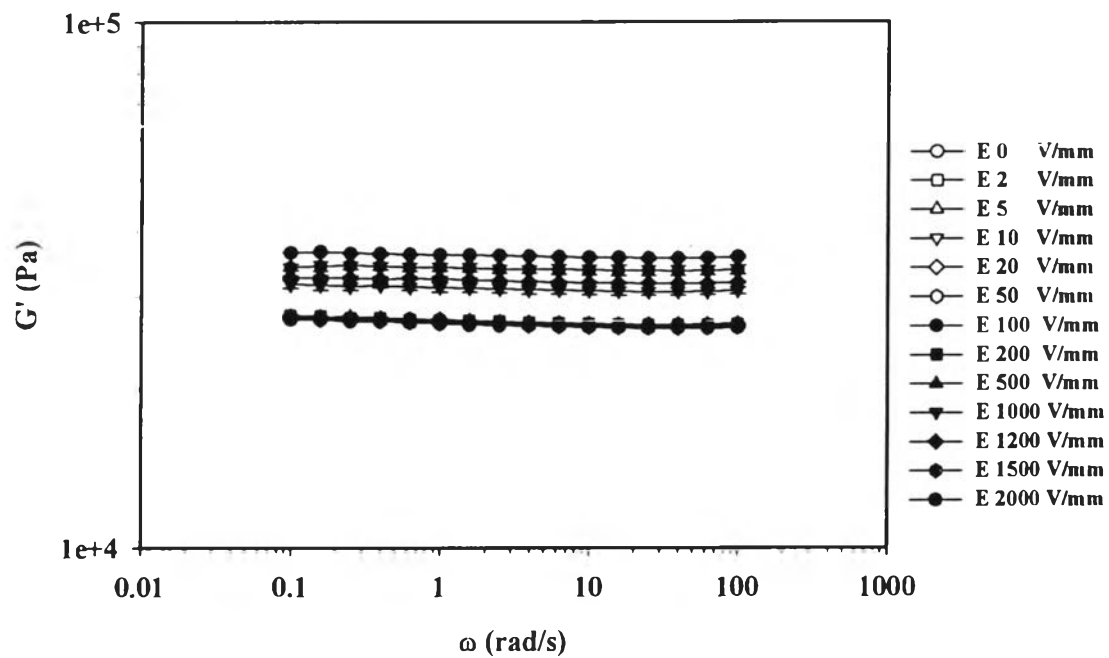


(a)

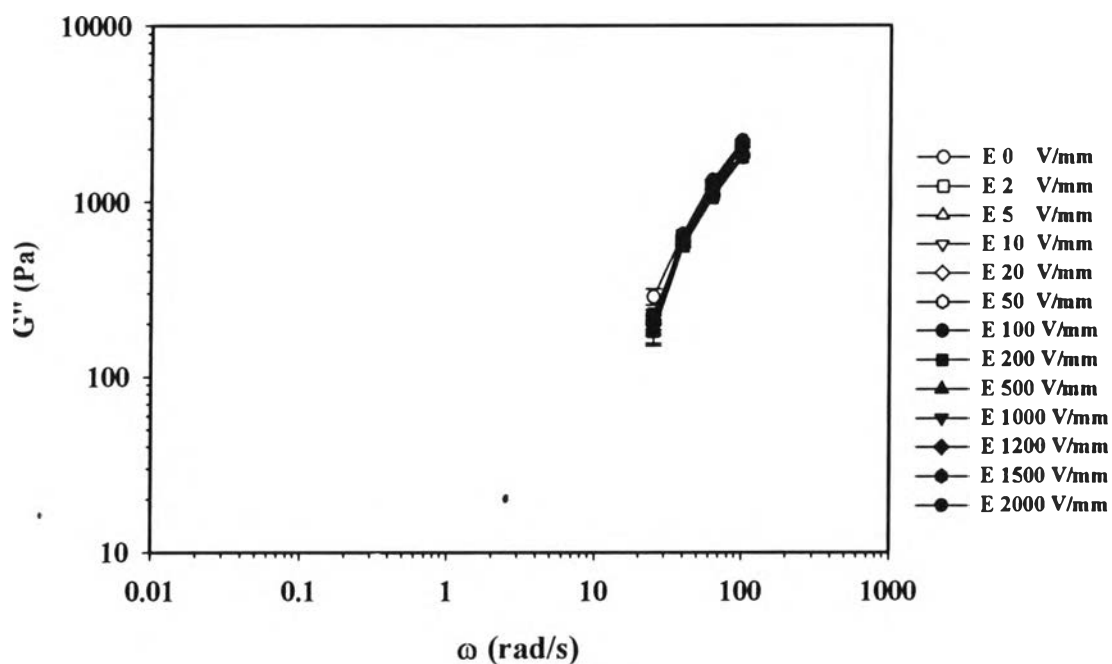


(b)

Figure K9 Frequency sweep tests of pure polyisoprene with crosslinking ratio of 5 (PI_05), strain 1.0%, 27°C, gap 0.917 mm, various electric field strength: a) G' ; b) G'' .

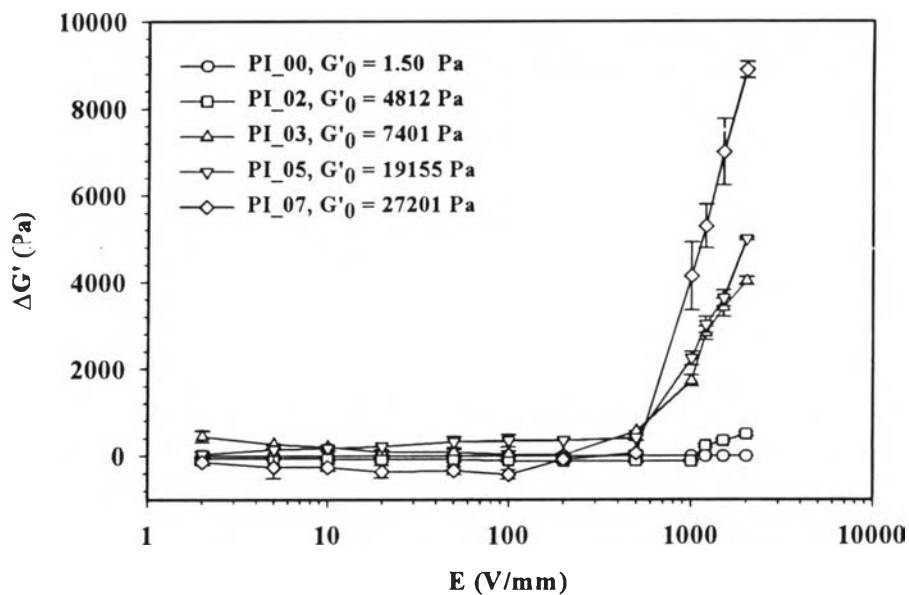


(a)

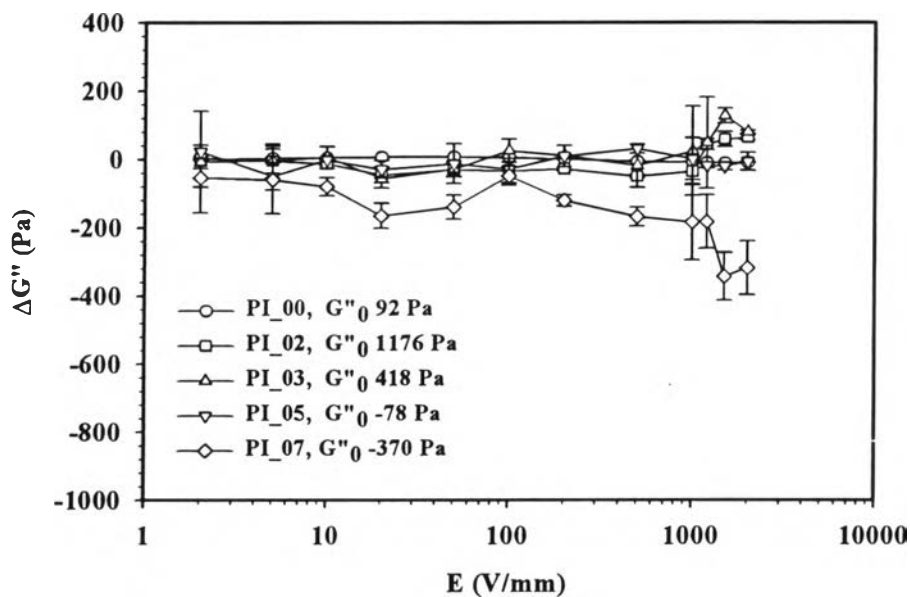


(b)

Figure K10 Frequency sweep tests of pure polyisoprene with crosslinking ratio of 7 (PI_07), strain 1.0%, 27°C, gap 0.895 mm, various electric field strengths: a) G' ; b) G'' .

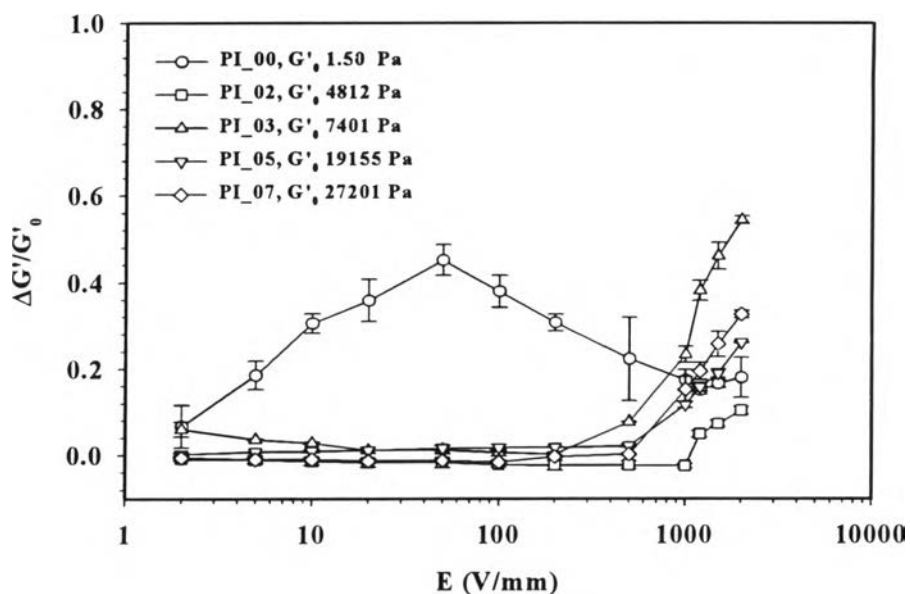


(a)

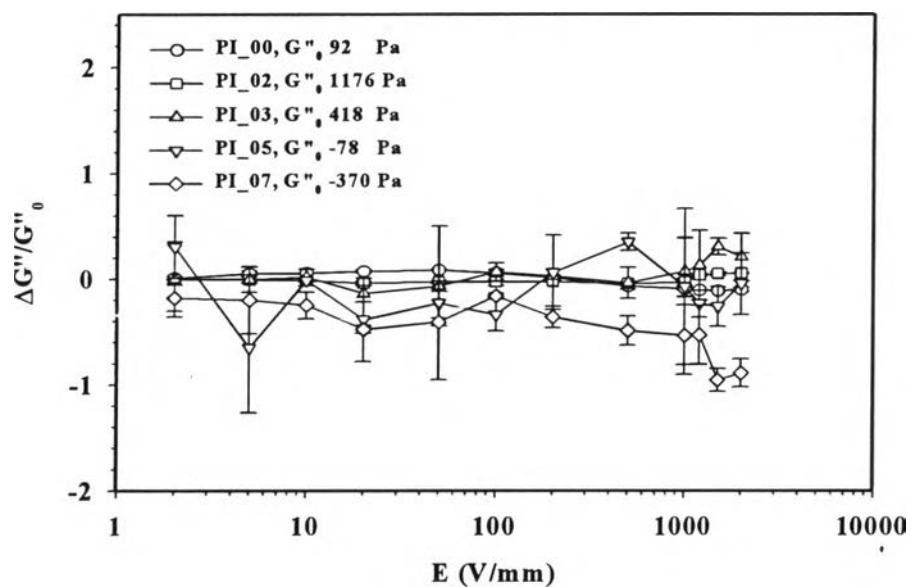


(b)

Figure K11 Responses of the storage and the loss moduli ($\Delta G'(\omega)$ and $\Delta G''(\omega)$) of the polyisoprenes at various crosslinking ratios vs. electric field strength, frequency 1.0 rad/s, strain 1%, (PI_00 system, strain 220%) at 27°C: (a) $\Delta G'(\omega)$; (b) $\Delta G''(\omega)$.

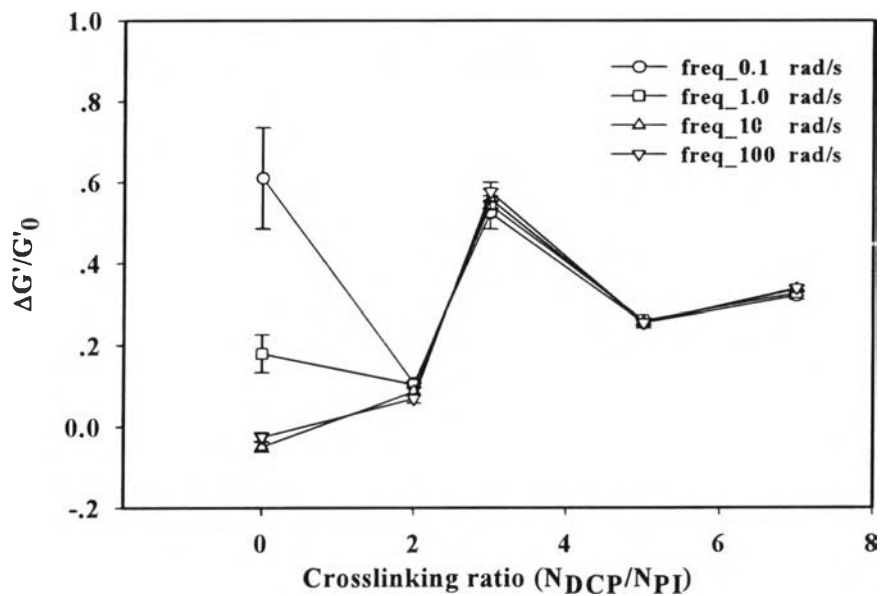


(a)

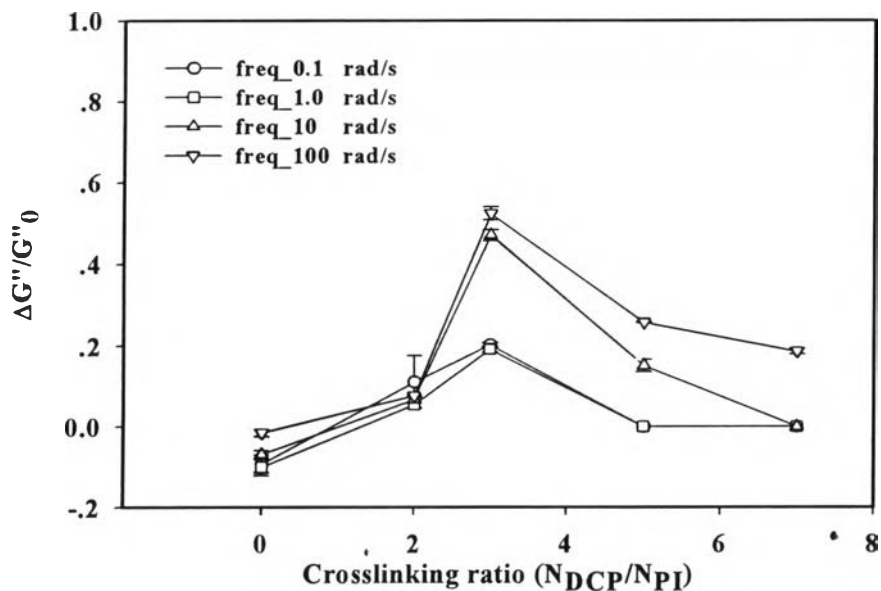


(b)

Figure K12 Sensitivity of the storage and loss moduli of the polyisoprenes at various crosslinking ratios vs. electric field strength, frequency 1.0 rad/s, strain 1%, (PI_00 system, strain 220%) at 27°C: (a) $\Delta G'/G'_0(\omega)$; (b) $\Delta G''/G''_0(\omega)$.



(a)



(b)

Figure K13 Sensitivity of the polyisoprenes as functions of various crosslinking ratios, 27°C, various frequencies, electric field strength 2 kV/mm: (a) $\Delta G'/G'_0$; (b) $\Delta G''/G''_0$.

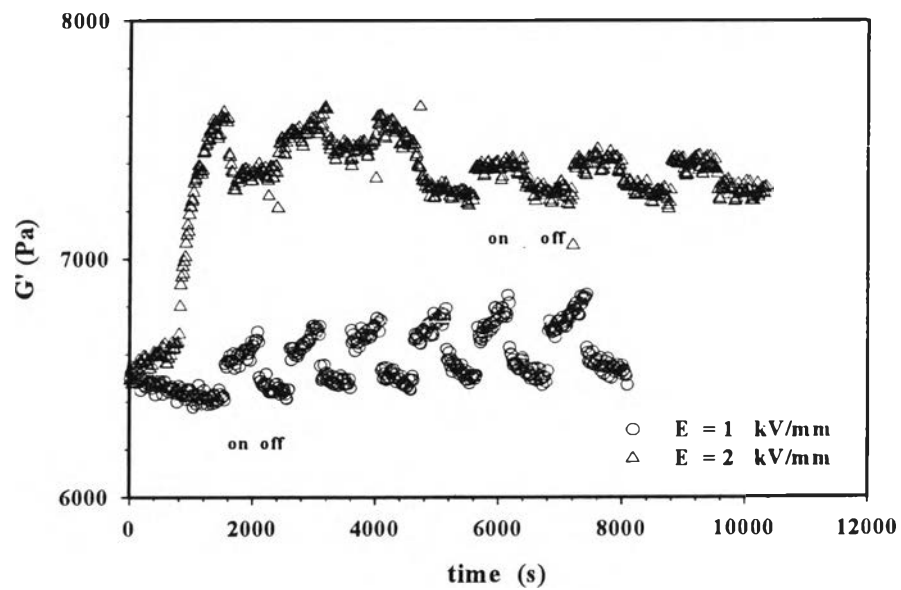


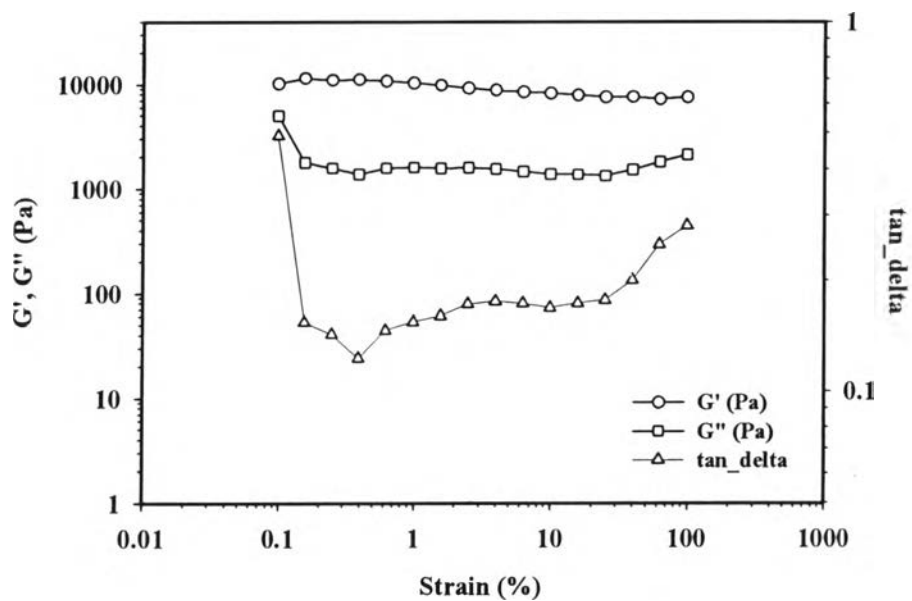
Figure K14 Temporal response of storage modulus (G') of PI_03 system at various electric field strengths (1 and 2 kV/mm).

Appendix L Electrorheological Properties Measurement of Polythiophene/ Polyisoprene Blends at various Polythiophene Particles Concentrations

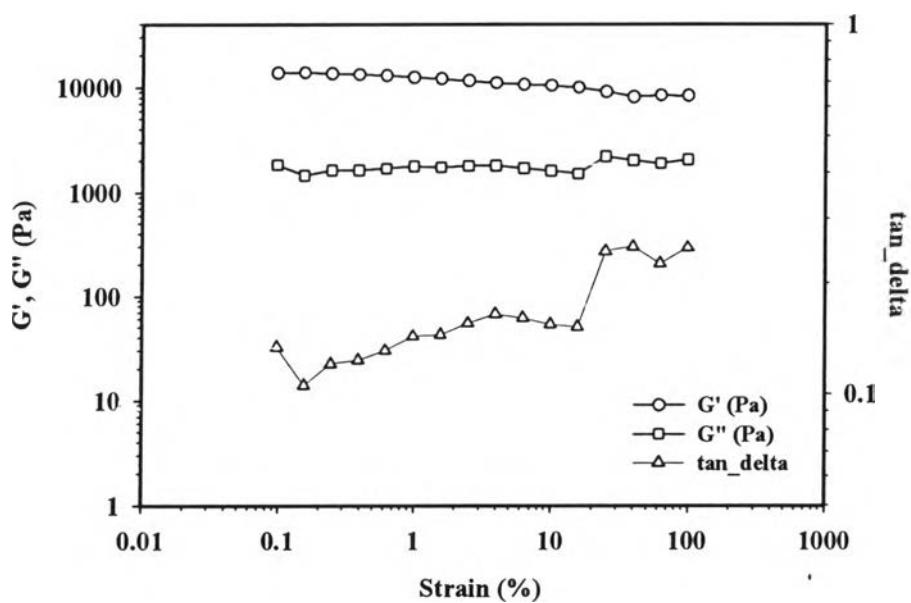
The electrorheological properties of polythiophene/polyisoprene blends at various polythiophene particle concentrations were measured by the melt rheometer (Rheometric Scientific, ARES) under oscillatory shear mode and applied electric field strength varying from 0 to 2 kV/mm. In these experiments, the dynamic moduli (G' and G'') were measured as functions of frequency and electric field strength. Strain sweep tests were first carried out to determine the suitable strain to measure G' and G'' in the linear viscoelastic regime as showed in Table L1.

Table L1 Summary the linear viscoelastic regime of polythiophene/polyisoprene blends at various polythiophene particle concentrations

Systems	Particles concentration (vol.%)	Linear Viscoelastic Range (% Strain)
PI 03	0	1
Pth U5/PI 03	5	1
Pth U10/PI 03	10	1
Pth U20/PI 03	20	1
Pth U30/PI 03	30	1

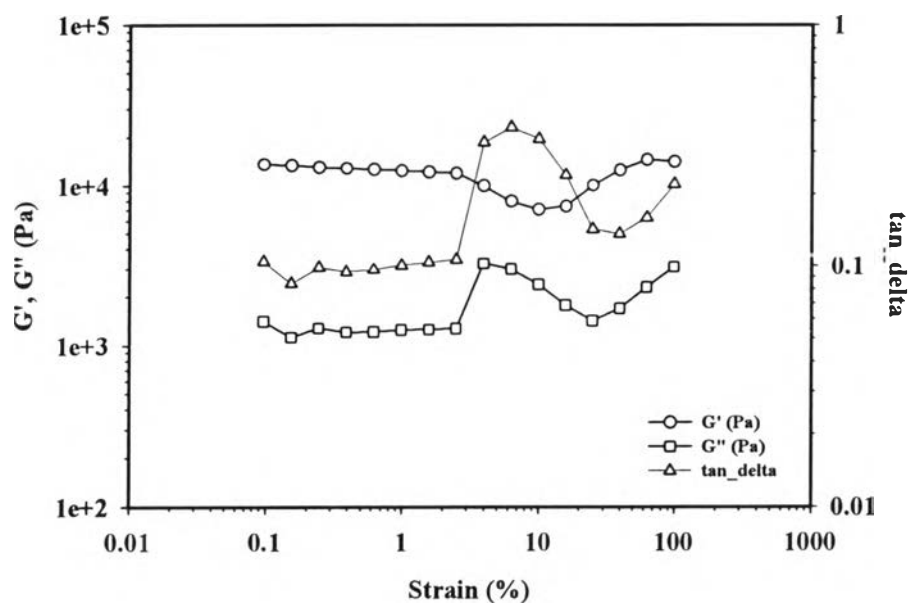


(a)

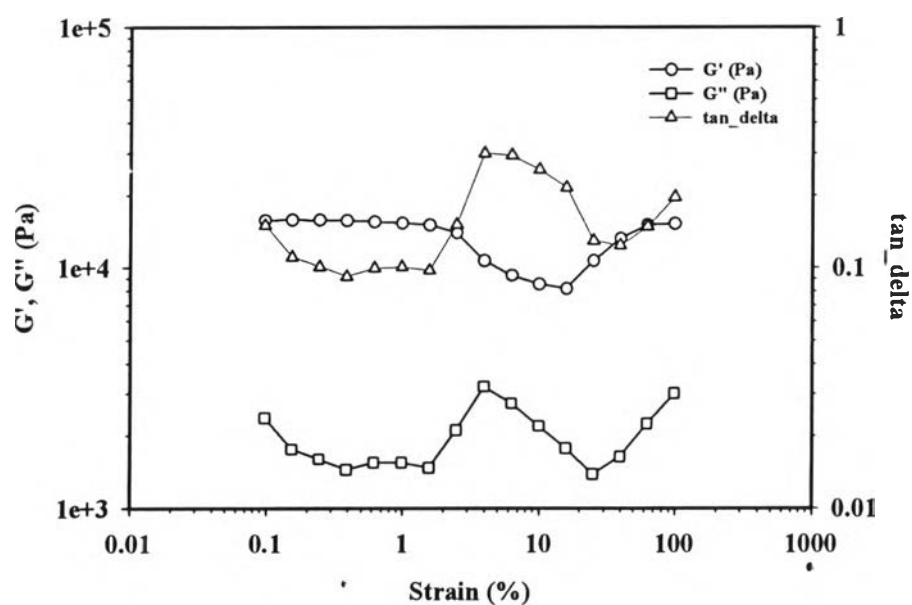


(b)

Figure L1 Strain sweep tests of polythiophene/polyisoprene blends with particle concentration of 5 vol.% (Pth_U5/PI_03), frequency 1.0 rad/s, 27°C, gap 0.900 mm: a) E 0 V/mm; b) E 2 kV/mm.

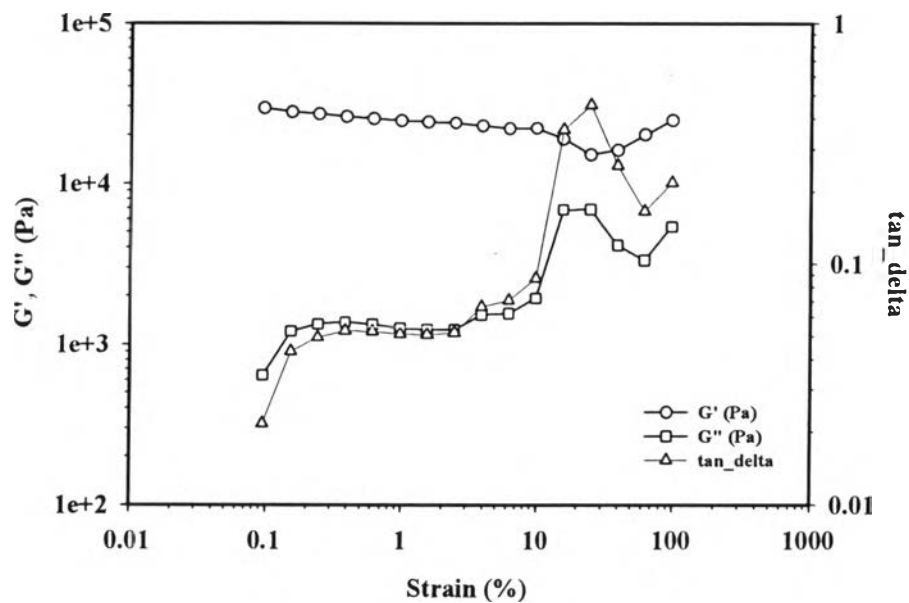


(a)

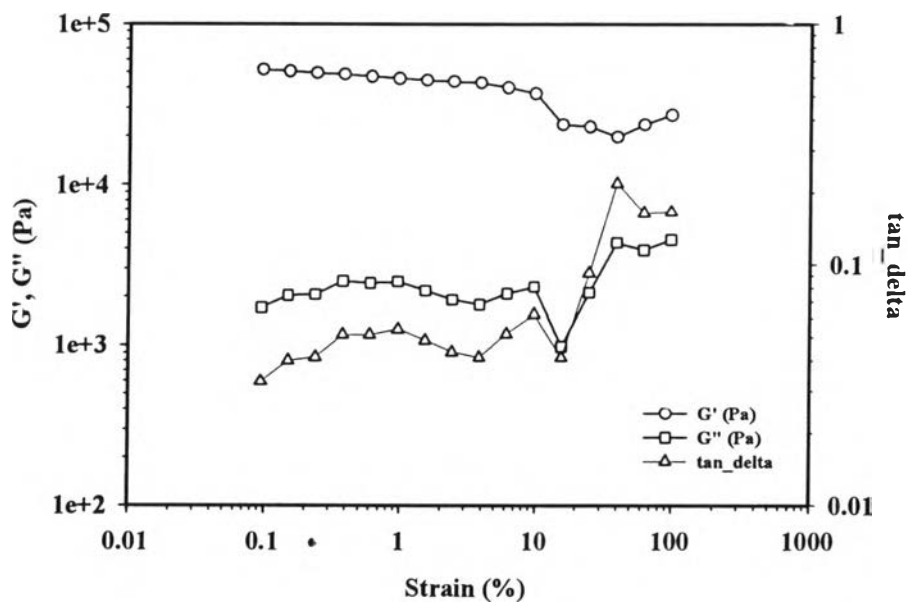


(b)

Figure L2 Strain sweep tests of polythiophene/polyisoprene blends with particle concentration of 10 vol.% (Pth_U10/PI_03), frequency 1.0 rad/s, 27°C, gap 0.870 mm: a) E 0 V/mm; b) E 2 kV/mm.

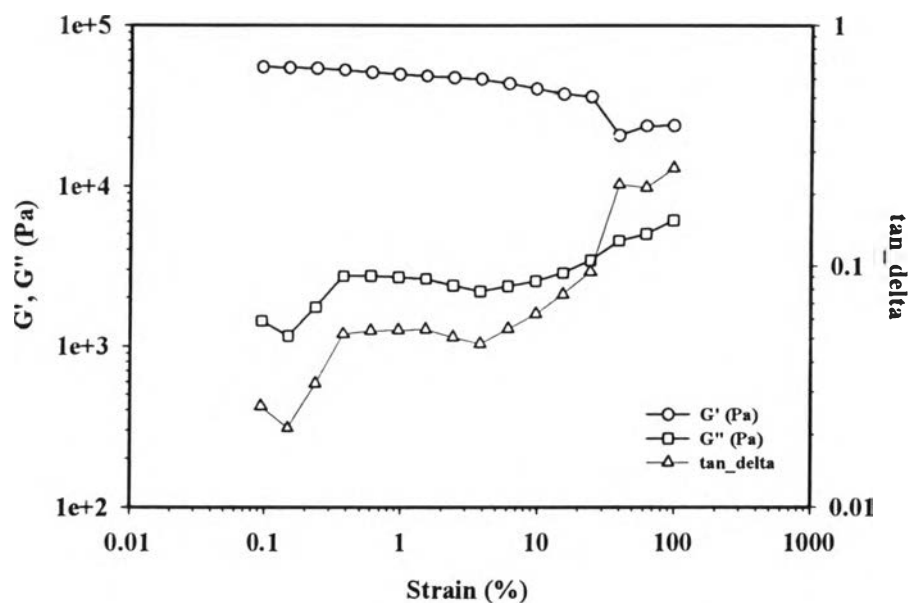


(a)

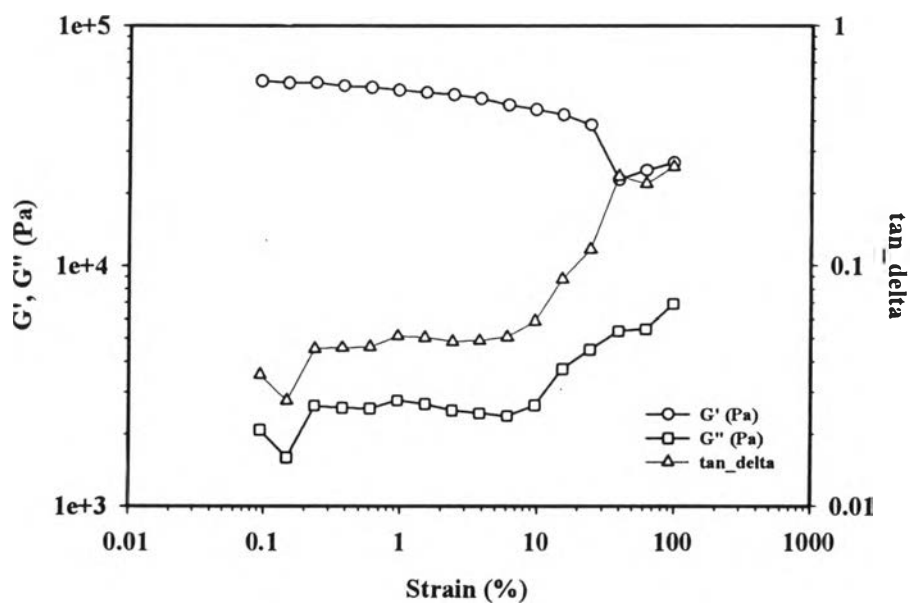


(b)

Figure L3 Strain sweep tests of polythiophene/polyisoprene blends with particle concentration of 20 vol.% (Pth_U20/PI_03), frequency 1.0 rad/s, 27°C, gap 0.960 mm: a) E 0 V/mm; b) E 2 kV/mm.

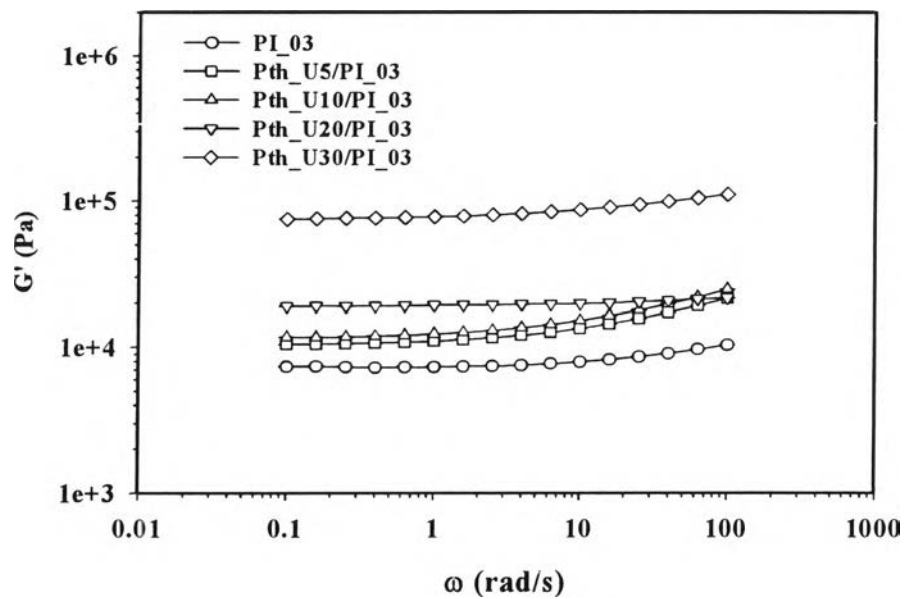


(a)

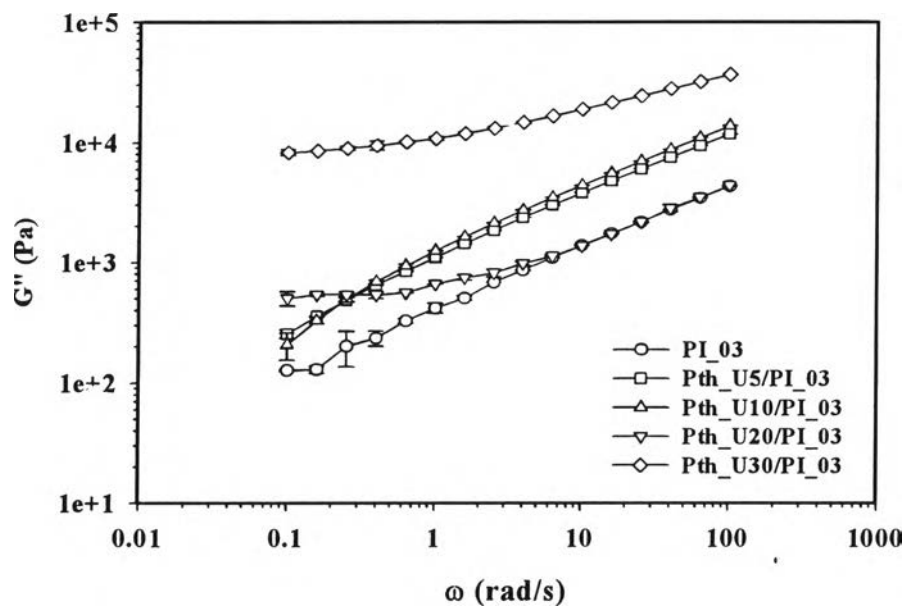


(b)

Figure L4 Strain sweep tests of polythiophene/polyisoprene blends with particle concentration of 30 vol.% (Pth_U30/PI_03), frequency 1.0 rad/s, 27°C, gap 0.960 mm: a) E 0 V/mm; b) E 2 kV/mm.

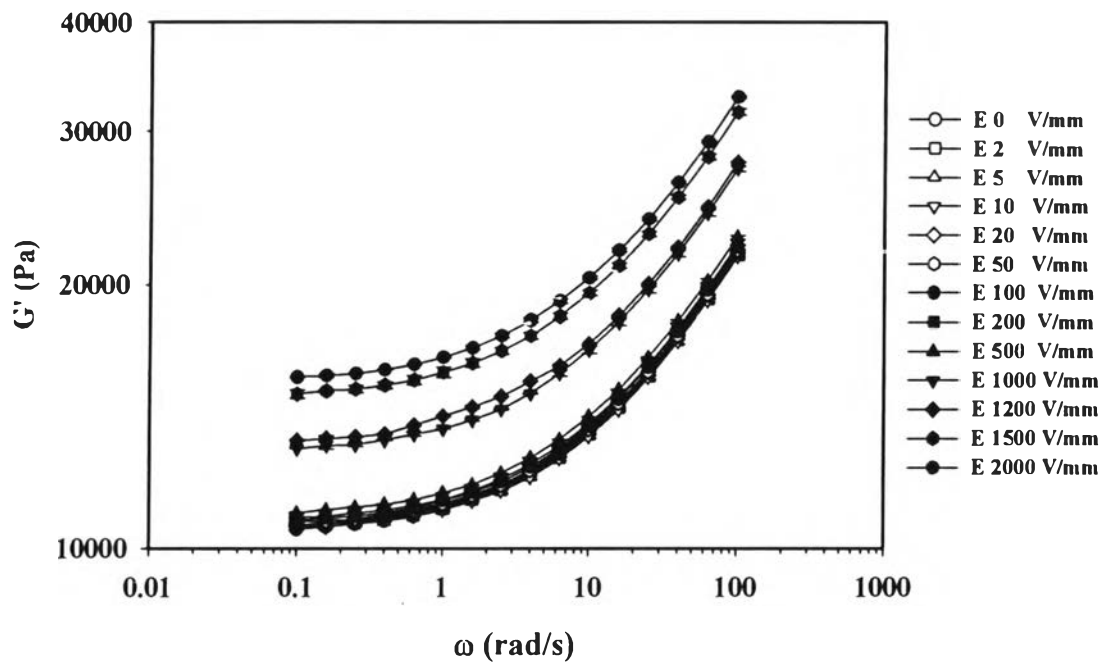


(a)

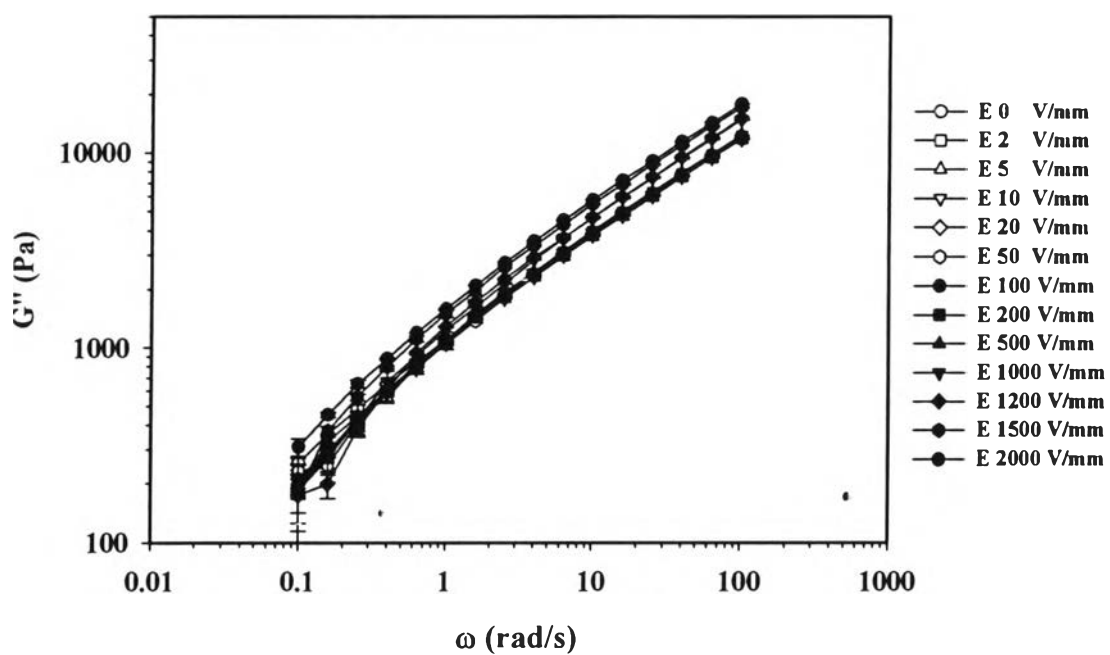


(b)

Figure L5 Comparison of the storage and the loss moduli of polyisoprene (PI_03) and Polythiophen/polyisoprene blends (Pth_U/PI_03) at various particle concentrations (5,10, 20, and 30 vol.%), strain 1%, 27°C, electric field strength 0 V/mm: (a) storage modulus, G' , (b) loss modulus, G'' .

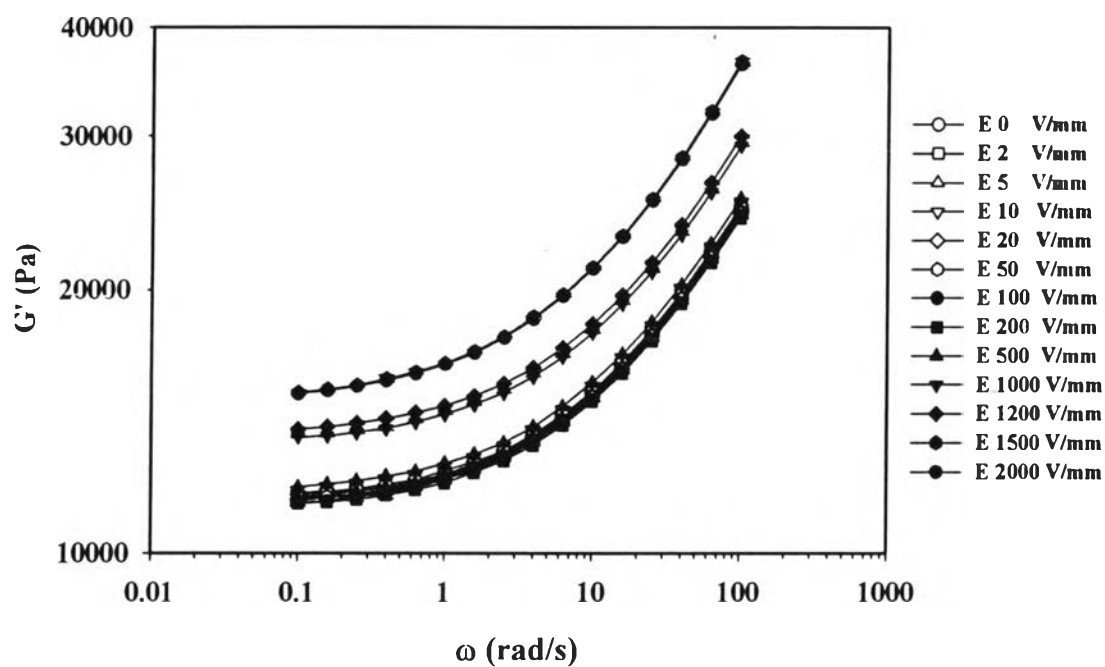


(a)

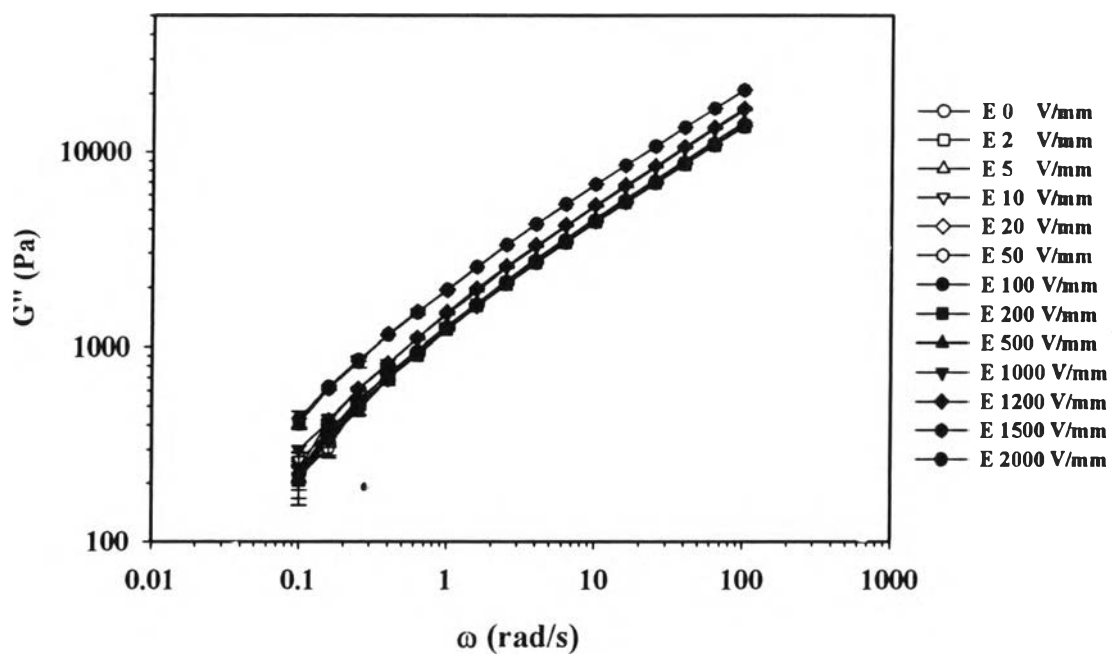


(b)

Figure L6 Frequency sweep tests of Pth_U5/PI_03, strain 1.0%, 27°C, gap 0.899 mm, various electric field strength: a) G' ; b) G'' .

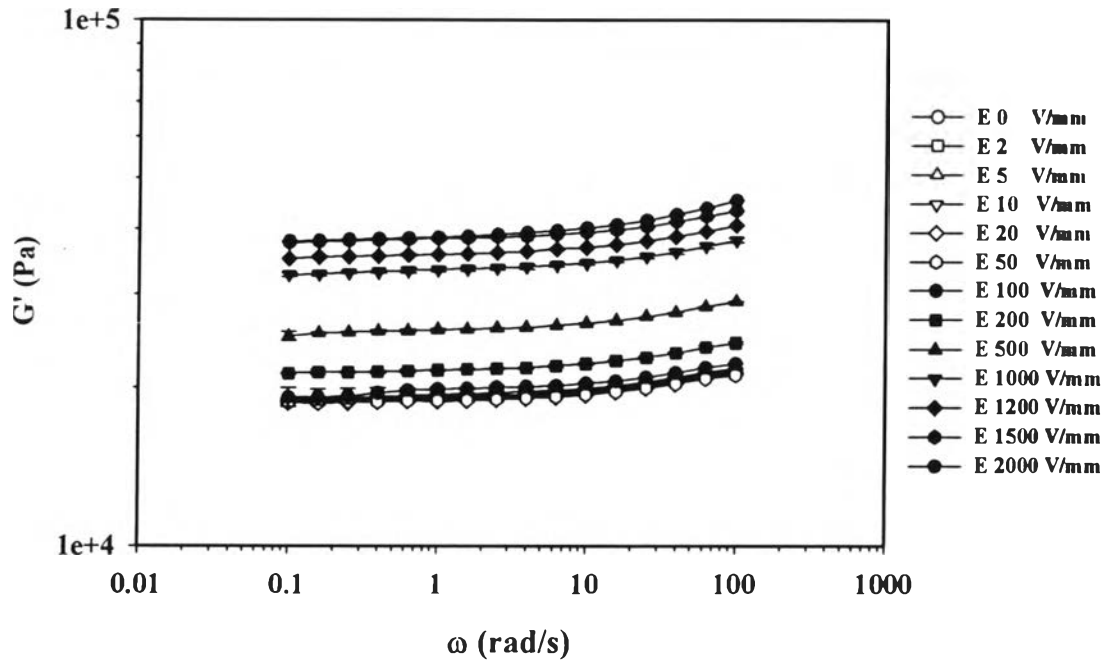


(a)

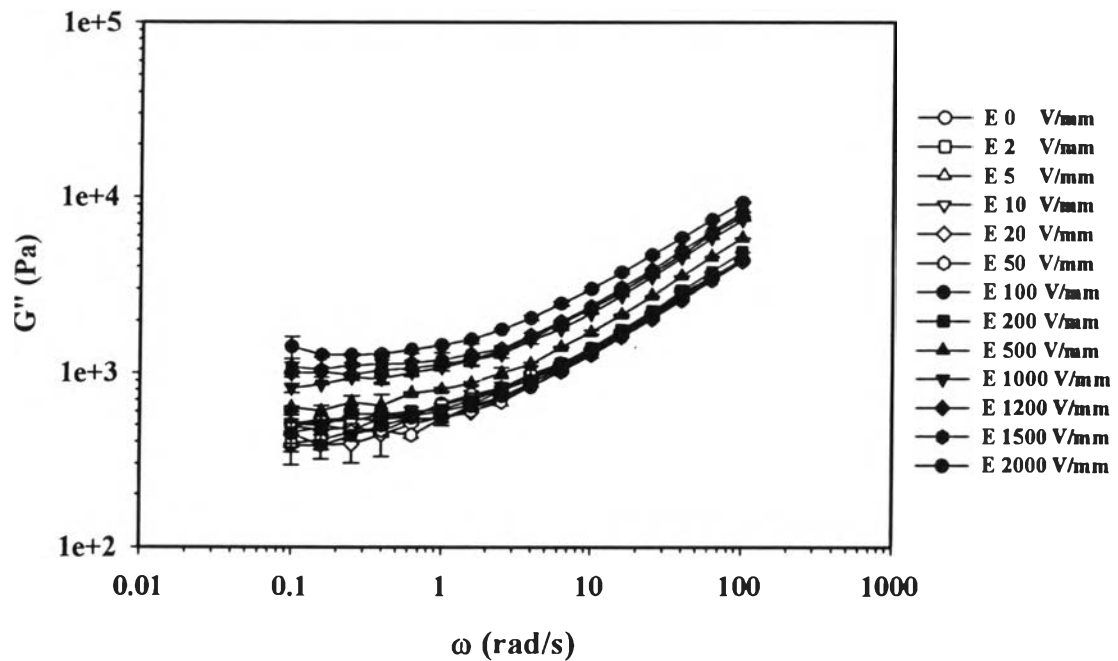


(b)

Figure L7 Frequency sweep tests of Pth_U10/PI_03, strain 1.0%, 27°C, gap 0.905 mm, various electric field strength: a) G' ; b) G'' .

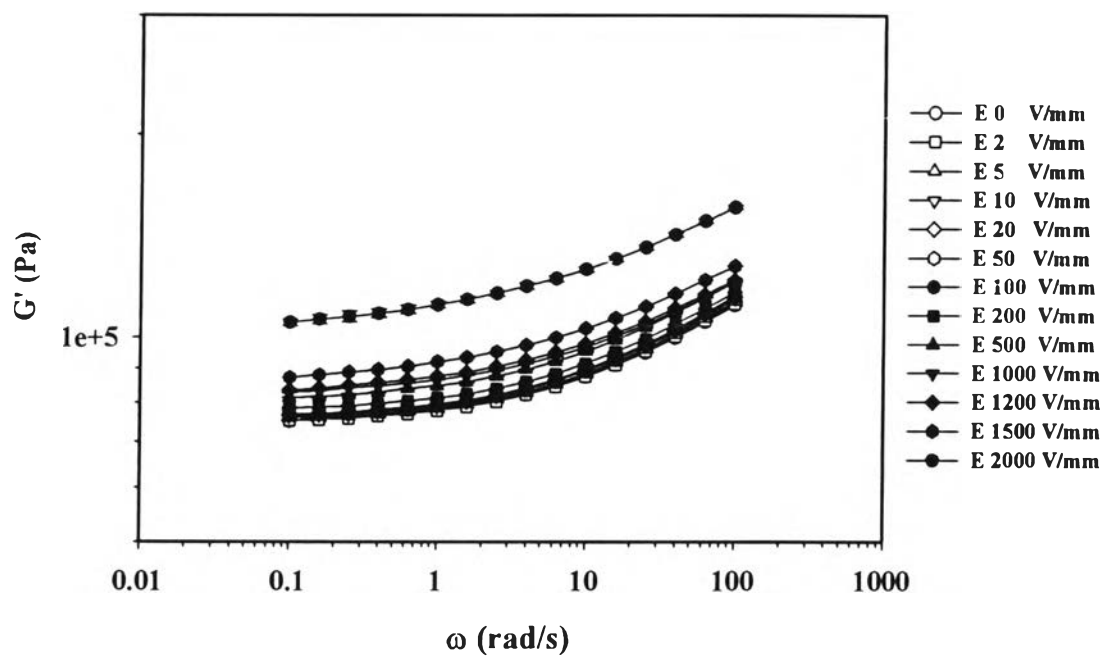


(a)

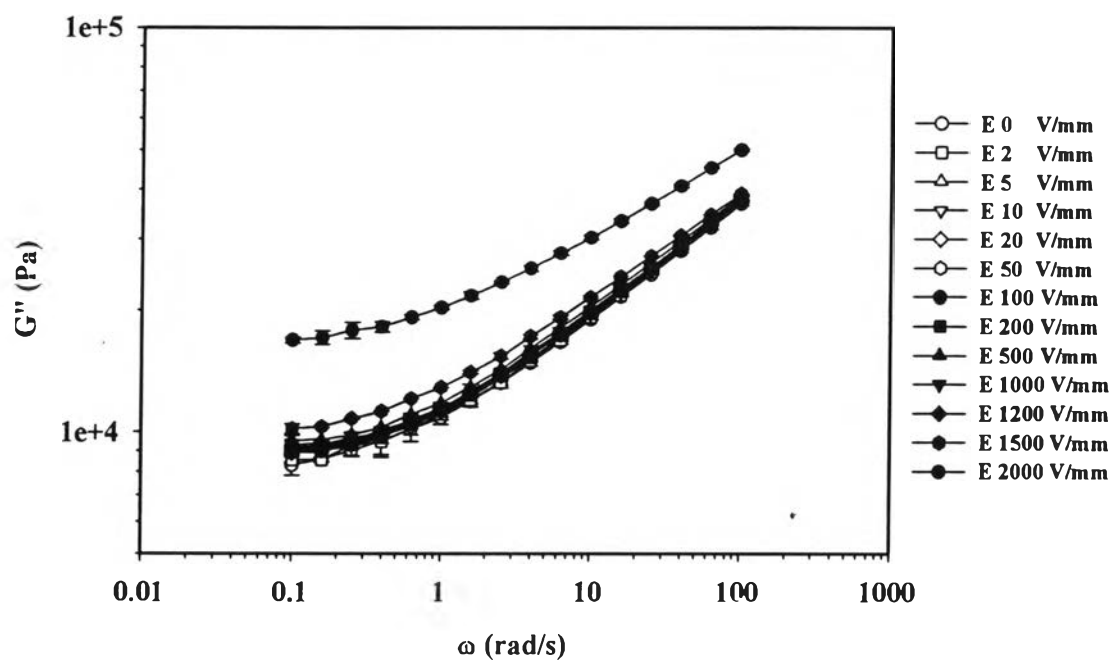


(b)

Figure L8 Frequency sweep tests of Pth_U20/PI_03, strain 1.0%, 27°C, gap 0.950 mm, various electric field strength: a) G' ; b) G'' .

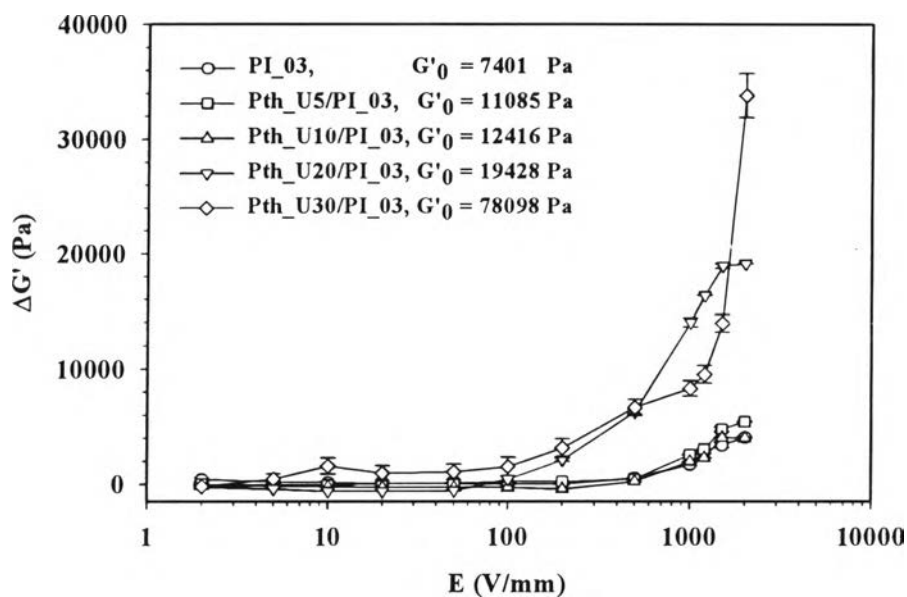


(a)

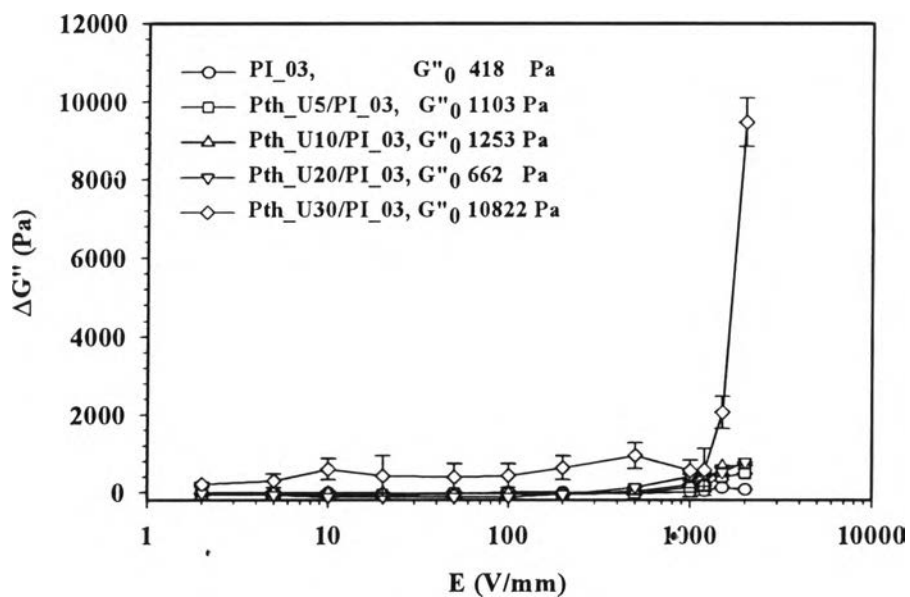


(b)

Figure L9 Frequency sweep tests of Pth_U30/PI_03, strain 1.0%, 27°C, gap 0.920 mm, various electric field strengths: a) G' ; b) G'' .

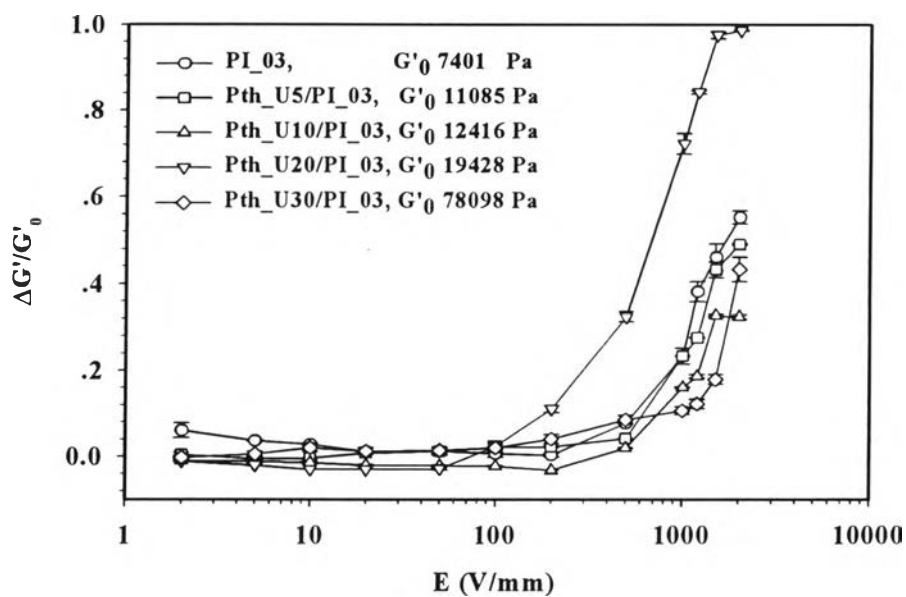


(a)

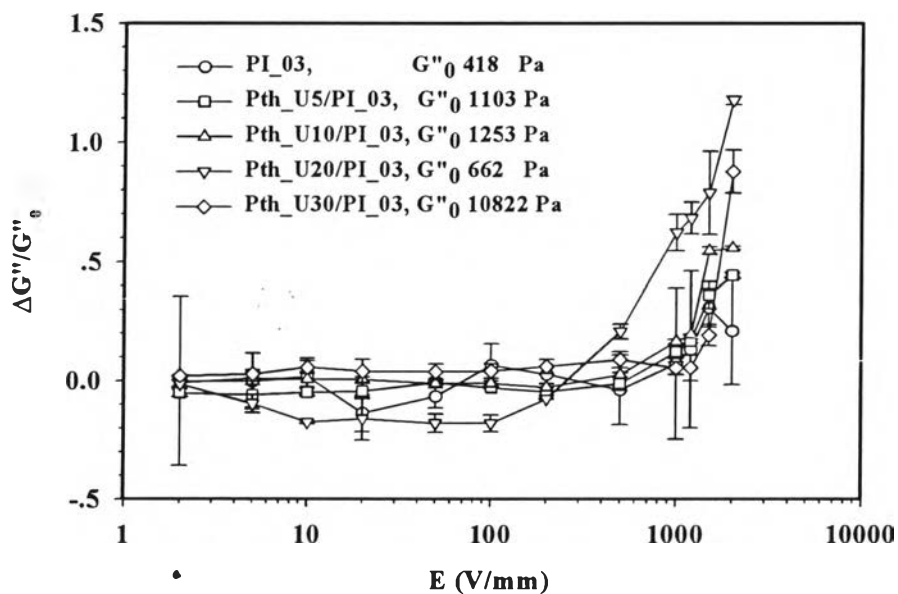


(b)

Figure L10 Responses of the storage and the loss moduli of the polythiophen/polyisoprene blends at various particle compositions vs. electric field strength, at frequency 1.0 rad/s, strain 1%, at 27°C: (a) $\Delta G'(\omega)$; (b) $\Delta G''(\omega)$.

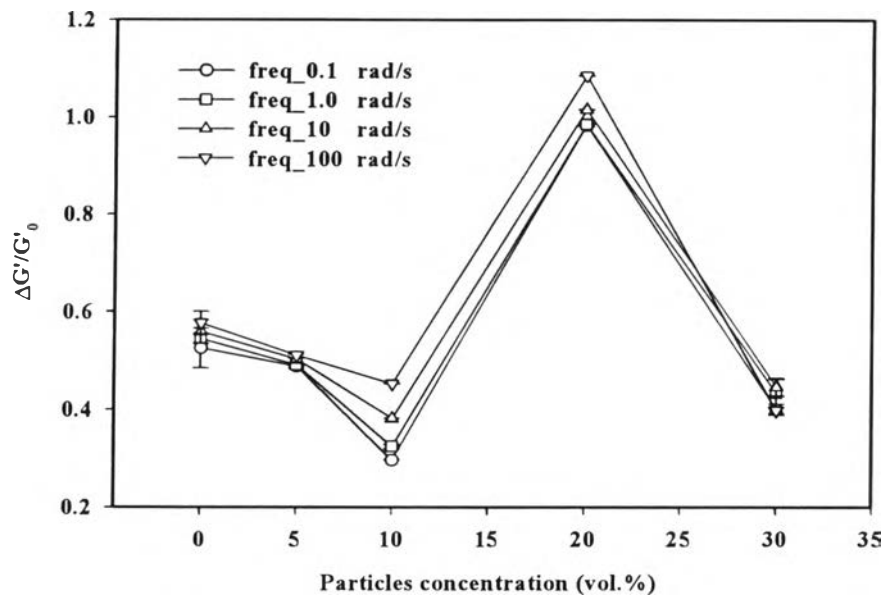


(a)

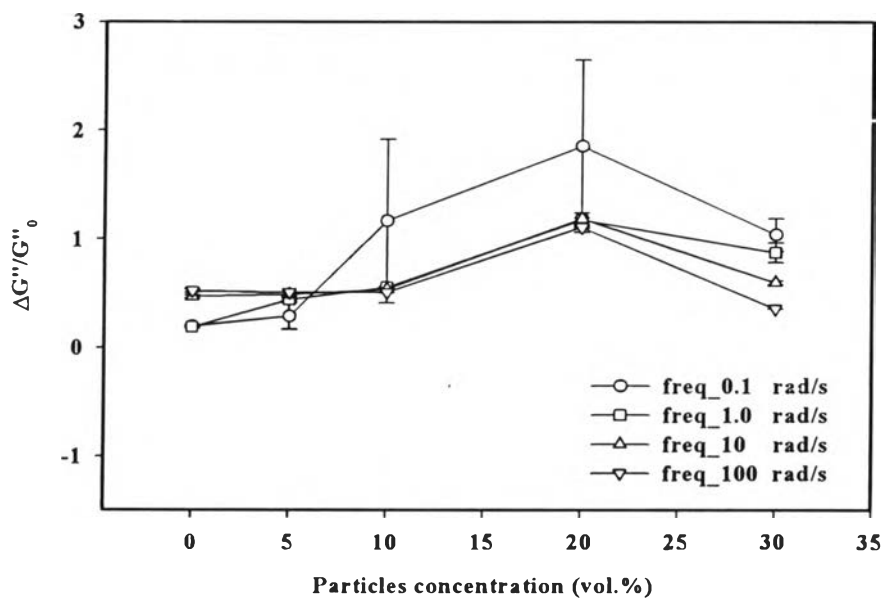


(b)

Figure L11 Sensitivity of the storage and the loss moduli of the Pth_U/PI_03 blends at various particle compositions vs. electric field strength, at frequency 1.0 rad/s, strain 1%, at 27°C: (a) $\Delta G'/G'_0(\omega)$; (b) $\Delta G''/G''_0(\omega)$.



(a)



(b)

Figure L12 Sensitivity of the polyisoprenes as functions of various polythiophene particle concentrations, 27°C, various frequencies, electric field strength 2 kV/mm: (a) $\Delta G'/G'_0$; (b) $\Delta G''/G''_0$.

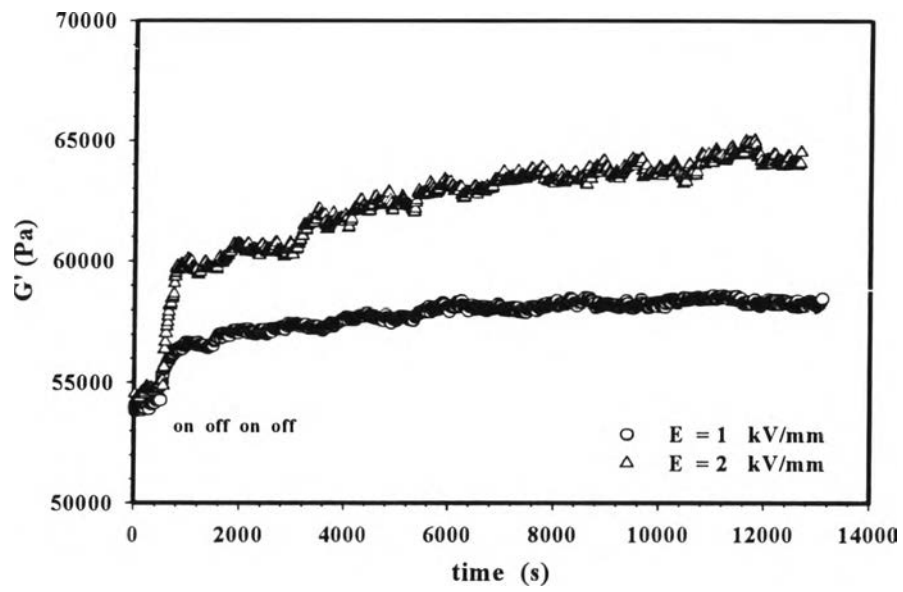


Figure L15 Temporal response of storage modulus (G') of Pth_U20/PI_03 system at various electric field strength (1 and 2 kV/mm).

Appendix M Electrorheological Properties Measurement of Polythiophene/ Polyisoprene Suspensions at various Polythiophene Specific Conductivity Polythiophene Particles Concentrations

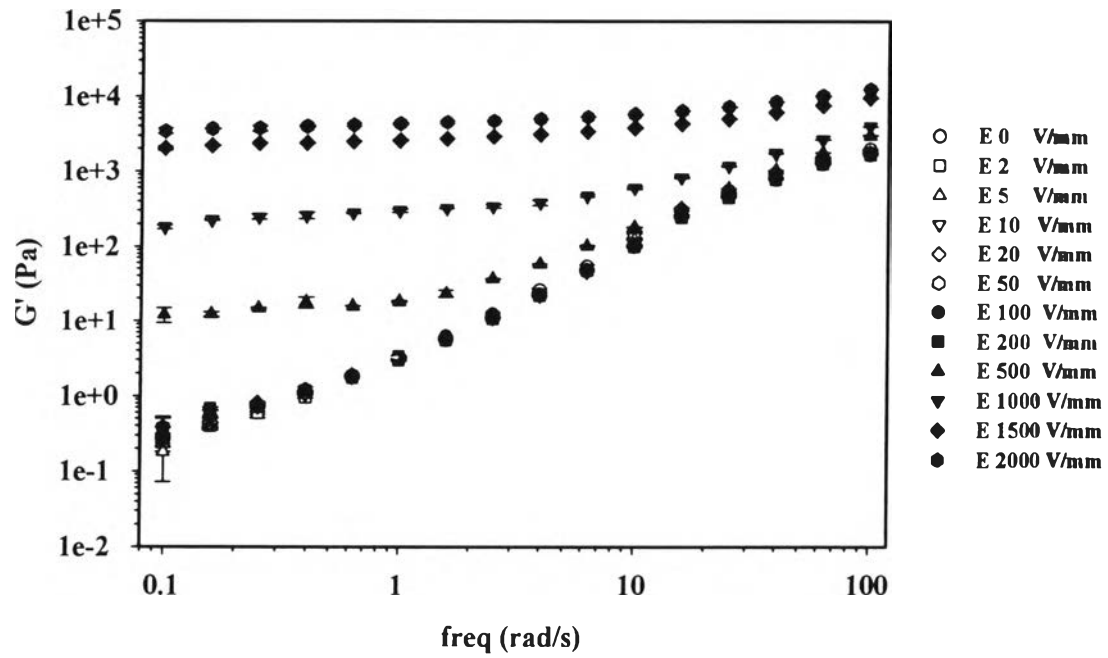
The electrorheological properties of polythiophene/polyisoprene suspensions at various polythiophene specific conductivity and polythiophene particle concentrations were measured by the melt rheometer (Rheometric Scientific, ARES) under oscillatory shear mode and applied electric field strength varying from 0 to 2 kV/mm. In these experiments, the dynamic moduli (G' and G'') were measured as functions of frequency and electric field strength. Strain sweep tests were first carried out to determine the appropriate strain to measure G' and G'' in the linear viscoelastic regime as showed in Table M1.

Table M1 Summary the linear viscoelastic regime of polythiophene/polyisoprene suspensions at various polythiophene particle concentrations

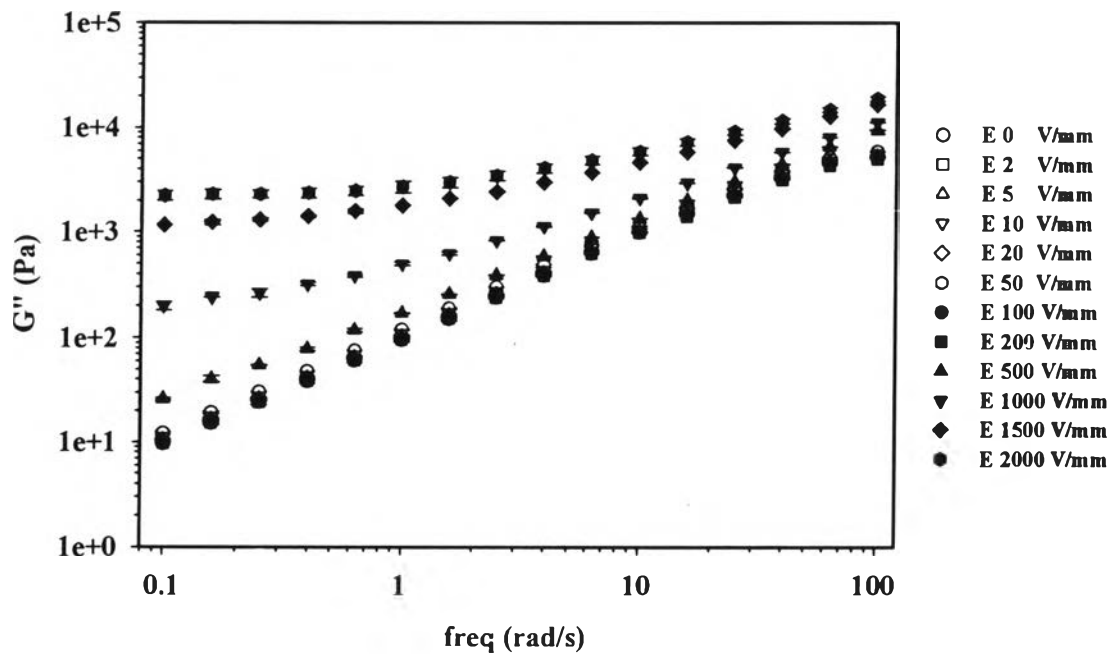
Systems	Particle concentration (vol.%)	Appropriate strain (%)			
		E (kV/mm)			
5Pth U/PI	5	0 - 0.2	0.5	1	1.5 - 2
		220	10	2	0.7
5Pth 1:1/PI	5	220	2	2	0.3
5Pth 10:1/PI	5	220	2	0.5	0.3
5Pth 200:1/PI	5	220	2	0.5	0.3
10Pth 200:1/PI	10	80	2	0.5	0.3
20Pth 200:1/PI	20	50	0.7	0.5	0.3

Table M2 Induction time and recovery times at 27°C of doped and undoped polythiophene/polyisoprene suspensions

Samples	Electric field (kV/mm)	Induction time (τ_{ind}) (s)	Recovery time (τ_{rec}) (s)	$\Delta G'_{ind}$ (Pa)	$\Delta G'_{rec}$ (Pa)	$\Delta G''_{ind}$ (Pa)	$\Delta G''_{rec}$ (Pa)
5Pth U/PI	2.0	34	62	25	24	148	122
5Pth_200:1/PI	2.0	33	173	61	57	303	277
20Pth_200:1/PI	0.5	62	70	10	8	89	61
	1.0	65	170	35	32	271	232
	2.0	67	206	133	125	772	699

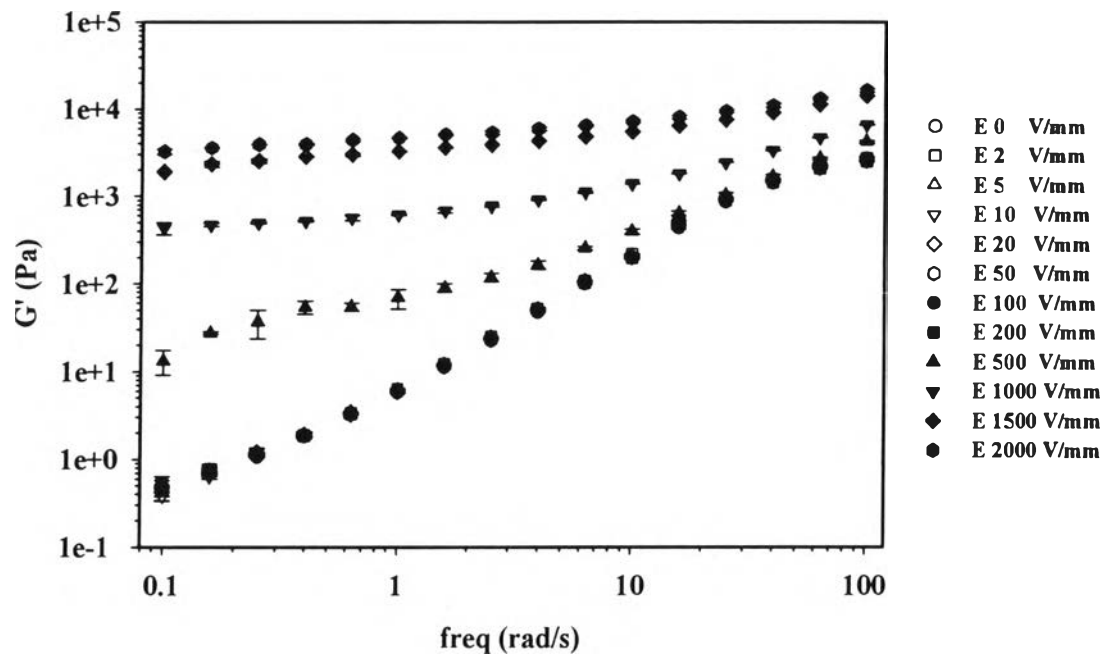


(a)

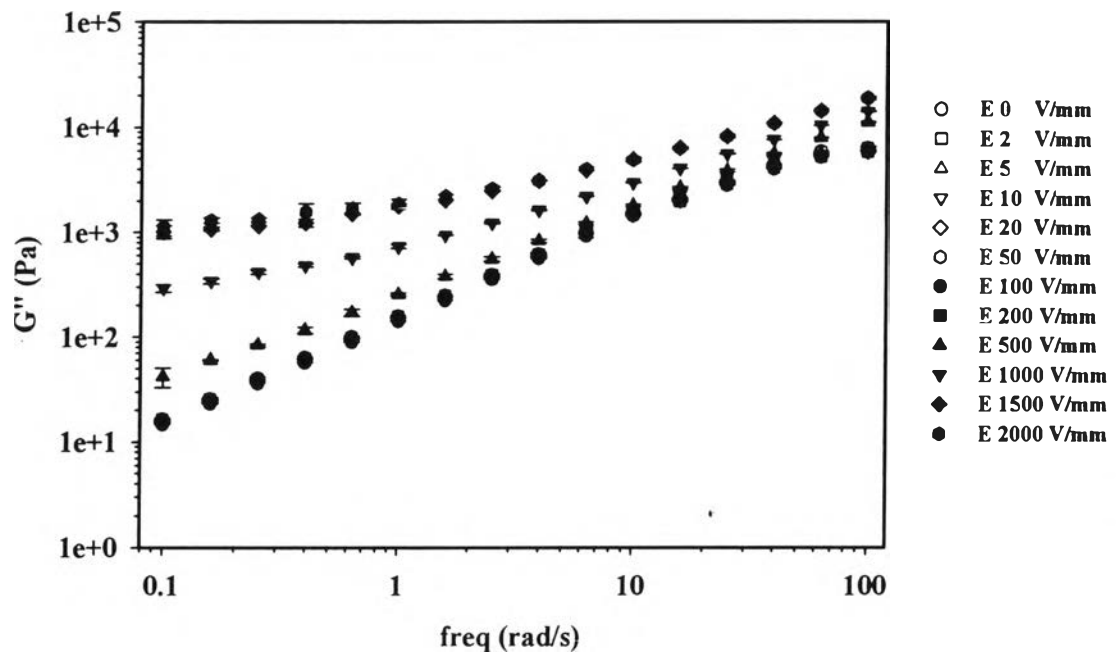


(b)

Figure M1 Frequency sweep tests of 5Pth_U/PI, gap 0.500 mm, various electric field strength, and at 27°C: a) G' ; b) G'' .

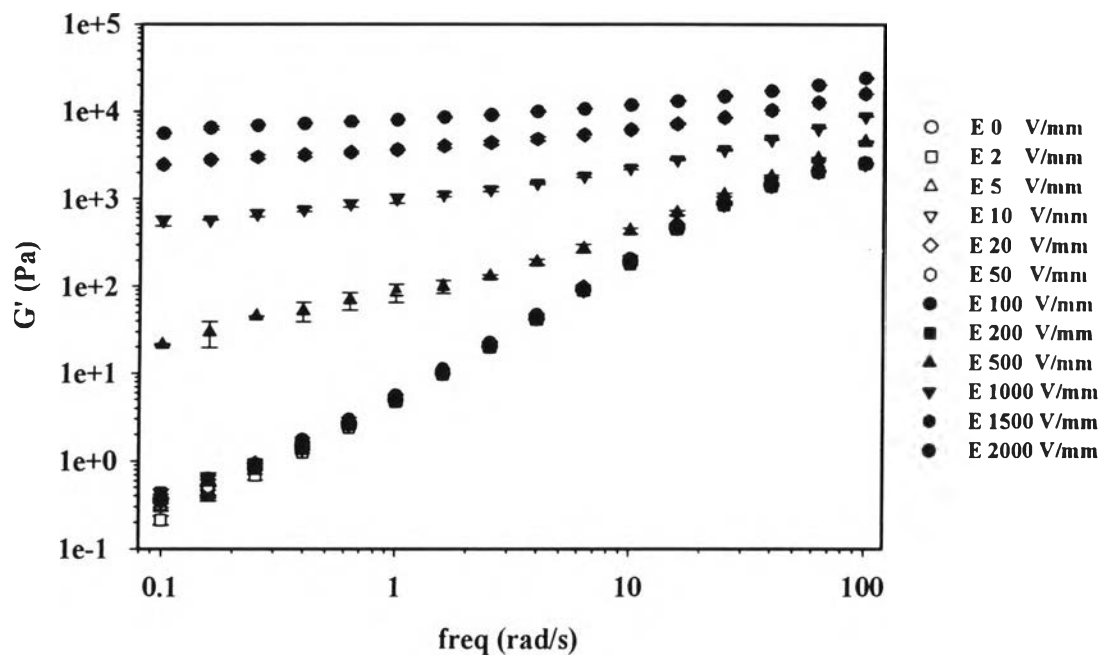


(a)

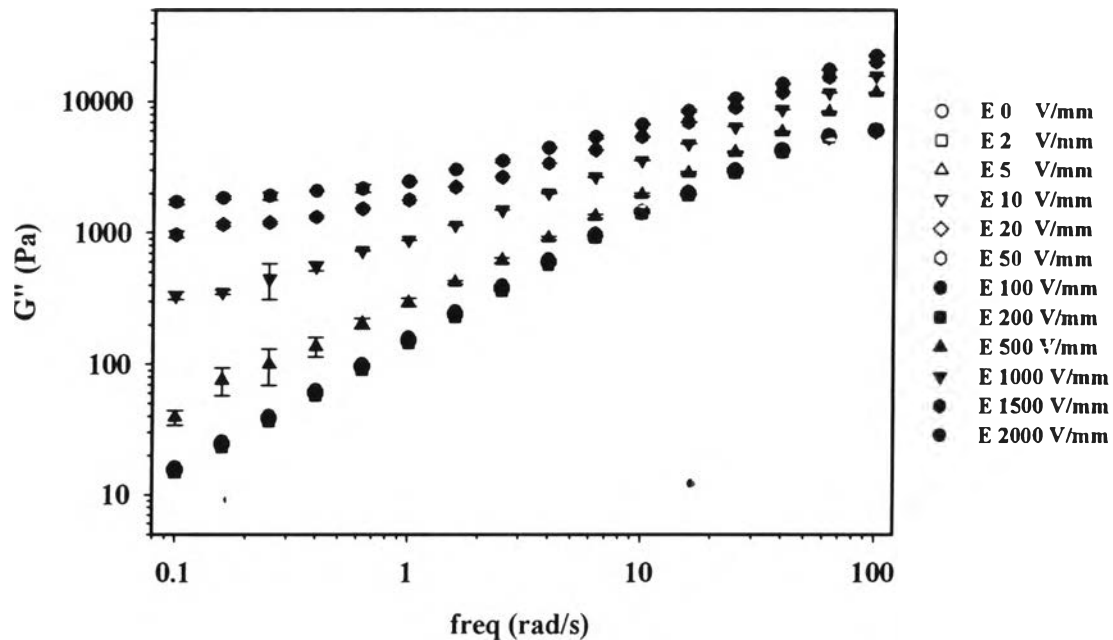


(b)

Figure M2 Frequency sweep tests of 5Pth_1:1/PI, gap 0.500 mm, various electric field strength, and at 27°C: a) G' ; b) G'' .

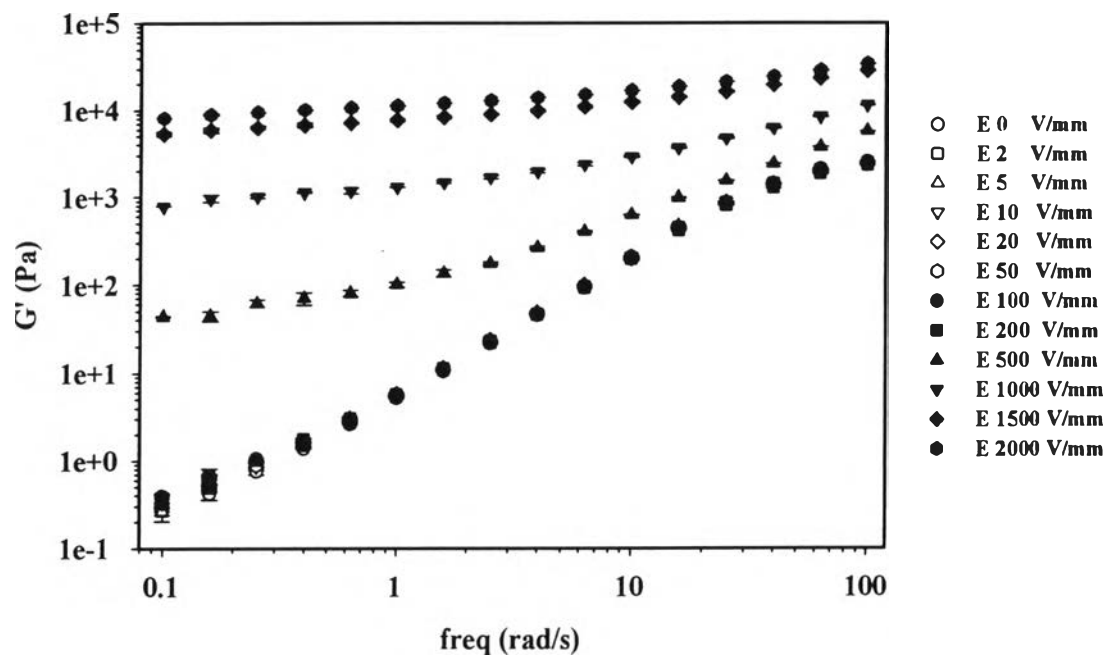


(a)

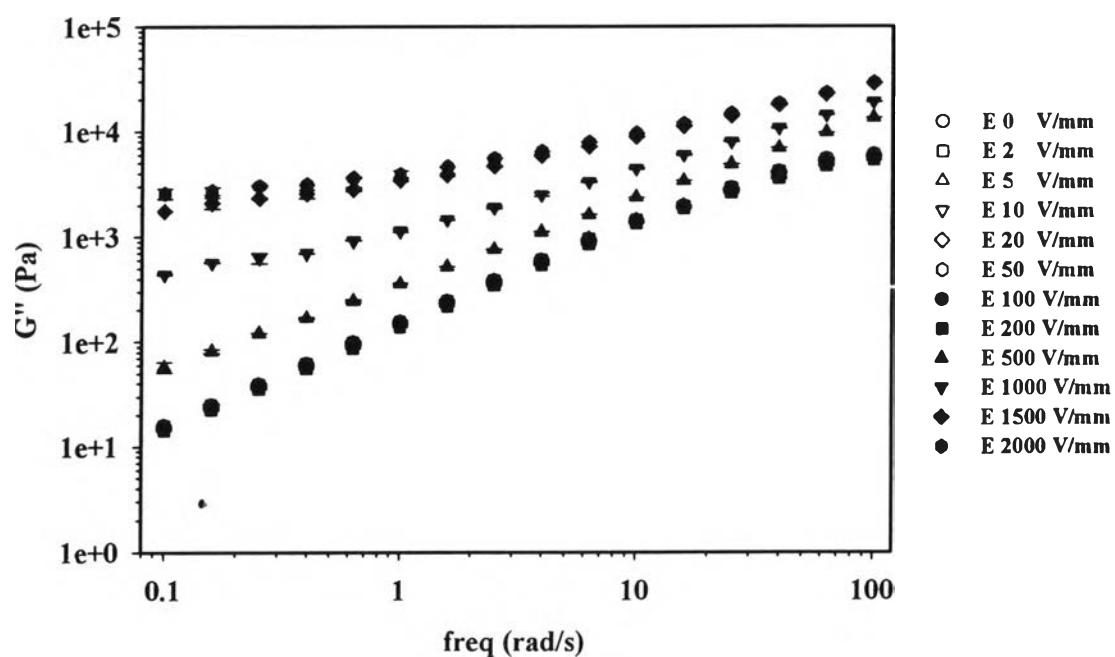


(b)

Figure M3 Frequency sweep tests of 5Pth_{10:1}/PI, gap 0.500 mm, various electric field strength, and at 27°C: a) G' ; b) G'' .

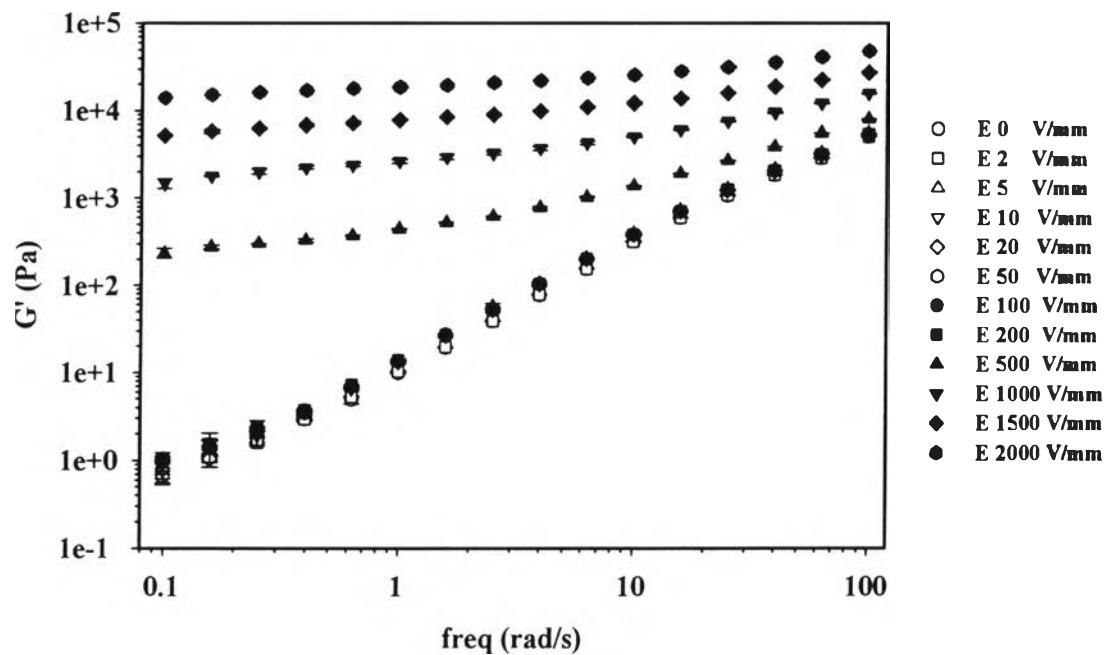


(a)

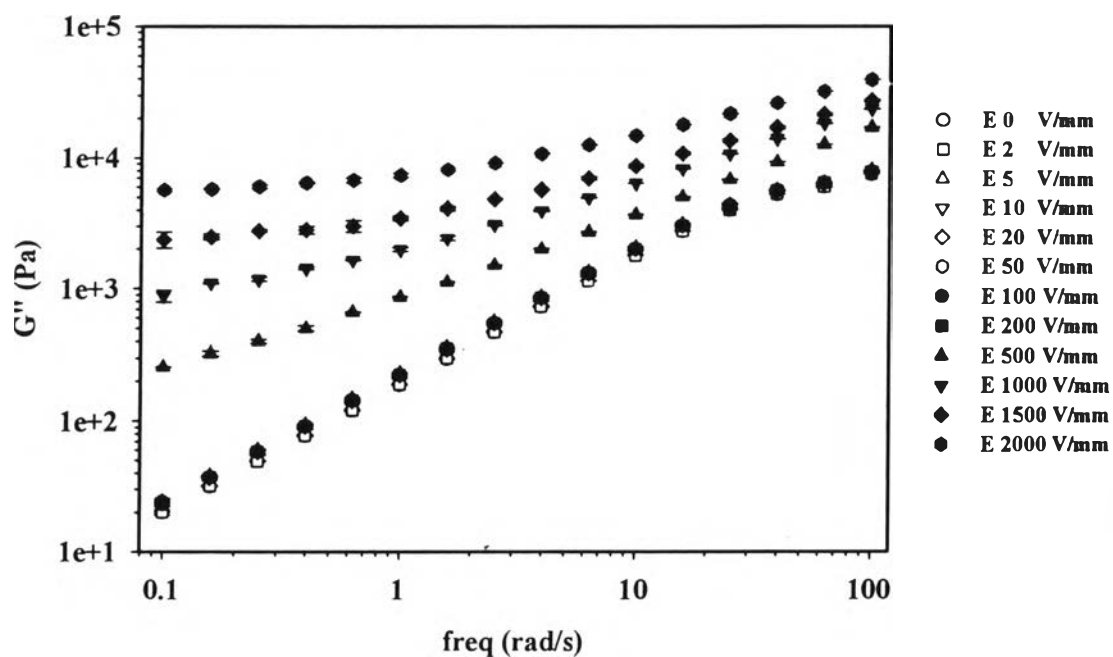


(b)

Figure M4 Frequency sweep tests of 5Pth_200:1/PI, gap 0.500 mm, various electric field strength, and at 27°C: a) G' ; b) G'' .

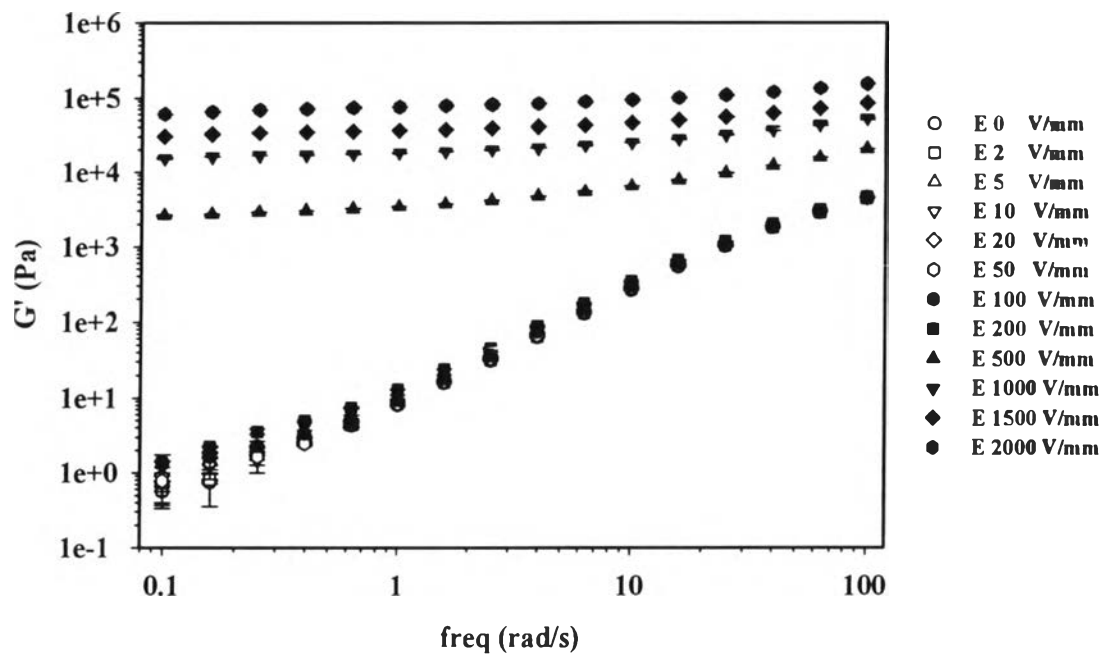


(a)

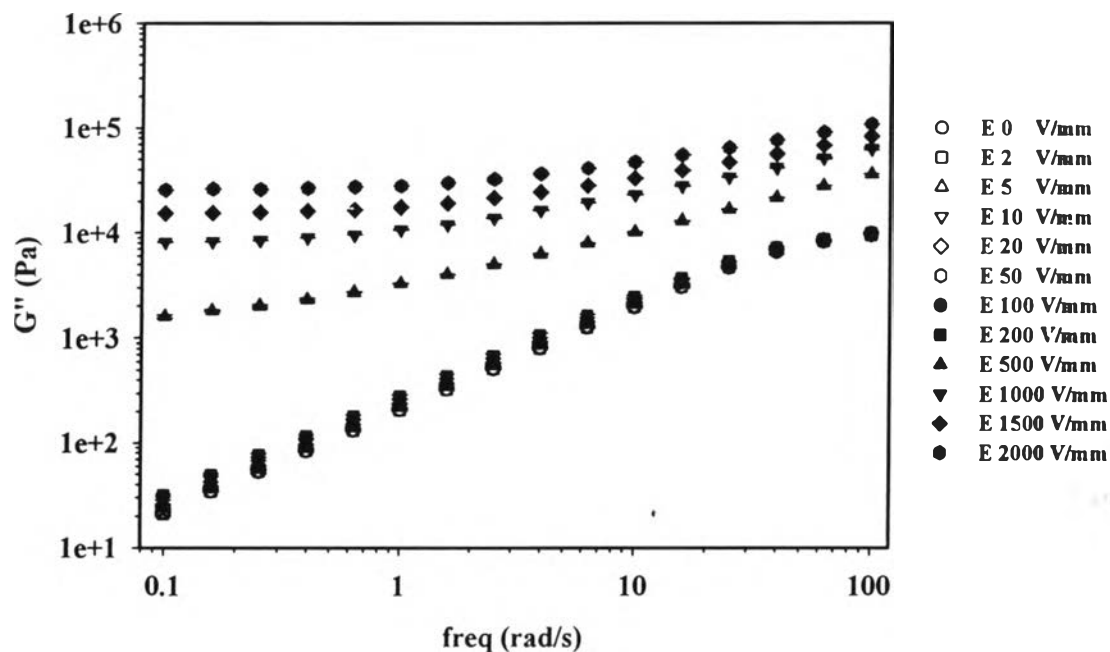


(b)

Figure M5 Frequency sweep tests of 10Pth_200:1/PI, gap 0.500 mm, various electric field strength, and at 27°C: a) G' ; b) G'' .

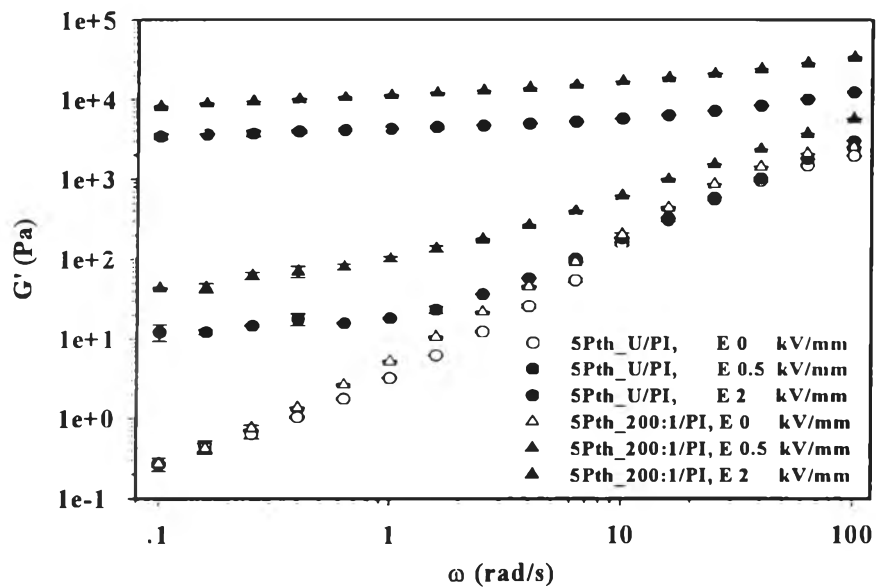


(a)

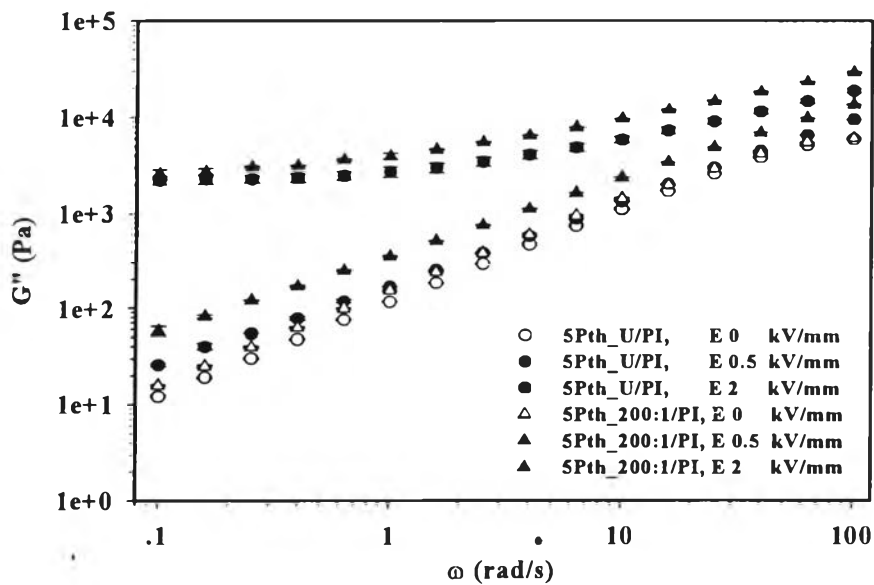


(b)

Figure M6 Frequency sweep tests of 20Pth_200:1/PI, gap 0.500 mm, various electric field strength, and at 27°C: a) G' ; b) G'' .

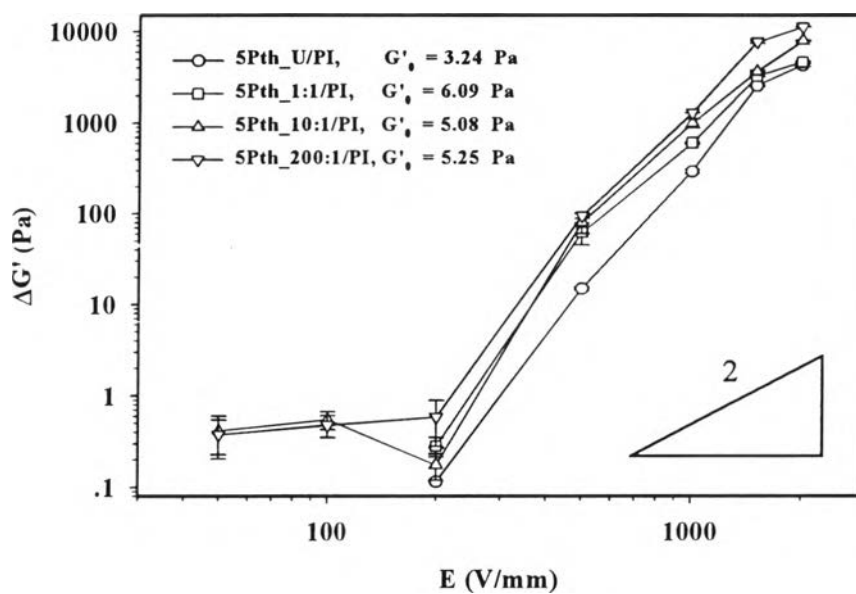


(a)

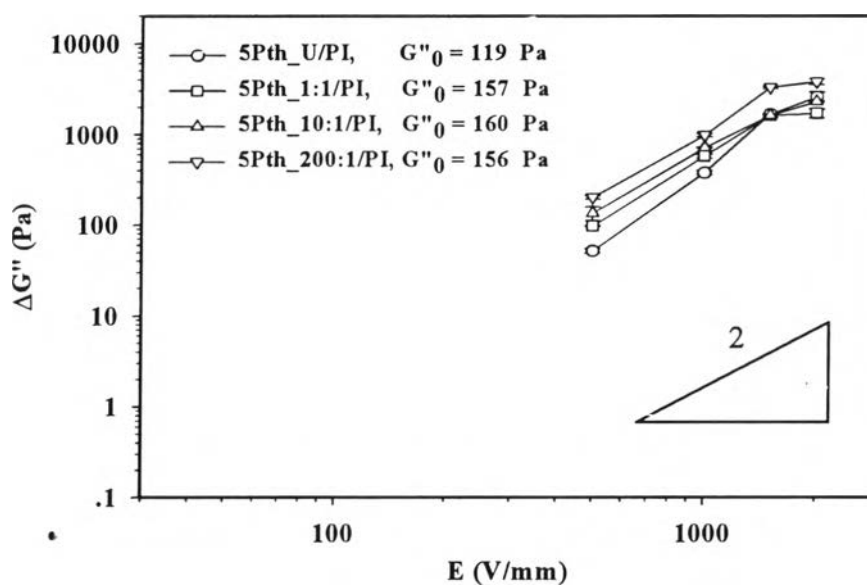


(b)

Figure M7 Storage and loss moduli of 5vol.% polythiophene/polyisoprene suspensions (5Pth/PI) at various doping ratios vs. frequency, 27°C: (a) storage modulus, $G'(\omega)$; (b) loss modulus, $G''(\omega)$.

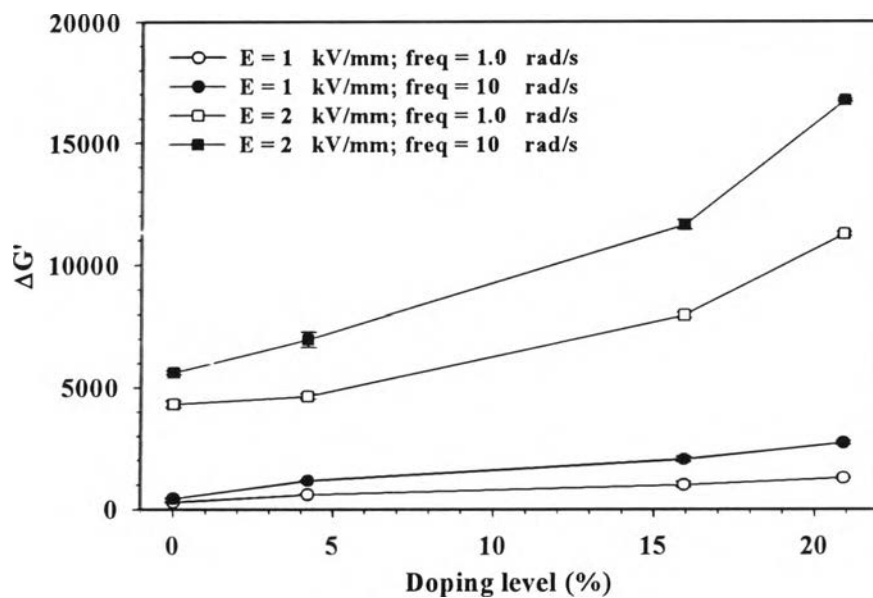


(a)

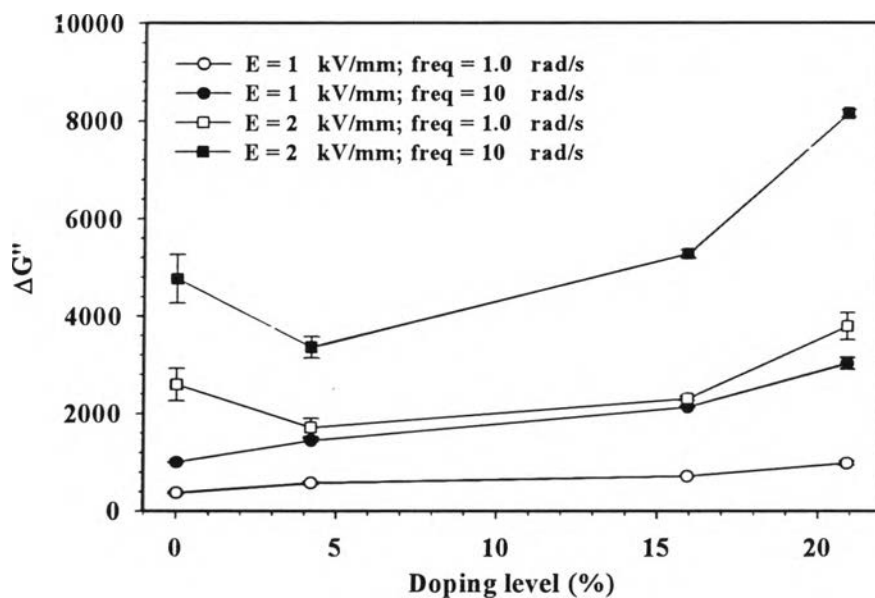


(b)

Figure M8 Storage modulus ($\Delta G'$) and loss modulus responses ($\Delta G''$) of 5vol.% polythiophene/polyisoprene suspension (5Pth/PI) at various doping ratios vs. electric field strength, at frequency of 1.0 rad/s, and at 27°C: (a) storage modulus response; (b) loss modulus response, which the data below 0.4 kV/mm are negligible.

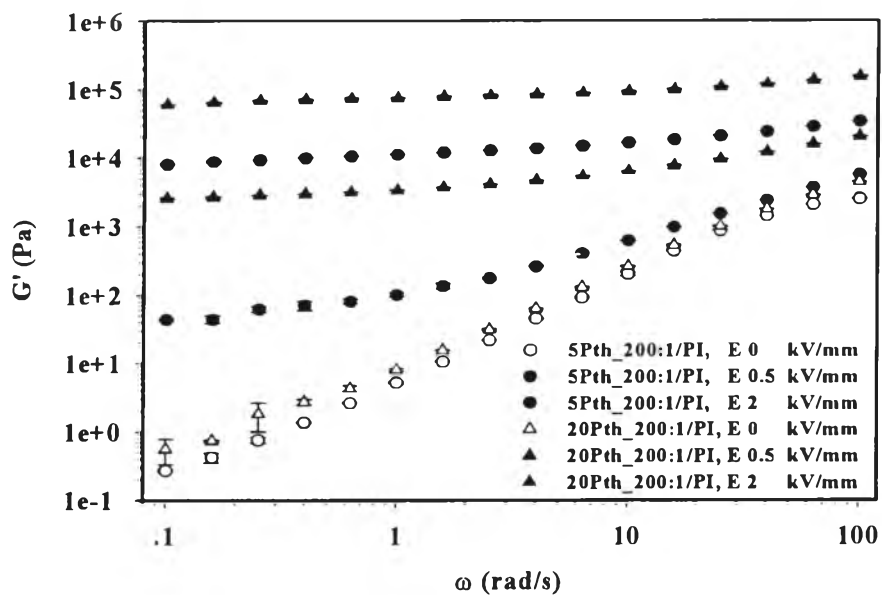


(a)

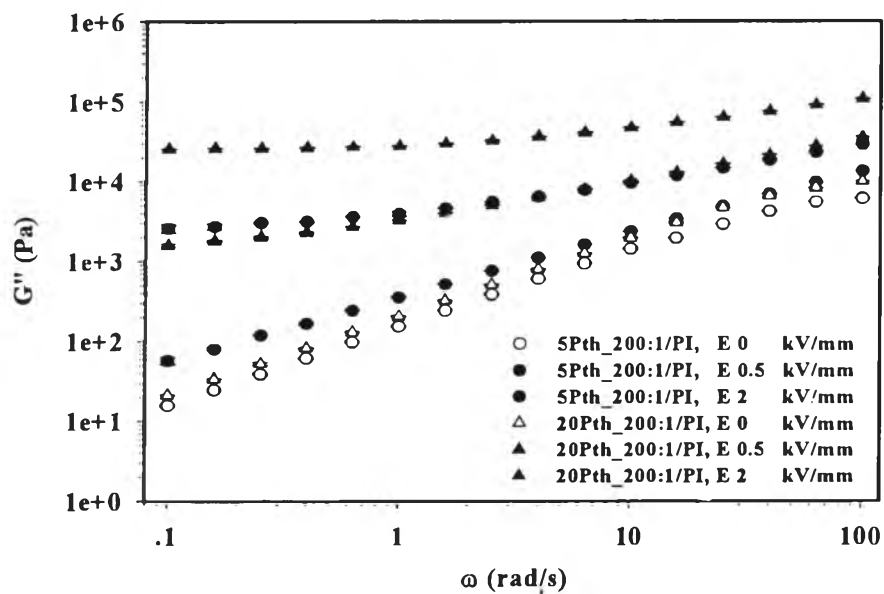


(b)

Figure M9 Storage modulus ($\Delta G'$) and loss modulus responses ($\Delta G''$) of doped polythiophene/polyisoprene suspensions as functions of doping level, 27°C, at various frequencies, and at electric field strengths of 1 and 2 kV/mm.

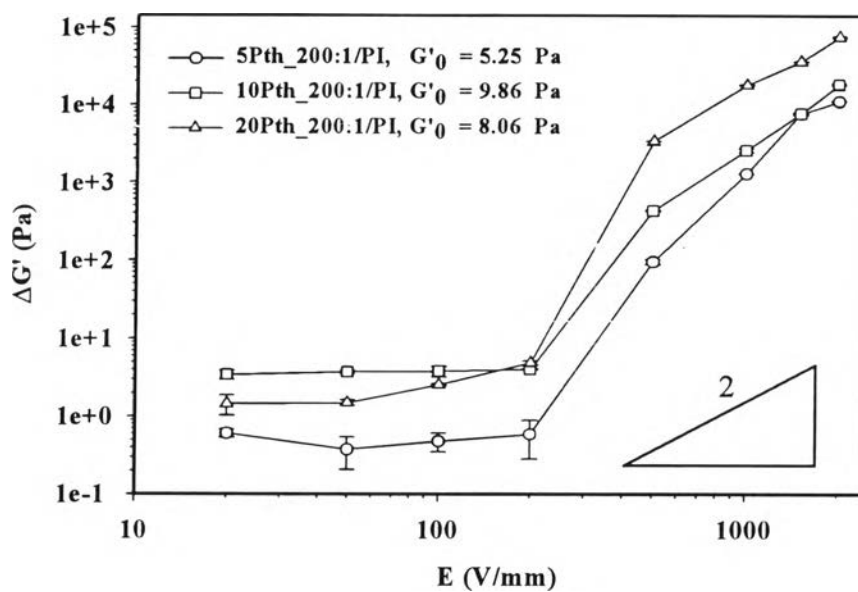


(a)

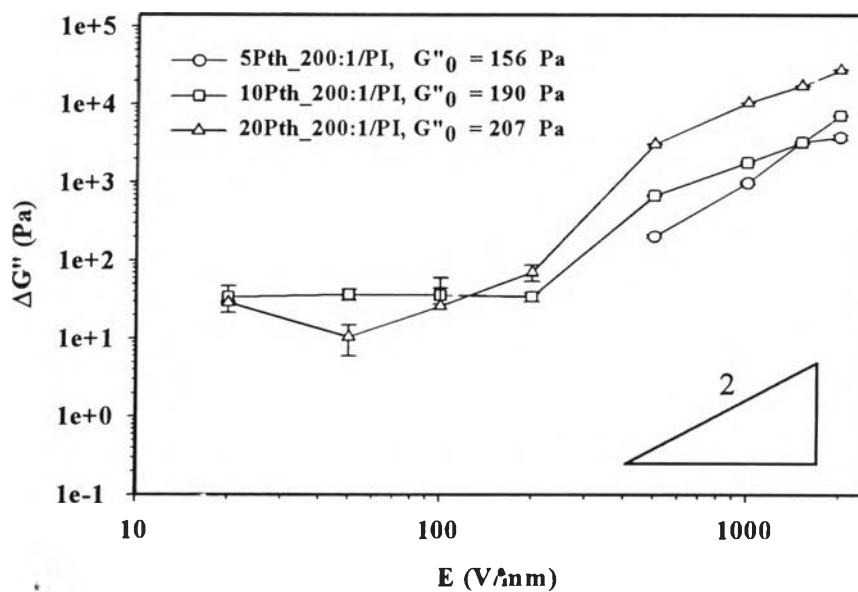


(b)

Figure M10 Storage and loss modulus of HClO_4 highly doped polythiophene/polyisoprene suspensions (Pth_200:1/PI) at various particle concentrations vs. frequency, 27°C : (a) storage modulus, $G'(\omega)$; (b) loss modulus, $G''(\omega)$.

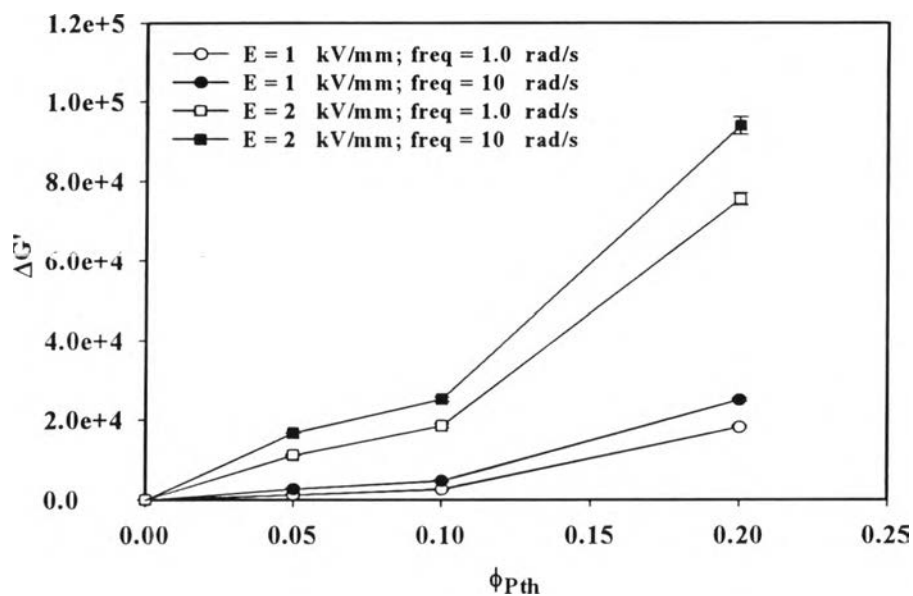


(a)

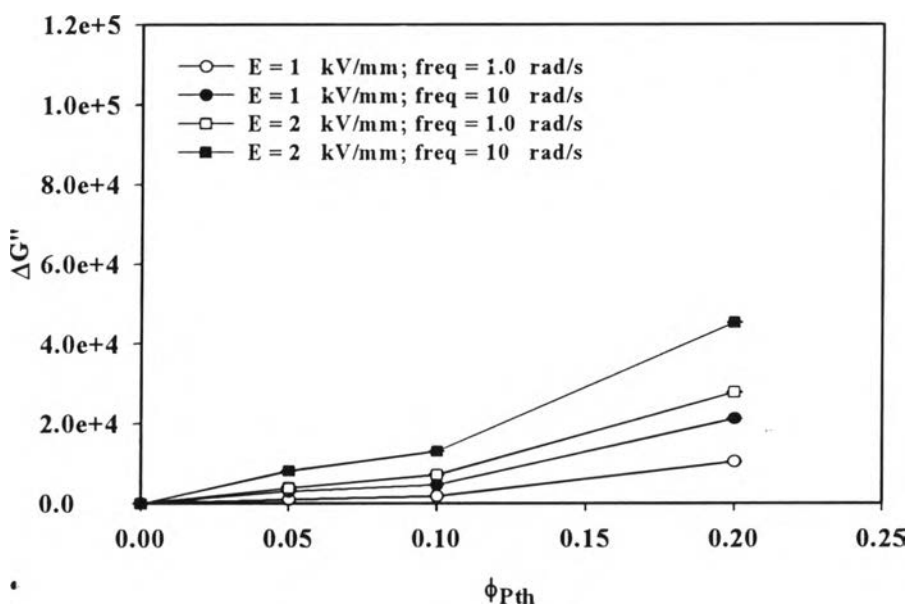


(b)

Figure M11 Storage modulus ($\Delta G'$) and loss modulus responses ($\Delta G''$) of HClO_4 highly doped polythiophene/polyisoprene suspensions (Pth_200:1/PI) at various particle concentrations vs. electric field strength, at frequency of 1.0 rad/s, at 27°C: (a) storage modulus responses; (b) loss modulus responses.

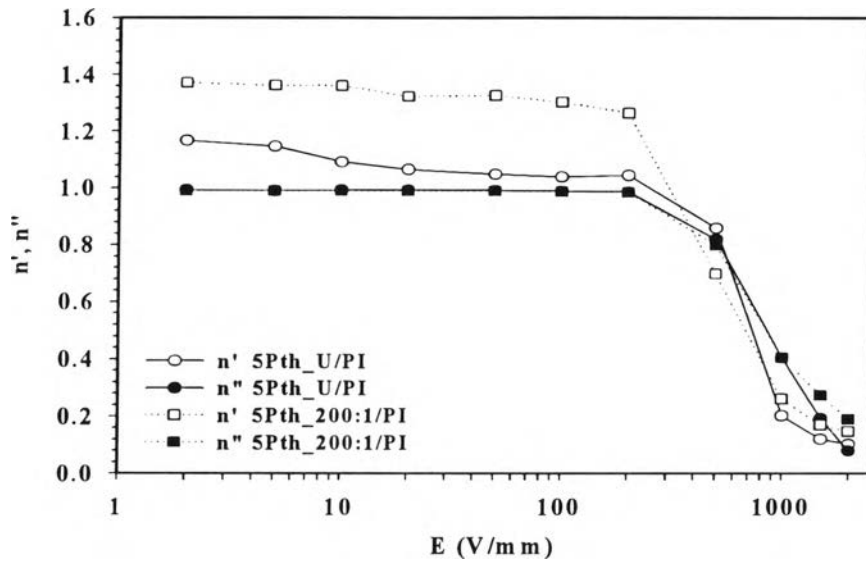


(a)

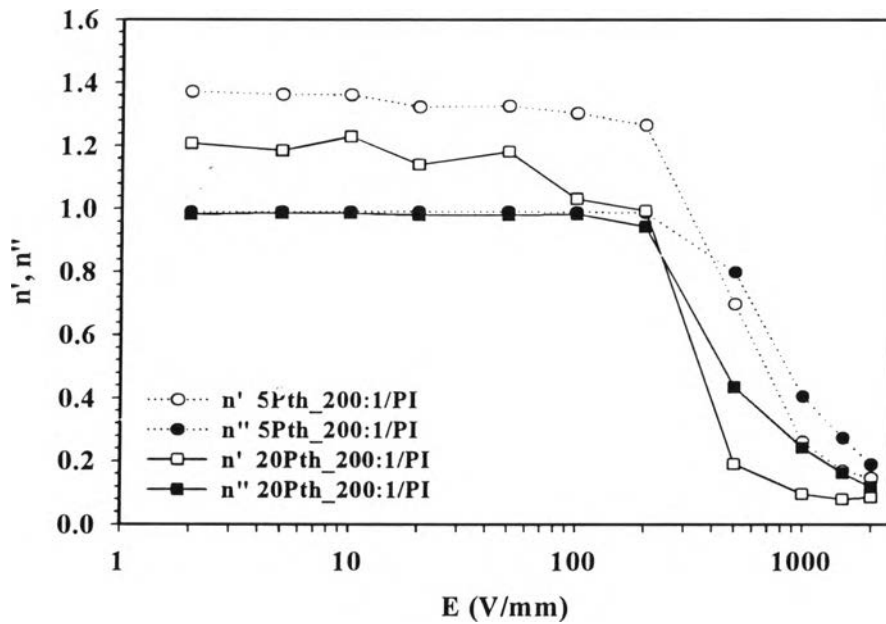


(b)

Figure M12 Storage modulus ($\Delta G'$) and loss modulus responses ($\Delta G''$) of HClO_4 highly doped polythiophene/polyisoprene suspensions as functions of particle concentration, 27°C , at various frequencies, and at electric field strengths of 1 and 2 kV/mm.

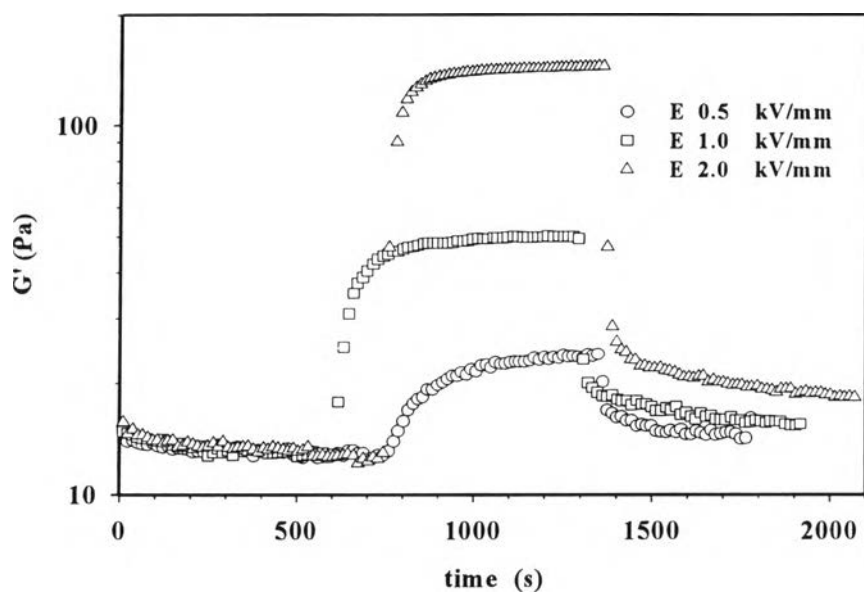


(a)

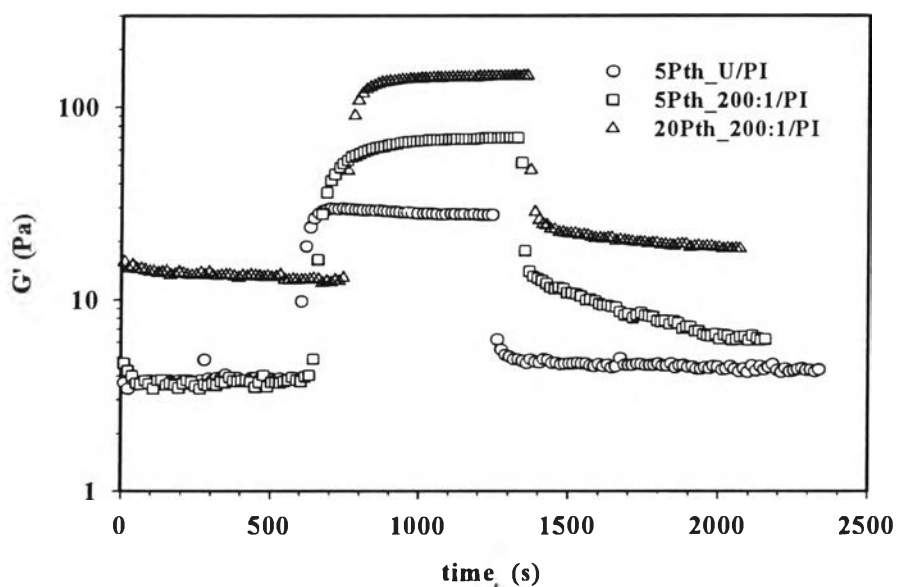


(b)

Figure M13 The scaling exponents n' and n'' vs. electric field strength of HClO_4 doped polythiophene/polyisoprene suspensions, and at temperature of 27°C : (a) Undoped and highly doped, 5 vol.%; (b) Highly doped at various particle concentrations.



(a)



(b)

Figure M14 Temporal response of storage modulus (G') of : (a) 20vol.% HClO_4 highly doped polythiophene/polyisoprene suspensions (20Pth_200:1/PI) at various electric field strengths; (b) Polythiophene/polyisoprene suspensions at various doping ratio and particle concentration, electric field strength of 2 kV/mm, and at 27°C.

CURRICULUM VITAE

Name: Mr. Toemphong Puvanatvattana

Date of Birth: September 19, 1981

Nationality: Thai

University Education:

1999-2002 Bachelor Degree of Petrochemical Engineer and Polymeric Materials, Faculty of Engineering and Industrial Technology, Silpakorn University, Nakornphathom, Thailand

Presentations:

1. Puvanatvattana, T., Sirivat, A., and Jamieson, A.M. (2004, December 1-3). Electroactive Polythiophene/Polyisoprene Elastomer Blends. Poster presented at International Conference on Smart Materials (SmartMat-'04), Chiang Mai, Thailand.